AD-A120 077   TEXAS UNIV AT AUSTIN APPLIED RESEARCH LABS   F/G 20/1
GENERATION AND ANALYSIS OF BOTTOM LOSS UPGRADE GEOACOUSTIC PARA--ETC(U)
AUG 82 D P KNOBLES, P J VIDMAR   N00014-82-C-0049
UNCLASSIFIED   ARL-TR-82-17   NL

1 OF 2
AD A
120077

UNCLASSIFIED

SECURITY CLASSIFICATION OF THIS PAGE (When Data Entered)

REPORT DOCUMENTATION PAGE

READ INSTRUCTIONS BEFORE COMPLETING FORM

1. REPORT NUMBER	2. GOVT ACCESSION NO. AD-A120077
3. RECIPIENT'S CATALOG NUMBER	
4. TITLE (and Subtitle) GENERATION AND ANALYSIS OF BOTTOM LOSS UPGRADE GEOACOUSTIC PARAMETERS FOR SPECIFIC LOCATIONS IN THE NORTHEAST PACIFIC	5. TYPE OF REPORT & PERIOD COVERED Technical Report
	6. PERFORMING ORG. REPORT NUMBER ARL-TR-82-17
7. AUTHOR(s) David Knobles, Paul Vidmar	8. CONTRACT OR GRANT NUMBER(s) N00014-82-C-0049
9. PERFORMING ORGANIZATION NAME AND ADDRESS Applied Research Laboratories, The University of Texas at Austin, Austin, TX 78712-8029	10. PROGRAM ELEMENT, PROJECT, TASK AREA & WORK UNIT NUMBERS
11. CONTROLLING OFFICE NAME AND ADDRESS Naval Ocean Research and Development Activity, NSTL Station, MS 39529	12. REPORT DATE 12 August 1982
	13. NUMBER OF PAGES 139
14. MONITORING AGENCY NAME & ADDRESS (if different from Controlling Office)	15. SECURITY CLASS. (of this report) UNCLASSIFIED
	15a. DECLASSIFICATION/DOWNGRADING SCHEDULE

16. DISTRIBUTION STATEMENT (of this Report)

Approved for public release; distribution unlimited.

17. DISTRIBUTION STATEMENT (of the abstract entered in Block 20, if different from Report)

OCT 1 2 1982

A

18. SUPPLEMENTARY NOTES

19. KEY WORDS (Continue on reverse side if necessary and identify by block number)

Bottom Loss Upgrade Program (BLUP)
geoacoustic profile
bottom loss
Pacific
thin sediment cover
basement reflection coefficient

20. ABSTRACT (Continue on reverse side if necessary and identify by block number)

Naval Air Development Center (NADC) octave-averaged bottom loss data were used as the primary resource in the generation of Bottom Loss Upgrade Program (BLUP) geoacoustic parameter sets for specific locations in the Northeastern Pacific Ocean. A ray trace simulator of the NADC measurement and analysis procedure was developed and used to determine the BLUP parameters. The BLUP parameters and a comparison of simulated bottom loss to data for each location are presented. Deficiencies in the comparison at each location and the suitability

DD FORM 1 JAN 73 1473 EDITION OF 1 NOV 65 IS OBSOLETE

UNCLASSIFIED

SECURITY CLASSIFICATION OF THIS PAGE (When Data Entered)

20. (cont'd)

of the BLUP parameter set for representing the acoustics of thin sediment areas are discussed.

TABLE OF CONTENTS

		Page
	LIST OF FIGURES	v
I.	INTRODUCTION	1
II.	BLUP GEOACOUSTIC PROFILE	5
III.	METHOD USED TO OBTAIN THE BLUP PARAMETERS	8
IV.	THE ONE-BOUNCE BOTTOM LOSS MEASUREMENT SIMULATOR	15
V.	PATTERNS IN THE COMPARISON OF BLUP PREDICTED AND NADC MEASURED BOTTOM LOSS	27
	A. Type 1	27
	B. Type 2	29
	C. Type 3	30
	D. Type 4	30
VI.	RESULTS	33
	A. Location 1	36
	B. Location 2	39
	C. Location 3	42
	D. Location 4	45
	E. Location 5	48
	F. Location 6	51
	G. Location 7	54
	H. Location 8	57
	I. Location 9	60
	J. Location 10	63
	K. Location 11	66
	L. Location 12	69
	M. Location 13	72
	N. Location 14	75

	Page
O. Location 15	78
P. Location 16	81
Q. Location 17	84
S. Location 19	90
T. Location 20-24 and 26-29	93
U. Location 25	114
V. Location 30	117
W. Location 31	120
VII. DISCUSSION	123
VIII. SUMMARY	129
ACKNOWLEDGMENTS	131
REFERENCES	133

LIST OF FIGURES

Figure		Page
1	Geometric and Sound Velocity Structure of BLUP Geoacoustic Model	6
2	NADC Eastern Pacific Data Collection Regions	11
3	Original NADC Data for Location 1	12
4	Smoothed NADC Data for Location 1	13
5	Relationship Between Critical Angle θ_c and Bottom Loss Curve	18
6	Reflection and Transmission Coefficients for the Three Ray Classes	24
7	Problem Types Associated with Fitting BLUP Model to NADC Pacific Data	28
	Octave Averaged Bottom Loss Predicted by Bottom Loss Upgrade Geoacoustic Profile versus NADC Bottom Loss Data at Location 1	37
	Difference Between BLUP Predicted Bottom Loss and NADC Data at Location 1	38
	Octave Averaged Bottom Loss Predicted by Bottom Loss Upgrade Geoacoustic Profile versus NADC Bottom Loss Data at Location 2	40
	Difference Between BLUP Predicted Bottom Loss and NADC Data at Location 2	41
	Octave Averaged Bottom Loss Predicted by Bottom Loss Upgrade Geoacoustic Profile versus NADC Bottom Loss Data at Location 3	43
	Difference Between BLUP Predicted Bottom Loss and NADC Data at Location 3	44

Figure		Page

Octave Averaged Bottom Loss Predicted by Bottom Loss Upgrade Geoacoustic Profile versus NADC Bottom Loss Data at Location 4 ... 46

Difference Between BLUP Predicted Bottom Loss and NADC Data at Location 4 ... 47

Octave Averaged Bottom Loss Predicted by Bottom Loss Upgrade Geoacoustic Profile versus NADC Bottom Loss Data at Location 5 ... 49

Difference Between BLUP Predicted Bottom Loss and NADC Data at Location 5 ... 50

Octave Averaged Bottom Loss Predicted by Bottom Loss Upgrade Geoacoustic Profile versus NADC Bottom Loss Data at Location 6 ... 52

Difference Between BLUP Predicted Bottom Loss and NADC Data at Location 6 ... 53

Octave Averaged Bottom Loss Predicted by Bottom Loss Upgrade Geoacoustic Profile versus NADC Bottom Loss Data at Location 7 ... 55

Difference Between BLUP Predicted Bottom Loss and NADC Data at Location 7 ... 56

Octave Averaged Bottom Loss Predicted by Bottom Loss Upgrade Geoacoustic Profile versus NADC Bottom Loss Data at Location 8 ... 58

Difference Between BLUP Predicted Bottom Loss and NADC Data at Location 8 ... 59

Octave Averaged Bottom Loss Predicted by Bottom Loss Upgrade Geoacoustic Profile versus NADC Bottom Loss Data at Location 9 ... 61

Difference Between BLUP Predicted Bottom Loss and NADC Data at Location 9 ... 62

Octave Averaged Bottom Loss Predicted by Bottom Loss Upgrade Geoacoustic Profile versus NADC Bottom Loss Data at Location 10 ... 64

Difference Between BLUP Predicted Bottom Loss and NADC Data at Location 10 ... 65

Figure		Page
	Octave Averaged Bottom Loss Predicted by Bottom Loss Upgrade Geoacoustic Profile versus NADC Bottom Loss Data at Location 11	67
	Difference Between BLUP Predicted Bottom Loss and NADC Data at Location 11	68
	Octave Averaged Bottom Loss Predicted by Bottom Loss Upgrade Geoacoustic Profile versus NADC Bottom Loss Data at Location 12	70
	Difference Between BLUP Predicted Bottom Loss and NADC Data at Location 12	71
	Octave Averaged Bottom Loss Predicted by Bottom Loss Upgrade Geoacoustic Profile versus NADC Bottom Loss Data at Location 13	73
	Difference Between BLUP Predicted Bottom Loss and NADC Data at Location 13	74
	Octave Averaged Bottom Loss Predicted by Bottom Loss Upgrade Geoacoustic Profile versus NADC Bottom Loss Data at Location 14	76
	Difference Between BLUP Predicted Bottom Loss and NADC Data at Location 14	77
	Octave Averaged Bottom Loss Predicted by Bottom Loss Upgrade Geoacoustic Profile versus NADC Bottom Loss Data at Location 15	79
	Difference Between BLUP Predicted Bottom Loss and NADC Data at Location 15	80
	Octave Averaged Bottom Loss Predicted by Bottom Loss Upgrade Geoacoustic Profile versus NADC Bottom Loss Data at Location 16	82
	Difference Between BLUP Predicted Bottom Loss and NADC Data at Location 16	83
	Octave Averaged Bottom Loss Predicted by Bottom Loss Upgrade Geoacoustic Profile versus NADC Bottom Loss Data at Location 17	85
	Difference Between BLUP Predicted Bottom Loss and NADC Data at Location 17	86

Figure		Page
	Octave Averaged Bottom Loss Predicted by Bottom Loss Upgrade Geoacoustic Profile versus NADC Bottom Loss Data at Location 18	88
	Difference Between BLUP Predicted Bottom Loss and NADC Data at Location 18	89
	Octave Averaged Bottom Loss Predicted by Bottom Loss Upgrade Geoacoustic Profile versus NADC Bottom Loss Data at Location 19	91
	Difference Between BLUP Predicted Bottom Loss and NADC Data at Location 19	92
	Octave Averaged Bottom Loss Predicted by Bottom Loss Upgrade Geoacoustic Profile versus NADC Bottom Loss Data at Location 20	96
	Difference Between BLUP Predicted Bottom Loss and NADC Data at Location 20	97
	Octave Averaged Bottom Loss Predicted by Bottom Loss Upgrade Geoacoustic Profile versus NADC Bottom Loss Data at Location 21	98
	Difference Between BLUP Predicted Bottom Loss and NADC Data at Location 21	99
	Octave Averaged Bottom Loss Predicted by Bottom Loss Upgrade Geoacoustic Profile versus NADC Bottom Loss Data at Location 22	100
	Difference Between BLUP Predicted Bottom Loss and NADC Data at Location 22	101
	Octave Averaged Bottom Loss Predicted by Bottom Loss Upgrade Geoacoustic Profile versus NADC Bottom Loss Data at Location 23	102
	Difference Between BLUP Predicted Bottom Loss and NADC Data at Location 23	103
	Octave Averaged Bottom Loss Predicted by Bottom Loss Upgrade Geoacoustic Profile versus NADC Bottom Loss Data at Location 24	104
	Difference Between BLUP Predicted Bottom Loss and NADC Data at Location 24	105

Figure		Page
	Octave Average Bottom Loss Predicted by Bottom Loss Upgrade Geoacoustic Profile versus NADC Bottom Loss Data at Location 26	106
	Difference Between BLUP Predicted Bottom Loss and NADC Data at Location 26	107
	Octave Averaged Bottom Loss Predicted by Bottom Loss Upgrade Geoacoustic Profile versus NADC Bottom Loss Data at Location 27	108
	Difference Between BLUP Predicted Bottom Loss and NADC Data at Location 27	109
	Octave Averaged Bottom Loss Predicted by Bottom Loss Upgrade Geoacoustic Profile versus NADC Bottom Loss Data at Location 28	110
	Difference Between BLUP Predicted Bottom Loss and NADC Data at Location 28	111
	Octave Averaged Bottom Loss Predicted by Bottom Loss Upgrade Geoacoustic Profile versus NADC Bottom Loss Data at Location 29	112
	Difference Between BLUP Predicted Bottom Loss and NADC Data at Location 29	113
	Octave Averaged Bottom Loss Predicted by Bottom Loss Upgrade Geoacoustic Profile versus NADC Bottom Loss Data at Location 25	115
	Difference Between BLUP Predicted Bottom Loss and NADC Data at Location 25	116
	Octave Average Bottom Loss Predicted by Bottom Loss Upgrade Geoacoustic Profile versus NADC Bottom Loss Data at Location 30	118
	Difference Between BLUP Predicted Bottom Loss and NADC Data at Location 30	119
	Octave Averaged Bottom Loss Predicted by Bottom Loss Upgrade Geoacoustic Profile versus NADC Bottom Loss Data at Location 31	121
	Difference Between BLUP Predicted Bottom Loss and NADC Data at Location 31	122

Figure		Page
8	Comparison of BLUP Predicted to Measured Bottom Loss at Location 8 for Sediment Thicknesses of 20, 40, 60 and 80 m	126

I. INTRODUCTION

The objective of the Bottom Loss Upgrade Program (BLUP), co-sponsored by the NORDA SEAS and TAEAS programs, is to increase the accuracy of low frequency acoustic predictions made by Fleet Numerical Oceanographic Center (FNOC) through an improved treatment of the acoustic interaction with the ocean floor. This objective is being achieved by replacing the limited set of bottom loss classes by a database containing a simplified set of geoacoustic parameters describing the ocean floor. Use of the BLUP database with suitably modified FNOC software will allow more accurate modeling of the effect of the ocean floor on both the amplitude and phase of the acoustic signal. The BLUP database will allow more detailed dependence on frequency, grazing angle, and location than is currently possible.

The geoacoustic profile is now generally accepted as the most flexible and useful means of characterizing the interaction of sound with the seafloor. Given the complete geoacoustic profile (the depth dependent density, velocity, and attenuation structure of the seafloor), it is theoretically possible to accurately predict bottom interaction effects on acoustic propagation. In practice it may not be possible or even necessary to determine the complete geoacoustic profile. The profile contained in the BLUP database is a simplified profile which, on the basis of recent research, is valid at low frequencies in many areas of the world.

The BLUP geoacoustic profile is based on recent research that has developed an understanding of the major processes governing low frequency bottom loss in areas of thick sediment cover in deep water environments. The successful analysis and interpretation of data from the BEARING STAKE exercise suggested a fairly simple geoacoustic profile containing the surficial sediment density and the depth dependent compressional wave velocity and attenuation. Results from the NAVELEX 612 Bottom Interaction Program have provided a firm theoretical foundation for the use of this profile at low frequencies in areas of thick, unlayered sediment cover by showing that complications due to shear wave excitation in the sediment, roughness of the sediment surface, density gradients in the sediment, and the properties of the substrate can be neglected. Other work from the Bottom Interaction Program to establish values and relations among geoacoustic parameters has successfully provided estimates of these parameters, consistent with those obtained from data analysis, and acceptable ranges for their values. With the exception of the surface layer and the substrate reflectivity parameter, the BLUP profile is based on this scientific foundation.

The initial values of BLUP geoacoustic parameters are based on analysis of Naval Air Development Center (NADC) bottom loss data, available information on sediment type and structure, and established empirical relationships between sediment parameters. It is expected that these initial parameter values will be changed as new acoustic data becomes available for analysis. The number and kind of geoacoustic parameters used in the BLUP profile are also expected to change in response to new research results which will allow more complex bottom structures and higher frequencies to be treated accurately.

As a result of the work carried out at Applied Research Laboratories, The University of Texas at Austin (ARL:UT), one of the now recognized deficiencies of the simplified BLUP profile is its inability to accurately represent the low frequency acoustics of areas with thin sediment cover. In particular, the effects of sediment shear wave excitation, interaction with the basalt substrate, and scattering from the rough basement are not modeled in a realistic fashion by the initial BLUP parameter set. They are currently included through a basement reflectivity factor which is assumed to be independent of frequency and grazing angle.

During FY 81, ARL:UT carried out a study of the use of the restricted BLUP geoacoustic parameter set to describe bottom loss in thin sediment areas in the Northeastern Pacific. This study had two major goals. The first was to develop BLUP parameter sets for NADC locations in the Pacific. These parameter sets served as part of the input data for use by Science Applications, Inc. (SAI), in their determination of the actual BLUP parameters for some areas in the Pacific for use in the initial version of the BLUP database for FNOC use. The second goal of these studies was to evaluate potential problems with using the BLUP parameter set in thin sediment areas.

This report presents the results of the ARL:UT study of the use of the initial BLUP parameter set in the thin sediment areas of the Northeastern Pacific. The acoustic data used in this study is NADC measured bottom loss at 31 locations in the Northeastern Pacific. The analysis relied on comparing measured bottom loss with bottom loss predicted by a ray theory simulator of the NADC measurement and analysis procedure. To obtain the best fit to the data, BLUP geoacoustic parameter values were changed but kept within accepted geophysical ranges. The difference between the best fit prediction and the data was analyzed at each location to determine the quality of the BLUP-based prediction.

This analysis resulted in the conclusion that the initial BLUP geoacoustic parameter set does not contain the parameters necessary to accurately predict bottom loss in thin sediment areas. This conclusion is based on the poor fits obtained for at least half of the 31 NADC sites analyzed. These poor fits are to be contrasted with the generally good fits to NADC data that can be obtained in areas of thick sediment cover for which the major physical mechanisms governing bottom interaction are now well understood and in fact form the basis for the BLUP parameter set. However, for thin sediments found in vast areas of the Pacific, a large portion of the incident energy interacts with a rough substrate, an interaction that has little importance in thick sediment areas. While shear wave generation at the substrate has been studied and can be modeled, scattering from the rough substrate is not well understood and cannot be included at this time in the BLUP parameter set. Uncertainties in sediment thickness in areas of thin sediment cover also play a role in the inadequacy of the BLUP parameter set.

The remainder of this report is organized as follows. Section II discusses the BLUP geoacoustic profile. Section III discusses the NADC data set used in this study and the procedure used to obtain the BLUP parameters from the data. Section IV presents the details of the ARL:UT bottom loss measurement simulator. Section V classifies and discusses patterns of the deficiencies in the fit of BLUP predicted bottom loss to the NADC data. Section VI contains the BLUP parameters giving the best fit to NADC data at each location and graphical comparisons of BLUP predicted and measured bottom loss. A discussion of the quality of the fit is given. Section VII presents a discussion of the deficiencies in the comparison of BLUP predicted and NADC measured bottom loss. Conclusions and suggestions for improvement are summarized in Section VII.

II. BLUP GEOACOUSTIC PROFILE

Figure 1 illustrates some features of the BLUP geoacoustic profile. The profile consists of a single fluid sediment layer overlying a flat substrate with the option to place a thin, isovelocity, surface layer (approximately 1 m thick) over the sediment. The profile represents the structure of the substrate by a reflection coefficient for the sediment-substrate interface that is independent of grazing angle and frequency. The sediment attenuation profile is linear with depth and the sediment density is a constant. The sediment sound velocity structure is given by the following formula:

$$C(z) = \sqrt{C_1^2(1+\beta)^2 + 2G(1+\beta)C_1 z} - \beta C_1 \quad ,$$

where C_1 is the surficial sediment sound velocity. The BLUP attenuation profile has a constant gradient and is given by $\alpha(z)=\alpha_o+\gamma z$. The parameters β, G, α_o, and γ are described below in the list of the BLUP parameters.

A total of nine parameters are used at this time to define the BLUP geoacoustic profile.

(1) R surficial sediment to bottom water velocity ratio
(2) ρ_2 surface layer density
(3) ρ_3 sediment density
(4) D thickness of surface layer
(5) G gradient of sound velocity at sediment surface
(6) β curvature parameter in BLUP sound velocity profile
(7) α_o sediment attenuation at sediment surface
(8) γ gradient of sediment attenuation
(9) R_{sub} the constant substrate reflectivity

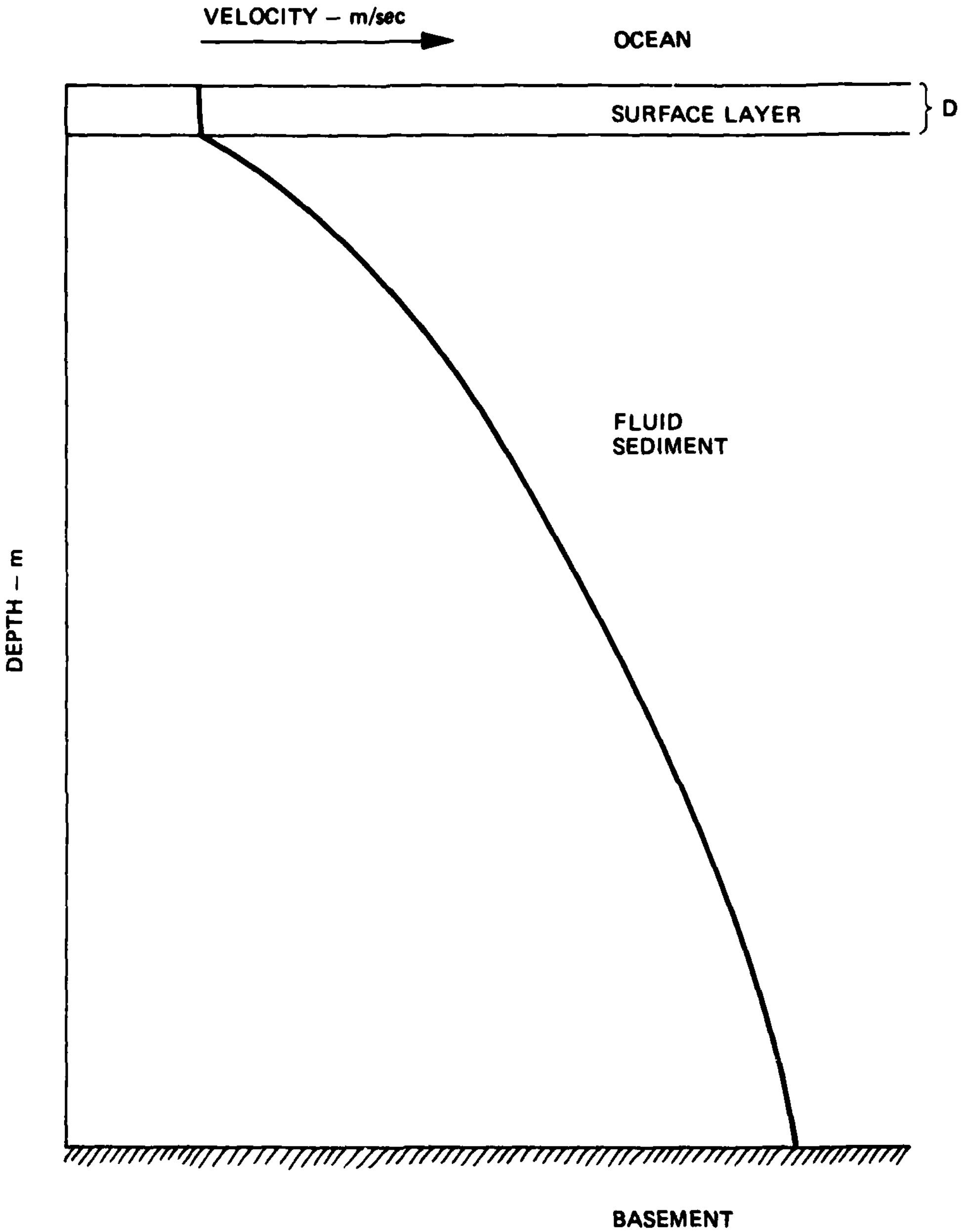

FIGURE 1
GEOMETRIC AND SOUND VELOCITY STRUCTURE
OF BLUP GEOACOUSTIC MODEL

ARL:UT
AS-82-336
DPK-GA
3-29-82

The BLUP geoacoustic profile is based on recent research that has developed an understanding of the major processes governing low frequency bottom loss in areas of thick sediment cover in deep water environments. The successful analysis and interpretation of data from the BEARING STAKE[1-3] exercise suggested a fairly simple geoacoustic profile containing the surficial sediment density and the depth dependent compressional wave velocity and attenuation. Results from the NAVELEX 612 Bottom Interaction Program have provided a firm theoretical foundation for the use of this profile at low frequencies in areas of thick, unlayered sediment cover by showing that complications due to shear wave excitation in the sediment,[4-5] roughness of the sediment surface,[6] density gradients in the sediment,[7] and the properties of the substrate[8] can be neglected. Other work from the Bottom Interaction Program to establish values and relations among geoacoustic parameters[9] has successfully provided estimates of these parameters, consistent with those obtained from data analysis, and acceptable ranges for their values. With the exception of the surface layer and the substrate reflectivity parameter, the BLUP profile is based on this scientific foundation.

The surface layer was added to the BLUP profile to allow the modeling of the anomalous frequency dependence of high angle, high frequency loss in nominally thick sediment areas in the Atlantic.[10] NADC bottom loss data from these areas can have octave averaged bottom loss at 1600 Hz as low as 5 dB at high grazing angles. For these thick sediment areas, one would expect that any high frequency energy entering the sediment at high grazing angles would be completely absorbed in the sediment and would not return to the water column. Bottom loss would then be given by the reflection coefficient of the water-sediment interface. For the sediment types typical of these deep ocean areas, the expected bottom loss would be about 15 dB. To cope with this large discrepancy compared to the measured 5 dB loss, the BLUP geoacoustic profiles for these areas contain a nonphysical, thin, high density, surface layer to enhance the reflected energy. Two mechanisms have been identified as potential sources of the loss: (1) the presence of near-surface fine scale layering[11] and (2) the occurrence of hydrated marine sediments.[12] These two mechanisms have different physical origins and produce different effects on cw bottom loss. Since the actual mechanism leading to the anomalous reflectivity is not yet known, there is concern about the correct means for extrapolating these BLUP profiles geographically to define areas of similar properties and also about their utility in eventual cw predictions.

For thin sediment structures the bottom interaction process is more complex than that in thick sediment layers, requiring additional loss mechanisms which are not needed to describe thick sediments. Previous work has shown that sediment shear wave excitation at the substrate interface can be a dominant loss process in thin sediments.[6,7] Scattering from a rough surface from the substrate interface is possibly a major loss process, but is not understood well enough for modeling applications at this time.

For the purposes of this report, it is important to note that the entire interaction with the substrate, important in areas of thin sediment cover, is contained in the single parameter R_{sub}, the substrate reflectivity. In the initial version of BLUP, R_{sub} is a constant, independent of angle and frequency. This form is known to be physically unrealistic and serves as an interim description for thin sediment areas. One of the purposes of this work was to evaluate the effectiveness of this parameter. At this time, R_{sub} is at best an empirical parameter used to fit the NADC data and has no clear relation to actual subbottom parameters. In improved versions of the BLUP database, it is hoped that R_{sub} can be replaced by geoacoustic parameters related to understood physical processes. Such a goal is worthwhile since only then will acoustic predictions in thin sediment areas be made with confidence.

III. METHOD USED TO OBTAIN THE BLUP PARAMETERS

This section describes the procedure used by ARL:UT to obtain the BLUP parameters for a given location. First is a discussion of how the NADC data were converted into the form used in this study. Next, a skeleton description of the procedure used to find the parameters is presented. A brief discussion of how initial estimates of the parameters were obtained precedes a more detailed account of the selection of the individual parameters.

The NADC bottom loss data set was the primary acoustic resource used in determining the BLUP geoacoustic profile parameter values. The limitations of this data set, its advantages, and its choice for use in the BLUP project are discussed in detail elsewhere.[10] Briefly, the NADC data are the result of a survey-like effort to acquire bottom loss data in support of air deployed sensor design. The NADC data provide wide geographic coverage, and up to 300 estimates of bottom loss at different grazing angles and frequencies at each measurement site. The principal limitations of the data are the accuracy of the reconstructed geometry and the measured signal levels. The inaccurate geometry does not lead to significant error in computed propagation loss but does prohibit correcting for image-interference effects at low frequencies and low angles. Hydrophone calibration errors have been observed, but their effects are usually reduced by taking the median value of the data in angle bins. The NADC data represent a significant resource which can be useful to the BLUP program provided that its limitations are recognized and attention given to using those aspects of the data that are reliable.

NADC reported octave averaged bottom loss versus grazing angle (0^o-90^o) data for 17 center frequencies including 50, 100, 200, 400, 800, and 1600 Hz at 31 locations within the region indicated in Fig. 2. The NADC data gives bottom loss values for each location, frequency, grazing angle, and the number of bottom bounces. The bottom bounce number ranges from 1 to 3. A typical example of the data is shown in Fig. 3. where the numbers on the graph represent the bottom bounce number. Also available are sound velocity profiles and the source and receiver depths.

This study used a smoothed version of the raw NADC data. The smoothing procedure is discussed in detail elsewhere.[13] Briefly, the procedure is outlined as follows. First, the data points were separated into grazing angle bins 2^o wide. The median bottom loss for each bounce number was then found. A weighting factor was assigned to each median value in accordance with its bottom bounce number: one to a one-bounce point, two to a two-bounce point, and three to a three-bounce point. A weighted average median bottom loss was then calculated for each bin. This weighting tends to minimize certain types of errors. With the grazing angle defined as the angle in the middle of the bin, a smoothed bottom loss versus grazing angle curve was constructed. Figure 4 shows the smoothed version of Fig. 3.

The method used by ARL:UT for finding the BLUP parameters for a given location had several steps. The first step was to construct an initial estimate for the parameter values. Then, a ray simulator of the NADC measurement and processing process, structured to use the BLUP profile, generated bottom loss curves for each frequency. In accordance with NADC processing procedures, bottom loss is defined here as the octave averaged transmission loss for rays within the water-sediment-substrate environment relative to a reference incoherent transmission loss for rays perfectly reflected from the sediment surface. The generated bottom loss curves are then compared to the NADC data. After adjusting the values for the parameters within reasonable geological limits to produce a better fit to the data, a second set of curves is

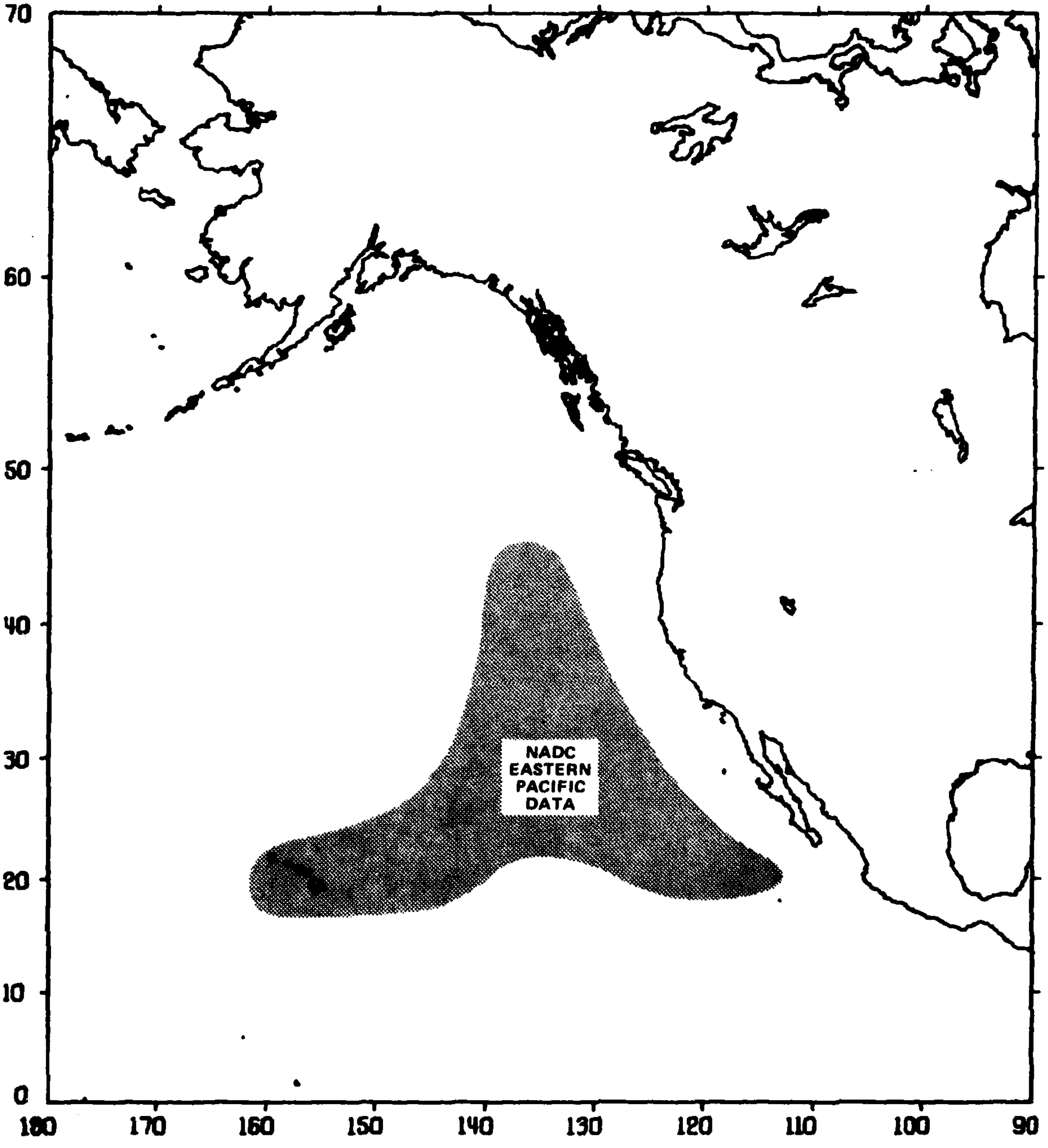

FIGURE 2
(U) NADC EASTERN PACIFIC DATA COLLECTION REGION

ARL:UT
AS-80-1375
JFL - GA
7 - 24 - 80

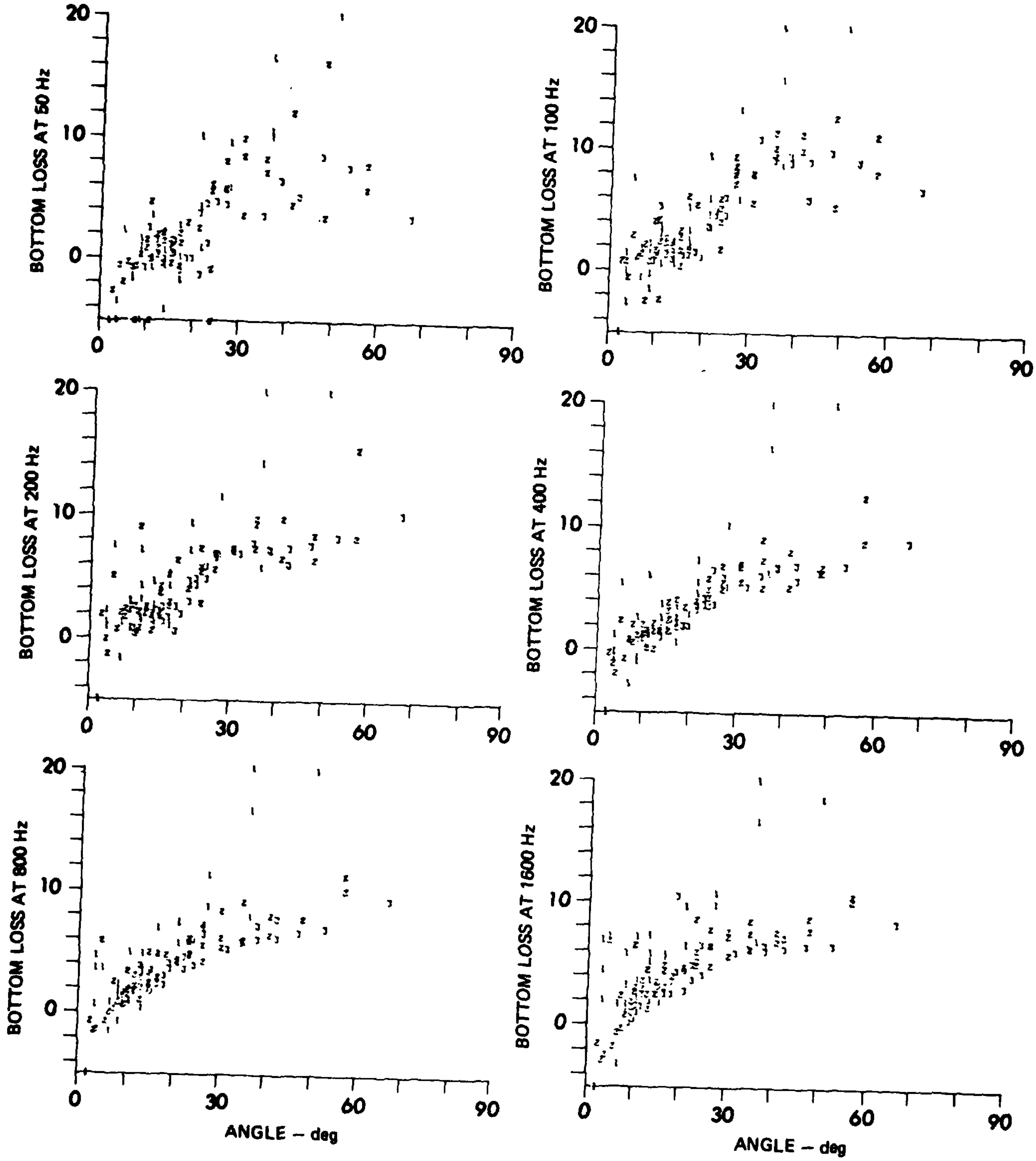

FIGURE 3
ORIGINAL NADC DATA FOR LOCATION 1

ARL:UT
AS-82-336
DPK - GA
3 - 29 - 82

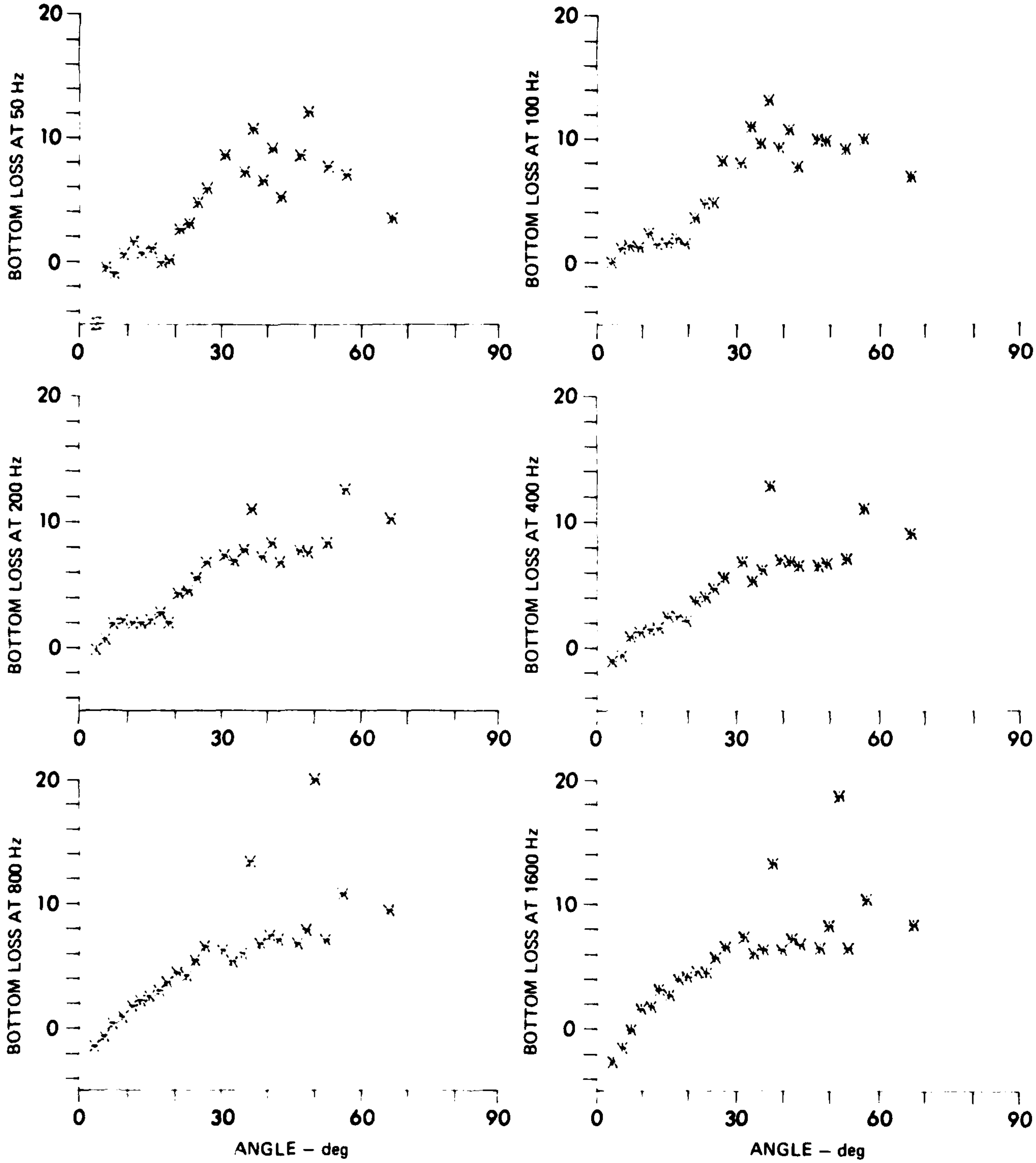

ARL:UT
AS-82-337
DPK - GA
3 - 29 - 82

FIGURE 4
SMOOTHED NADC DATA FOR LOCATION 1

produced and also compared to the data. This process is repeated until the best fit to the data is found. The best overall fit in frequency and grazing angle was determined by an "eyeball average." The major assumption in this procedure is that the BLUP parameters are those parameters that correspond to the best fit to the data.

The sources of information used to construct initial estimates for the BLUP parameters are E. L. Hamilton's work[9] concerning ocean geoacoustic parameters, results of the Deep Sea Drilling Project (DSDP), and oceanographic maps supplied by the U.S. Naval Oceanographic Office. Hamilton's paper provides average values of velocity ratios, sediment densities, surface sediment attenuation, and sound speed gradients for various geological environments. DSDP data provides information on types of sediments and sediment thicknesses at locations near some NADC sites. Oceanographic maps supply information concerning surface sediment types, physiographic provinces, sediment thicknesses, and surficial sediment velocities.

The first step in constructing initial estimates for a BLUP geoacoustic profile is to identify the sediment type. The NADC data used in this report comes from an area classified as an abyssal hill environment. The sediment in this region is classified as deep sea ("red") pelagic clay which comes in three types according to decreasing grain size: clayey silt, silty clay, and clay.

Even though sediment thickness is not a BLUP geoacoustic profile parameter, all geoacoustic modeling of the ocean floor needs this important parameter. Our region of interest has thin sediment cover ranging from 0 to 160 m overlying a basaltic substrate. Sediment thickness for each location can be obtained from two-way travel time maps. Unfortunately, these maps have a resolution of only ± 80 m. The bottom loss data itself provided a finer estimate of the thickness for some locations. For a few locations, these estimated thicknesses differed significantly from those indicated on maps.

The BLUP parameters can be separated into two groups: normal and abnormal. The abnormal parameters are those not directly related to subbottom geoacoustic features. They are the thickness and density of the thin surface layer and the substrate reflectivity. The substrate reflectivity is included in this group because of its non-physical description of the acoustic interaction with the substrate. The normal group contains the remaining BLUP parameters which are directly associated with the physical and acoustical properties of the sediment. Although it is certainly possible to have a thin, near-surface layer physically present in a particular area, this layer in the BLUP model is normally used to represent the effects of a process as yet unknown. The layer parameters (thickness and density) are chosen to fit the bottom loss data at high frequencies. Similarly, a constant reflection loss at the basement may be a reasonable method for dealing with substrate scattering loss. The way this method is implemented in BLUP leads to non-physical aspects.

Below is a description of how each BLUP parameter for a given location was obtained.

1. R, the surficial sediment to bottom water velocity ratio:

Table I contains average values provided by Hamilton[2] for velocity ratios for the various types of ocean geographic environments. The range of values for R in the abyssal hill environment is from 0.976 to 0.995. In our study the higher value of R was used at some locations to decrease the impedance contrast of the water-sediment interface. This allows more energy to enter the sediment. The lower value of R was used for the opposite effect, namely to increase the reflection coefficient at the interface, which decreases the influence of the sediment-substrate environment.

2. β, curvature parameter in BLUP sediment sound velocity profile:

The BLUP velocity increases approximately linearly with depth for the first 200 m for geologically reasonable values[10] of β between

TABLE I

ABYSSAL PLAIN AND ABYSSAL HILL ENVIRONMENTS; SEDIMENT DENSITIES, POROSITIES, SOUND VELOCITIES, AND VELOCITY RATIOS*

Environment	Density[a] (g/cm^3)		Porosity[a] (%)		Velocity[a] (m/s)		Velocity Ratio[a]	
Sediment Type	Av	SE	Av	SE	Av	SE	Av	SE
Abyssal Plain								
Clayey silt	1.454	0.022	74.2	1.58	1528	3	0.999	0.002
Silty clay	1.348	0.014	80.5	0.98	1515	2	0.991	0.001
Clay	1.352	0.037	80.0	2.20	1503	2	0.983	0.001
Bering Sea and Okhotsk Sea (siliceous-diatomaceous)								
Silt	1.447	...	70.8	...	1546	...	1.011	...
Clayey silt	1.228	0.019	85.8	0.86	1534	2	1.003	0.001
Silty clay	1.214	0.008	86.8	0.43	1525	2	0.997	0.001
Abyssal hill								
Deep-sea ("red") pelagic clay								
Clayey silt	1.347	0.020	81.3	0.95	1522	3	0.995	0.002
Silty clay	1.344	0.011	81.2	0.60	1508	2	0.986	0.001
Clay	1.414	0.012	77.7	0.64	1493	1	0.976	0.001
Calcareous pelagic sediment								
Sand-silt-clay	1.435	0.007	75.3	0.38	1556	2	1.017	0.001
Silt-clay	1.404	0.011	76.9	0.64	1536	1	1.004	0.001

[a]Laboratory values: 23°C, 1 atm pressure; density: Saturated bulk density; porosity: Salt free; velocity ratio: Velocity in sediment/velocity in sea water at 23°C, 1 atm, and salinity of sediment pore water; SE: Standard error of the mean.

*Taken from: E. L. Hamilton, "Geoacoustic Modeling of the Sea Floor", J. Acoust. Soc. Am., 68, 1313-1340 (1980).

± 1. Since the largest sediment thickness at the 31 locations analyzed for this report was about 150 m, the value of β is not important. Rather, the near-surface gradient determines the profile. Hence, in our analysis, we have set $\beta=0$ for all 31 locations.

3. G, the gradient term in BLUP sediment sound velocity profile:

The term G represents the surficial sound speed gradient. The values of G used in this report range from 0.9 to 1.275 sec^{-1}. The value of G was estimated using the following reasoning. Figure 5 exhibits a typical bottom loss versus grazing angle curve along with a ray diagram. Here the critical angle θ_c is defined as the lowest grazing angle for which the ray strikes the substrate. The ray associated with θ_c is the one with the longest path length through the sediment. For angles greater than θ_c, the path length through the sediment becomes shorter. This causes a decrease in the absorption which in turn causes a decrease in the predicted bottom loss. The simulator gives each ray that interacts with the substrate the <u>same</u> reflection coefficient R_{sub}. Thus, excluding the effects of a surface layer, the BLUP profile predicts an increasing bottom loss followed by a decreasing bottom loss where the peak loss corresponds to the ray for which $\theta=\theta_c$. A fair amount of Pacific data exhibits this phenomenon. This form of BLUP predictions is especially pronounced for 800 and 1600 Hz since the absorption is proportional to the frequency. This property of the data was used to obtain G from an estimate of θ_c. Since the bottom water velocity is a known quantity, one can use Snell's law to find the bottom sediment velocity. Sediment thickness data obtained from a map then allows one to determine G by dividing the velocity change by the thickness.

4. D and ρ_2, thickness and density of surface layer:

A surface layer parameter is used when the measured bottom loss for the higher frequencies is lower than the bottom loss predicted by expected attenuation and reflection coefficients.[10] The surface

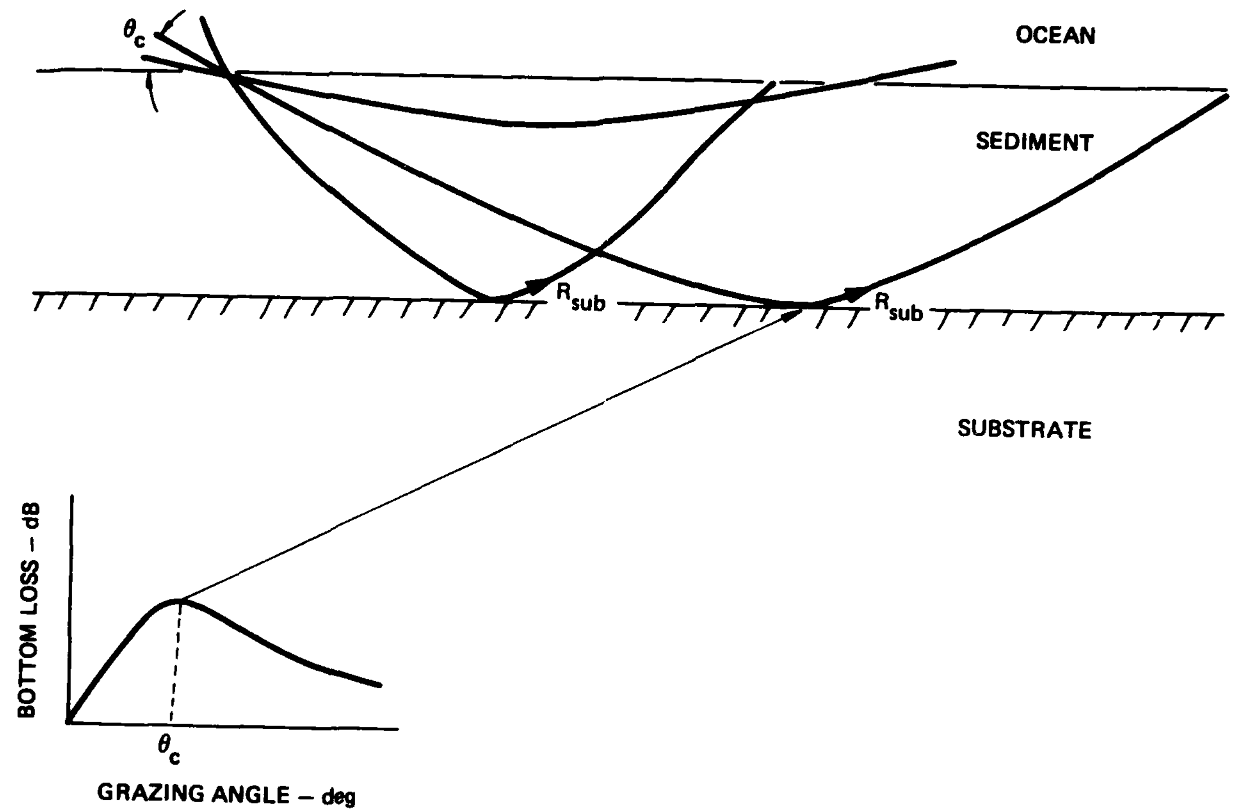

FIGURE 5
RELATIONSHIP BETWEEN CRITICAL ANGLE θ_c AND BOTTOM LOSS CURVE

ARL:UT
AS-82-338
DPK - GA
3 - 29 - 82

layer acts to reflect the energy of the higher frequencies causing a decrease in bottom loss. Atlantic data exhibits this phenomenon most vividly. The use of a surface layer parameter in the analysis of the Pacific data was held to a minimum. Its major use came in attempting to model an area north of the Hawaiian Islands. The values of D and ρ_2 are empirical, determined by fitting the data, and at this time have no clear relationship to physical properties of the sediment.

5. R_{sub}, the substrate reflectivity:

The general method used to obtain this parameter is to examine the bottom loss for high angles at 50 Hz. The important loss mechanisms here are those associated with the substrate. The bottom loss for the higher grazing angles at 50 Hz is turned into substrate reflectivity by the formula, substrate reflectivity = $10^{-BL/20}$. To better fit the higher frequencies, some cases involved use of a higher bottom loss or lower reflectivity than that corresponding to 50 Hz.

6. ρ_3, the sediment density:

Table I also provides some typical values for sediment density in the abyssal hills. These values range from 1.347 to 1.414 g/cc. The average value used here was 1.4; however, in a few locations values of 1.5 and 1.6 were used. The higher values were used to increase reflection at the water-sediment interface.

7. α_o, the sediment attenuation at surface:

Typical values noted by Hamilton for attenuation in clay sediments are 0.01-0.05 dB/m-kHz. The value used at all 31 NADC sites was approximately 0.015 dB/m-kHz. This value is in the lower part of the range given by Hamilton but agrees with recent measurements.[3]

8. <u>γ, the gradient of sediment attenuation</u>:

For geologically reasonable values, this parameter was found to have little influence on bottom loss for the thin sediment area studied. For most cases it was set equal to zero. In a few cases, however, it was found that introducing a small positive or negative gradient could slightly improve the fit to the data.

In summary, the values for BLUP geoacoustic parameters are determined by comparing measured bottom loss with bottom loss predicted by a measurement simulator which treats the bottom using the BLUP profile. Those parameter values found to give the best overall fit to the data are taken to be the BLUP parameters. The parameters fall into two categories, normal and abnormal. Normal parameters are defined as those directly related to the geoacoustic structure of the sediment. The values of these parameters are constrained to fall within accepted geological parameter ranges. Those parameters not intended to be related directly to the actual sediment structure are referred to as abnormal. These parameters include those of the surface layer and the substrate reflectivity. Abnormal parameters are adjusted to improve the comparison of the data and predictions.

IV. THE ONE-BOUNCE BOTTOM LOSS MEASUREMENT SIMULATOR

This section contains a description of the ray simulator which computes octave averaged bottom loss as a function of grazing angle for a given frequency.

Source receiver geometry along with a BLUP sediment sound velocity profile and the measured sound velocity structure of the water column are input to a ray trace computer program.[14] For each range the program finds eigenrays (rays connecting source and receiver) which reflect from the sediment and those that penetrate the sediment. Three classes of rays are found. The one-bounce eigenrays for the case of a perfectly reflecting water-sediment interface (no sediment penetration) are defined as class 1 rays. For complete sediment penetration, the rays characterized by one sediment refraction are called class 2 rays, and the rays which bounce off the substrate once are referred to as class 3 rays.

There are normally four eigenrays (multipaths) associated with each ray class for a given source and receiver geometry. For an isovelocity sound velocity profile there are always four eigenrays. However, for typically measured deep water profiles (especially those with a surface duct) there may be more than four rays.

Each of the eigenrays for a given class is characterized by a pressure amplitude, a frequency independent phase change, a travel time, a horizontal phase velocity, and a grazing angle at the water-sediment interface. The pressure at 1 m from the source is used as a reference pressure.

Now we describe the calculation of the octave averaged coherent transmission loss. Bottom loss is defined as the difference between the measured one-bounce transmission loss and a reference one-bounce transmission loss computed using a perfectly reflecting seafloor. In accordance with the NADC analysis procedure, the reference loss is the incoherent sum of the intensities of the individual class 1 eigenrays. This incoherent reference introduces artifacts into the reported bottom loss data. These artifacts, such as a negative bottom loss, are most important at low angles and at low frequencies.

The total pressure field is

$$P = \sum_j p_j \, Q_j(\omega) \, e^{i\phi_j} \, e^{i\omega t_j} \, e^{-\omega A_j} \quad ,$$

where the sum is over all the rays within the water-sediment environments; i.e., sum over all class 1, class 2, and class 3 rays. In this expression the subscripts identify the particular ray. The term p_j is the pressure, ϕ_j is the frequency independent phase, t_j is the travel time, and ω is the angular frequency. The term Q_j represents the total effect of the reflection and transmission coefficients encountered by a ray. Since absorption within the sediment is proportional to frequency, the total attenuation along the ray path through the sediment is given by ωA_j, where

$$A_j = \frac{\ell n(10)}{2\pi 10000} \int_0^z \frac{\alpha(z')dz'}{\sqrt{1 - a_j^2 C^2(z')}} \quad ,$$

$\alpha(z)$ is the BLUP attenuation profile, $C(z)$ is the BLUP sound speed profile, and a_j is the Snell's law constant for the ray.

The Q_j are related to the interface reflection and transmission coefficients for fluid-fluid interfaces

$$r_{ij} = \frac{\rho_j C_j \sin\theta_i - \rho_i C_i \sin\theta_j}{\rho_j C_j \sin\theta_i + \rho_i C_i \sin\theta_j} \quad ,$$

and

$$t_{ij} = \left(\frac{2\rho_i}{\rho_j}\right) \frac{\rho_j C_j \sin\theta_i}{\rho_j C_j \sin\theta_i + \rho_i C_i \sin\theta_j} \quad .$$

In our geometry the subscript values of 1, 2, and 3 refer to the water, the surface layer, and the top of the sediment. Here, r_{ij} is the reflection coefficient, t_{ij} is the transmission coefficient, ρ_j is the density, C_j is the sound speed, and θ_j is the grazing angle.

The total reflection and transmission coefficients (R_{13} and T_{13}) for the surface layer are

$$R_{13} = \frac{r_{12} + r_{23}\, e^{2i\kappa_2 D}}{1 + r_{12} r_{23}\, e^{2i\kappa_2 D}}$$

and

$$T_{13} = \frac{t_{12} t_{23}\, e^{i\kappa_2 D}}{1 + r_{12} r_{23}\, e^{2i\kappa_2 D}} \quad ,$$

where

$$\kappa_2 = \frac{\omega}{C_2} \sin\theta_2 \quad .$$

For the situation in which no surface layer is used, D=0 and R_{13} and T_{13} reduce to r_{13} and t_{13}, the reflection and transmission coefficients of the water-sediment interface.

Figure 6 illustrates the three ray classes and the makeup of the Q_j for each ray class. The value of Q_j is given by

$$Q_j = \begin{cases} R_{13} & \text{for class 1 rays} \\ T_{13}\, T_{31} & \text{for class 2 rays} \\ T_{13}\, T_{31}\, R_{sub} & \text{for class 3 rays.} \end{cases}$$

The total one-bounce pressure field is used to form the coherent intensity, CI, through

$$CI = \sum_j \sum_k p_j p_k Q_j Q_k^*$$

$$\times e^{i(\phi_j - \phi_k)} e^{i\omega(t_j - t_k)} e^{-\omega(A_j + A_k)} \quad .$$

Here the asterisk denotes the complex conjugate. The octave average of CI is given by

$$OCI = \frac{1}{\omega_2 - \omega_1} \int_{\omega_1}^{\omega_2} d\omega \, CI$$

$$= \frac{1}{\omega_2 - \omega_1} \sum_j \sum_k p_j p_k \, e^{i(\phi_j - \phi_k)} I_{jk} \quad ,$$

where $\omega_1 = \omega_0/\sqrt{2}$, $\omega_2 = \omega_0\sqrt{2}$, ω_0 is the angular frequency for the octave band, and

$$I_{jk} = \int_{\omega_1}^{\omega_2} d\omega \, Q_j Q_k^* \, e^{\omega\chi} \quad .$$

Here $\chi = -(A_j + A_k) + i(t_j - t_k)$. The integral in I_{jk} is performed numerically in the ARL:UT measurement simulator.

The incoherent reference transmission loss is given by

$$ITL = -10 \log_{10} IC \quad ,$$

where IC is the frequency independent incoherent one-bounce intensity for class 1 rays evaluated for a perfectly reflecting sediment surface, i.e.,

$$IC = \sum_j p_j^2$$

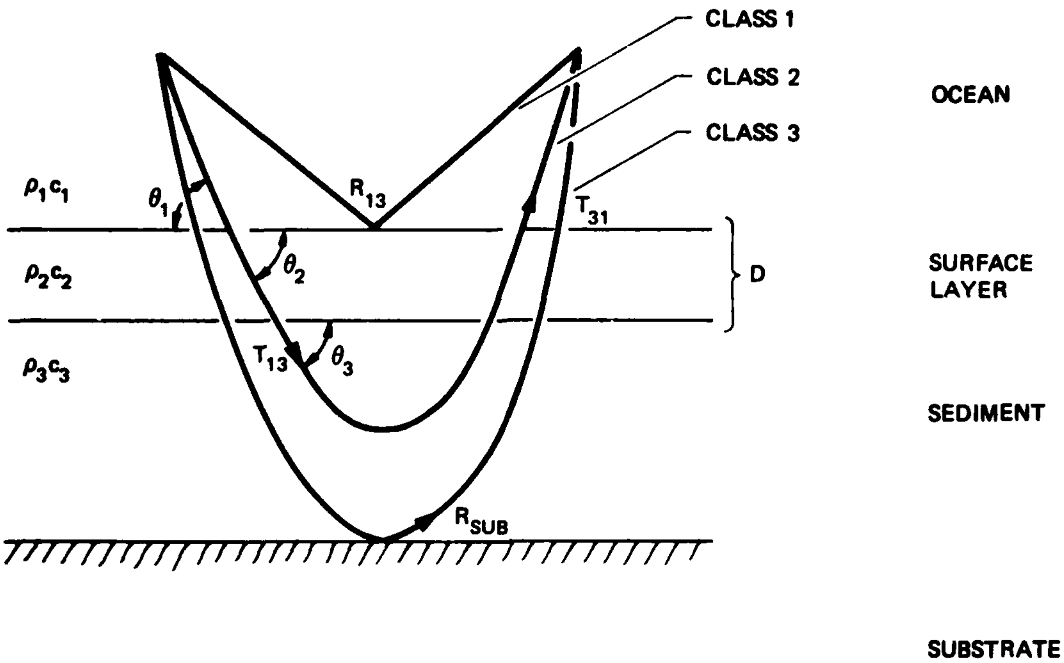

FIGURE 6
REFLECTION AND TRANSMISSION COEFFICIENTS
FOR THE THREE RAY CLASSES

ARL:UT
AS-82-339
DPK-GA
3-29-82

The simulator finally produces bottom loss defined as BL=CTL-ITL. The corresponding grazing angle is the average of the angles of the class 1 eigenrays with the water-sediment interface.

In summary, the ARL:UT bottom loss measurement simulator was designed to reproduce the measurement and analysis procedures used by NADC in their bottom loss measurements. The effects of water sound velocity profile, source and receiver geometry, BLUP format subbottom structure, and octave averaging are accurately treated by the simulator. The major assumptions embodied in the simulator are the use of ray theory to treat propagation and the BLUP profile to treat bottom interaction effects.

V. PATTERNS IN THE COMPARISON OF BLUP PREDICTED AND NADC MEASURED BOTTOM LOSS

The differences between BLUP predicted bottom loss and data for all 31 locations can be described by four problem types. The simple logic used is to divide angles into high and low regions. A "fuzzy" region about the critical angle separates the two regions. One problem type occurs when the model predictions fall below the data and another when the model predictions exceed the data. This occurs at both high and low angles. This simple approach categorizes the patterns observed in our analysis.

A. Type 1

Figure 7(a) illustrates problem type 1 which occurs when the predictions exceed the data for the lower grazing angles with a maximum difference occurring around θ_c. This problem type is usually associated with higher frequencies, i.e., 800 and 1600 Hz. It is related to the loss due to absorption along a ray path which increases linearly with frequency. As seen in Fig. 5, the longest path lengths are those near θ_c, which then produces a peak bottom loss near θ_c, particularly at high frequencies. In some cases this peak can be related to the grazing angle at which transmission into the sediment is a maximum. Whenever the data exhibits an absence of a pronounced bottom loss peak at high frequencies, problem type 1 will occur. This argument does not always hold when the thickness of the surface layer in the BLUP profile is on the order of a wavelength.

In general, it is difficult to remove type 1 problems by changing the BLUP parameter values without introducing problems at other frequencies and grazing angles. Decreasing the sediment attenuation causes the predictions to fall below the data for the higher grazing angles. Increasing the substrate reflectivity to correct the low

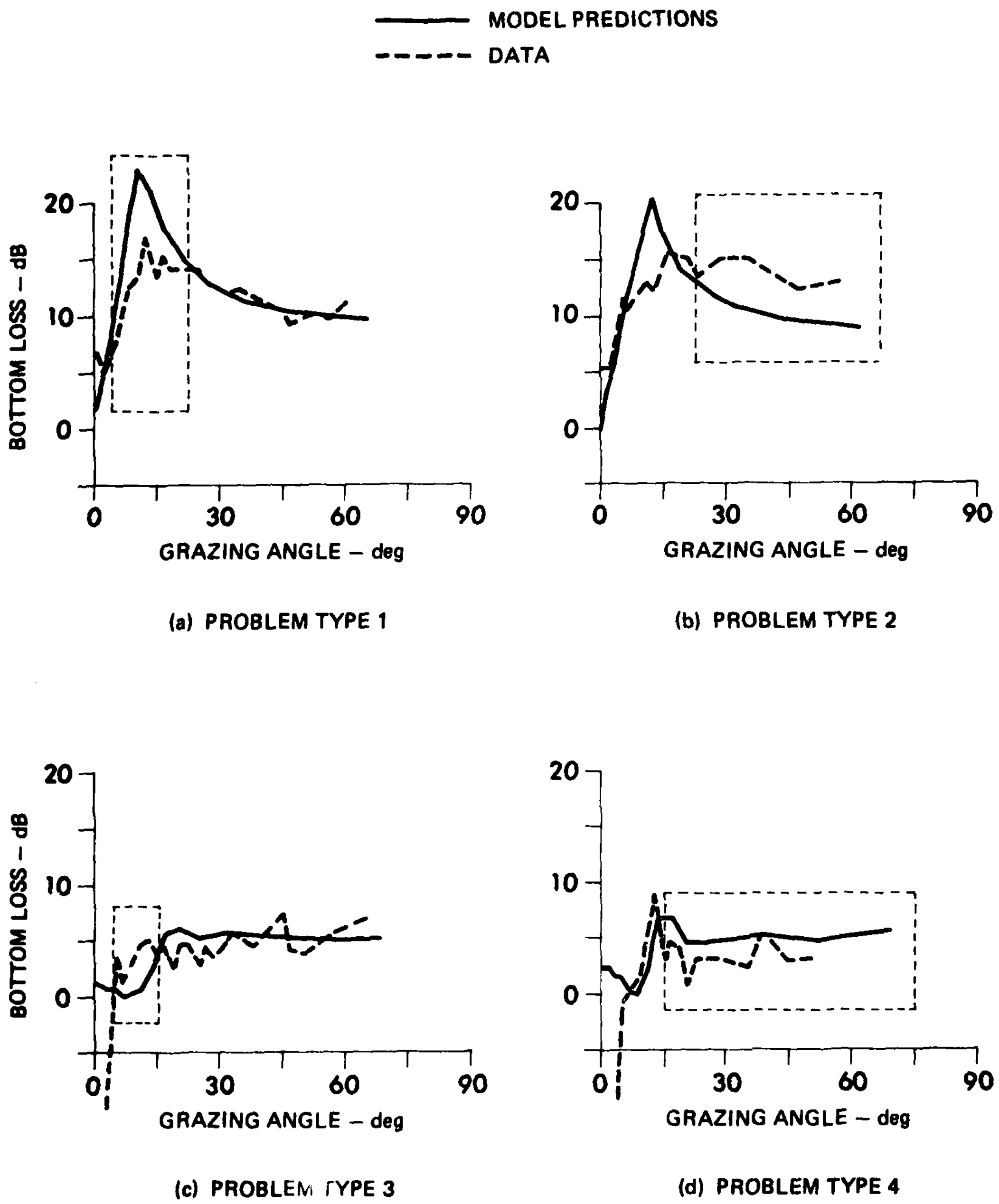

FIGURE 7
PROBLEM TYPES ASSOCIATED WITH FITTING BLUP MODEL TO NADC PACIFIC DATA

ARL:UT
AS-82-340
DPK - GA
3 - 29 - 82

grazing angle problem will worsen the high angle problem (see problem type 2). Since substrate reflectivity is independent of frequency and grazing angle, an increase in this parameter will decrease the model's bottom loss prediction for all angles for each frequency. Usually this action is undesirable. One can also attempt to correct the low angle problem by decreasing the transmission into the sediment by increasing the impedance difference at the water-sediment interface. This action has the effect of decreasing the bottom loss due to sediment absorption, which has the same effect as decreasing the sediment attenuation.

B. Type 2

Figure 7(b) illustrates problem type 2 which is characterized by the BLUP predictions falling below the data for the higher grazing angles. Problem type 2 usually occurs in combination with problem type 1. Whenever NADC data for 200, 400, 800, and 1600 Hz exhibits a lack of angular dependence or increase in loss at higher angles, problem type 2 occurs. This happens because the BLUP profile always predicts a decreasing bottom loss past θ_c due to the decrease in ray path length within the sediment. Again, as in problem type 1, the above argument does not hold when the thickness of the surface layer is on the order of a wavelength.

Attempts to remove type 2 problems in general lead to undesirable results. Increasing the sediment attenuation will increase the bottom loss for the higher grazing angles thus reducing the type 2 problem. Unfortunately, this action also causes an increase in bottom loss for the lower grazing angles for the high frequencies (800 and 1600 Hz) which usually creates or worsens a problem of type 1. Decreasing the substrate reflectivity can also be used to raise the predicted bottom loss for the higher grazing angles. This action also raises the bottom loss for all the frequencies at all the grazing angles by the same amount, usually leading to problems at lower frequencies. One can also raise the bottom loss predictions for the higher angles by increasing the transmission into the sediment. This can be accomplished by adjusting the impedance at the water-sediment interface. An increased transmission into the sediment means an increase in bottom loss due to sediment attenuation. While correcting problem type 2 this action will, however, again create or worsen a problem of type 1.

C. Type 3

Figure 7(c) illustrates problem type 3 which occurs when the BLUP predictions fall below the data for the lower grazing angles. This problem type usually occurs for the lower frequencies.

Two methods have been tried to remove type 3 problems. As mentioned earlier, sediment thickness maps have a resolution of only ± 80 m. This allows one to use the thickness value within a 160 m range which best fits the data. By reducing the sediment thickness one can decrease θ_c. This has the effect of increasing the bottom loss predicted by BLUP for the lower grazing angles because of the additional loss associated with the substrate. For 800 and 1600 Hz this causes a substantial decrease in bottom loss due to a decrease in sediment attenuation. This decrease in attenuation, however, creates problems of type 2. One can also try to increase the sediment attenuation to increase BLUP predictions for the lower angles. Unfortunately, this causes BLUP to predict much higher values of bottom loss for the higher frequencies since attenuation depends linearly on frequency.

D. Type 4

Figure 7(d) illustrates problem type 4 which is characterized by the BLUP predictions exceeding the data at higher angles, especially for 50 Hz. As mentioned earlier, the bottom loss data at 50 Hz associated with the higher grazing angles is usually used to determine the substrate reflectivity. However, there are cases when a decrease in the substrate reflectivity will, while decreasing the quality of the comparison for 50 Hz, improve the overall fit for the rest of the frequencies. One might argue that problem type 4 results from deliberately placing a large error in the 50 Hz fit. For several cases, however, creating a problem of type 4 has the benefit of greatly improving the fit at all other frequencies.

32- Blank

VI. RESULTS

This section presents the BLUP geoacoustic profiles determined by the best fit to the NADC data of model predictions obtained using the ARL:UT bottom loss measurement simulator. Table II lists the BLUP parameters for each site as determined by the best fit of simulated bottom loss to the data. Table II also contains the sediment thickness used to model each location and the bottom water velocity.

The deficiencies in the comparison at each site are discussed quantitatively. Each deficiency is assigned a problem type from those discussed in Section V and illustrated in Fig. 7. For each location a direct graphical comparison is given followed by an illustration showing the difference curve (measured subtracted from predicted bottom loss) for each frequency.

TABLE II

BLUP PARAMETERS FOR NADC NE PACIFIC LOCATIONS

LOCATION	R	ρ_2 (g/cm^3)	ρ_3 (g/cm^3)	D (m)	G (S^{-1})	β	α_o (dB/m kHz)	γ ($dB/m^2 kHz$)	R_{sub}	Bottom Water Velocity (m/sec)	Sediment Thickness (m)
1	.995	2.7	1.75	1.0	1.08	0.0	.01	0.0	.28	1524	154
2	.995	1.41	1.41	0.0	1.20	0.0	.02	0.0	.501	1539	40
3	.995	1.41	1.41	0.0	1.24	0.0	.02	0.0	.447	1550	39
4	.994	1.41	1.41	0.0	1.27	0.0	.02	0.0	.550	1551	32
5	.995	1.41	1.41	0.0	1.25	0.0	.02	0.0	.562	1550	50
6	.995	1.41	1.41	0.0	1.27	0.0	.02	0.0	.513	1547	49
7	.972	1.41	1.41	0.0	.90	0.0	.015	0.0	.501	1537	70
8	.969	1.41	1.41	0.0	.90	0.0	.015	0.0	.501	1540	60
9	.970	1.41	1.41	0.0	1.26	0.0	.01	0.0	.447	1541	60
10	.973	1.41	1.41	0.0	.90	0.0	.015	0.0	.447	1534	60
11	.973	1.53	1.53	0.0	1.0	0.0	.015	-4.22×10^{-5}	.398	1534	71
12	.973	1.55	1.55	0.0	.90	0.0	.02	8.33×10^{-5}	.501	1534	60
13	.970	1.41	1.41	0.0	1.01	0.0	.015	0.0	.355	1538	70
14	.969	1.8	1.41	1.0	1.25	0.0	.03	0.0	.501	1540	81
15	.995	1.41	1.41	0.0	1.17	0.0	.015	0.0	.501	1528	36

TABLE II

BLUP PARAMETERS FOR NADC NE PACIFIC LOCATIONS (Continued)

LOCATION	R	ρ_2 (g/cm^3)	ρ_3 (g/cm^3)	D (m)	G (S^{-1})	β	α_o (dB/m-kHz)	γ (dB/m^2-kHz)	R_{sub}	Bottom Water Velocity (m/sec)	Sediment Thickness (m)
16	.980	1.41	1.41	0.0	1.0	0.0	.01	0.0	.398	1524	50
17	.989	1.5	1.5	0.0	1.0	0.0	.01	0.0	.630	1510	60
18	.980	1.40	1.40	0.0	1.0	0.0	.015	0.0	.501	1523	60
19	.981	1.41	1.41	0.0	1.25	0.0	.02	0.0	.531	1544	40
20	.979	1.84	1.45	1.0	1.21	0.0	.015	4.17×10^{-5}	.562	1548	120
21	.974	1.84	1.45	1.0	1.21	0.0	.015	4.17×10^{-5}	.562	1550	120
22	.974	1.84	1.45	1.0	1.21	0.0	.015	4.17×10^{-5}	.562	1549	120
23	.974	1.84	1.45	1.0	1.21	0.0	.015	4.17×10^{-5}	.562	1550	120
24	.974	1.84	1.45	1.0	1.21	0.0	.015	4.17×10^{-5}	.562	1550	120
25	.967	1.84	1.75	1.0	1.15	0.0	.02	0.0	.507	1544	20
26	.978	1.84	1.45	1.0	1.21	0.0	.015	4.17×10^{-5}	.562	1549	120
27	.976	1.84	1.45	1.0	1.21	0.0	.015	4.17×10^{-5}	.562	1553	120
28	.974	1.84	1.45	1.0	1.21	0.0	.015	4.17×10^{-5}	.562	1550	120
29	.976	1.84	1.45	1.0	1.21	0.0	.015	4.17×10^{-5}	.562	1552	120
30	.963	1.6	1.6	0.0	1.25	0.0	.01	0.0	.501	1551	80
31	.967	1.8	1.41	1.0	1.25	0.0	.03	0.0	.473	1544	80

A. Location 1

1. Deficiencies

(1) For 200 and 400 Hz in the angular region $30^{o}<\theta g<65^{o}$, BLUP predictions fall below the data (maximum difference of 5 dB at 55^{o} for 200 Hz and 6.5 dB at 35^{o} for 400 Hz). Also, for 1600 Hz in the region $30^{o}<\theta g<65^{o}$, predictions fall below the data (maximum difference of 12 dB at 50^{o}). In addition to the above, predictions for 800 Hz in the region $25^{o}<\theta g<65^{o}$ fall below the data (maximum difference of 11 dB at 50^{o}) (problem type 2).

(2) For 800 Hz in the region $0^{o}<\theta g<25^{o}$, BLUP predictions exceed the data (maximum difference of 4 dB at 4^{o}). Also for 1600 Hz in the region $0^{o}<\theta g<30^{o}$, predictions exceed the data (maximum difference of 7 dB at 4^{o}) (problem type 1).

2. Comments

Even though sediment thickness maps report a thickness of 400 m, a thickness of 154 m is used here. This is a case in which only the data was used to estimate sediment thickness.

A surface layer is used here to allow bottom loss to increase with angle for 800 Hz. A 1 m surface layer maximizes the transmission into the sediment for the higher grazing angles for 800 Hz and minimizes transmission for the lower ones.

The data has very large peaks at two grazing angles. These are particularly noticeable at 800 Hz and 1600 Hz. These peaks are probably due to problems involving data collection or analysis.

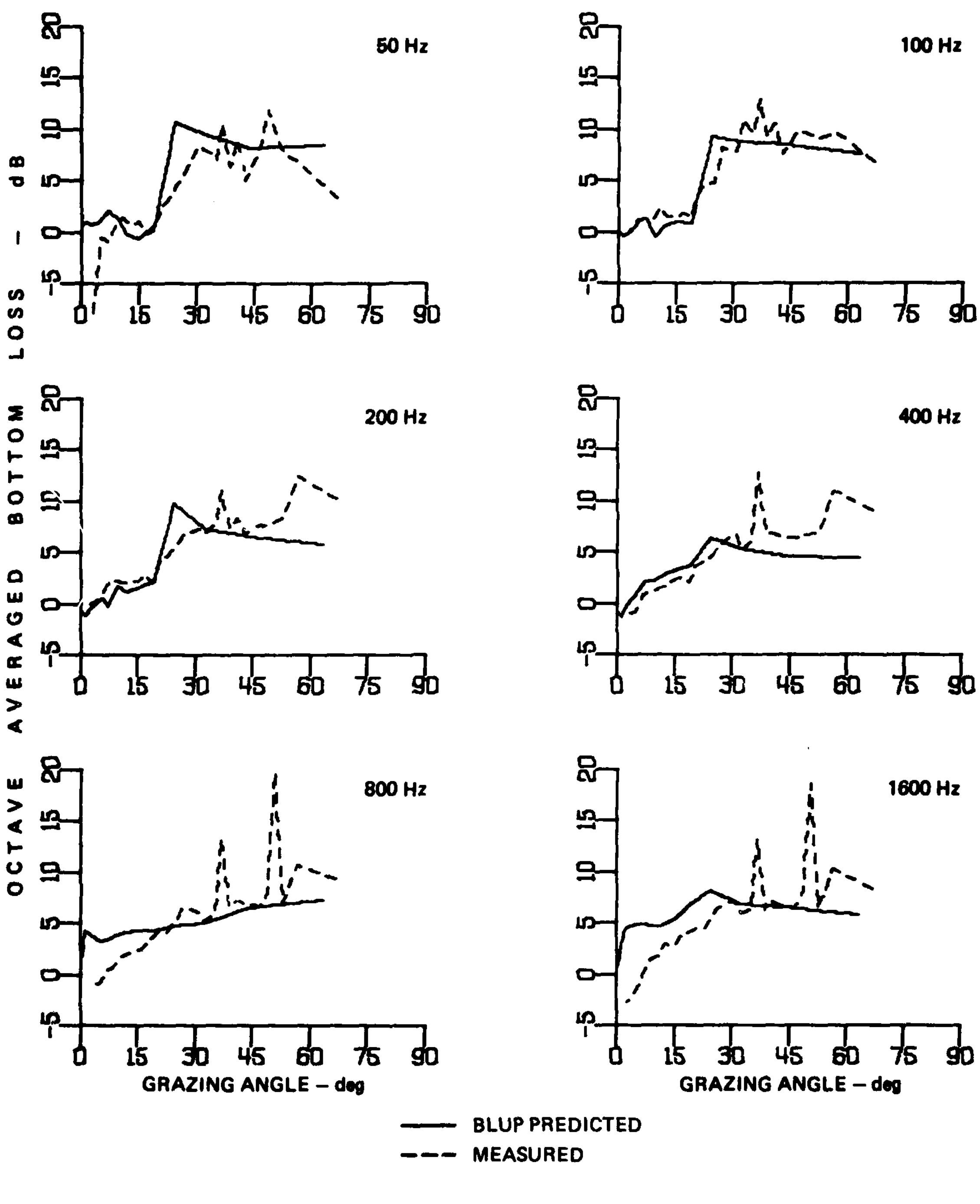

OCTAVE AVERAGED BOTTOM LOSS PREDICTED BY BOTTOM LOSS UPGRADE GEOACOUSTIC PROFILE versus NADC BOTTOM LOSS DATA AT LOCATION 1

ARL:UT
AS-81-1125
DPK - GA
9 - 17 - 81

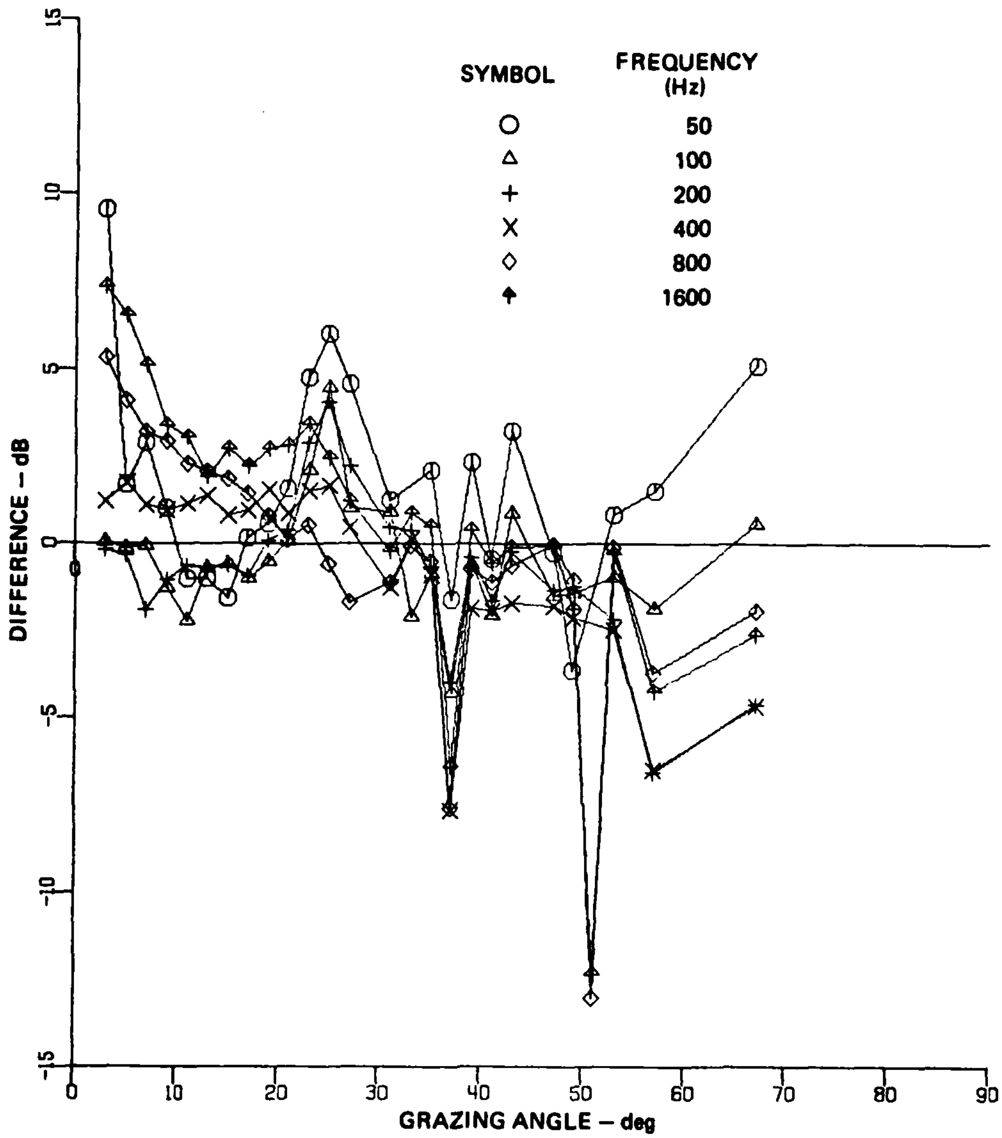

DIFFERENCE BETWEEN BLUP PREDICTED BOTTOM LOSS AND NADC DATA AT LOCATION 1

ARL:UT
AS-81-1156
DPK - GA
9 - 17 - 81

B. Location 2

1. Deficiencies

(1) For the frequencies 50, 100, 200, and 400 Hz in the angular region $5^{o}<\theta g<15^{o}$, BLUP predictions fall below the data (maximum difference of 7 dB at 12^{o} for 100 Hz) (problem type 3).

(2) For the frequencies 50, 100, and 200 Hz in the angular region $40^{o}<\theta g<65^{o}$, predictions are greater than the data (maximum of 2 dB at 43^{o} for 50 Hz) (problem type 4).

(3) For 1600 Hz, predictions are above the data (maximum difference of 7.5 dB at 10^{o}) (problem type 1).

2. Comments

Even though sediment thickness maps report a thickness of 80 m, a thickness of 40 m is used here. This thickness is consistent with DSDP sites 37 and 38 which report thicknesses of 31 and 48 m, respectively, near location 2.

Surface sediment acoustic velocity maps prepared by the U.S. Naval Oceanographic Office show a surface velocity of 1,495 m/sec in this region. A value of 1,531.3 m/sec associated with a 0.995 velocity ratio (within the range expected for pelagic clays) was used to obtain the fit to the data shown here.

Location 2 has the best fit to the data of all 31 locations.

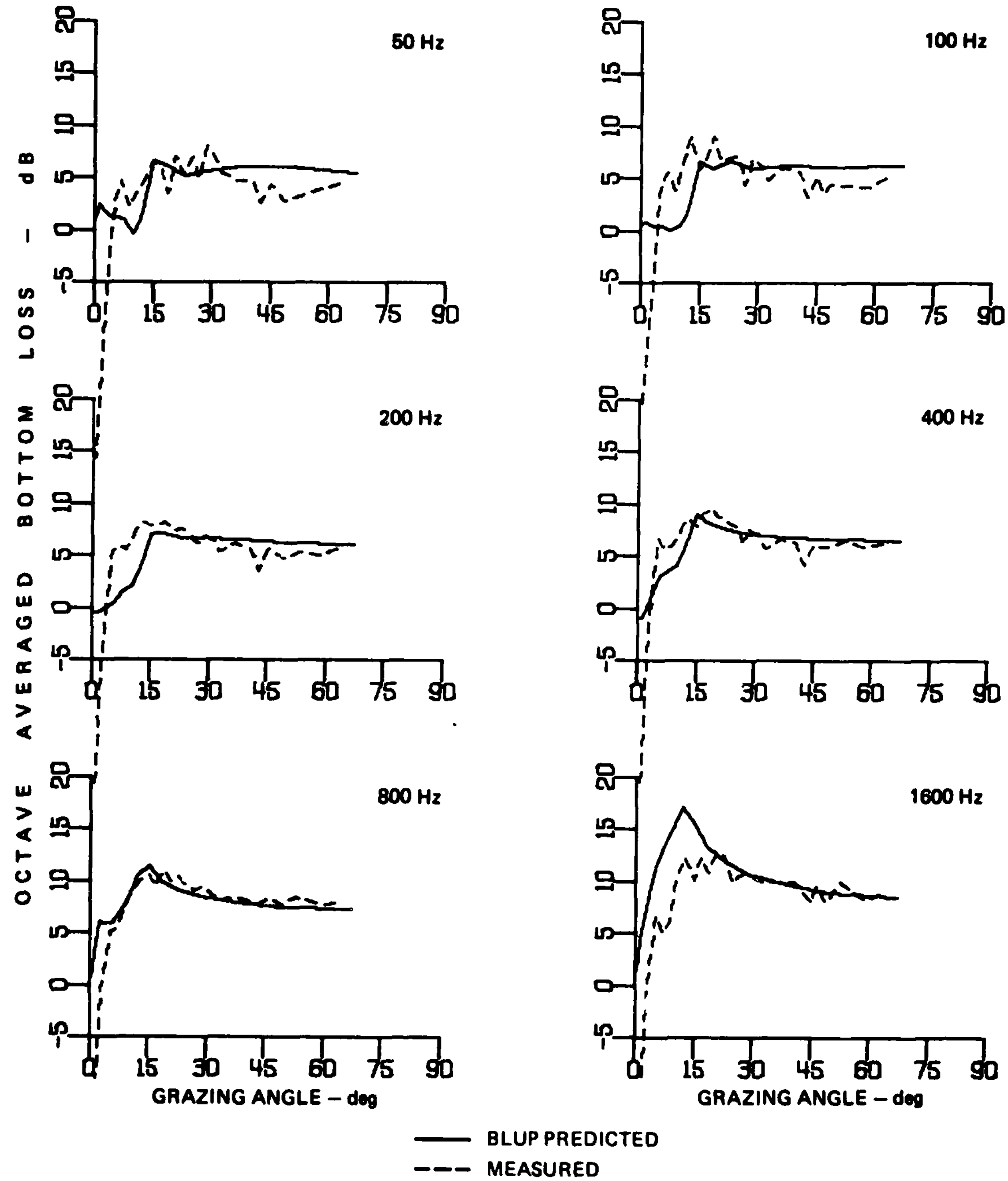

OCTAVE AVERAGED BOTTOM LOSS PREDICTED BY BOTTOM LOSS UPGRADE GEOACOUSTIC PROFILE versus NADC BOTTOM LOSS DATA AT LOCATION 2

ARL:UT
AS-81-1126
DPK - GA
9 - 17 - 81

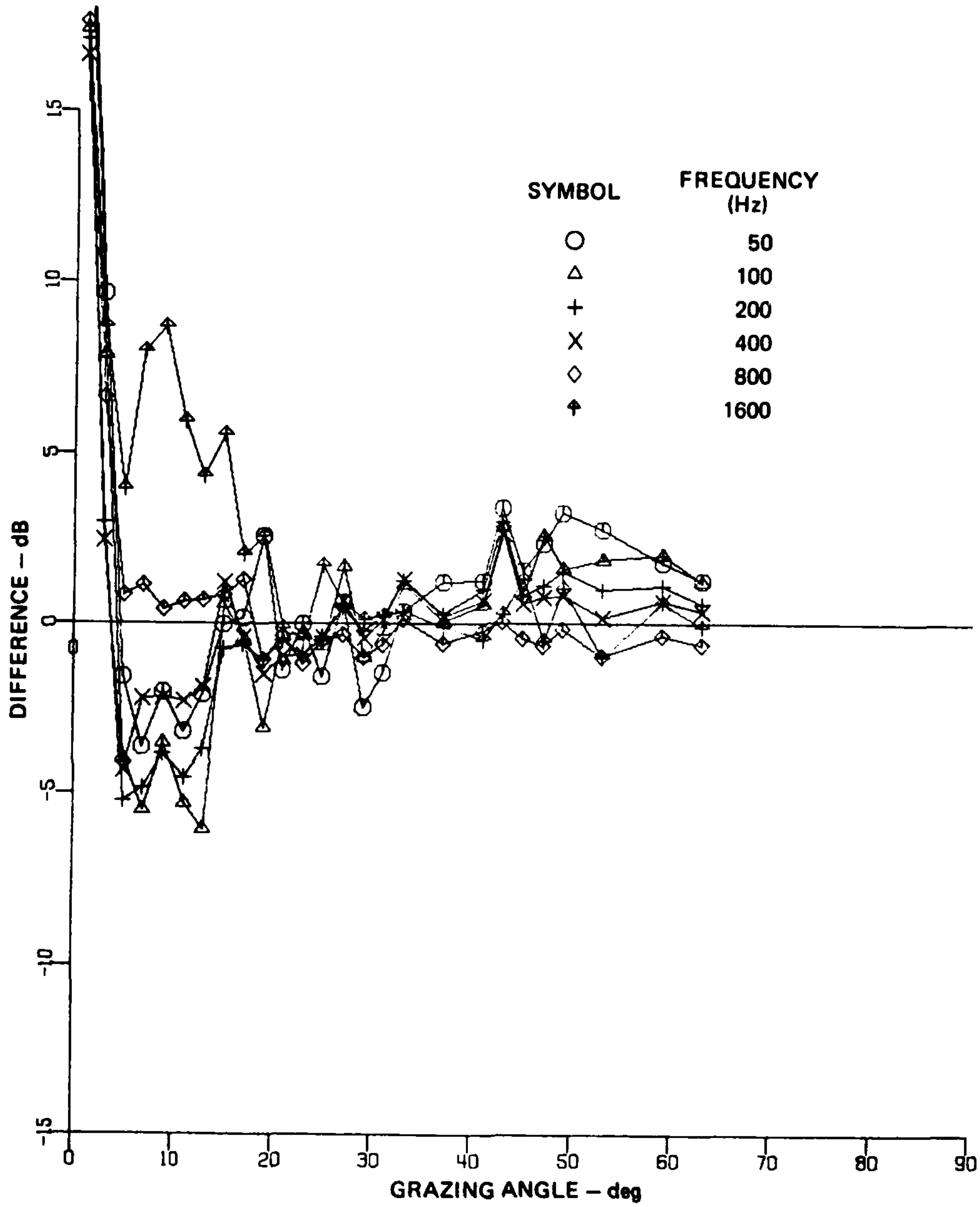

DIFFERENCE BETWEEN BLUP PREDICTED BOTTOM LOSS AND NADC DATA AT LOCATION 2

ARL:UT
AS-81-1157
DPK - GA
9 - 17 - 81

C. Location 3

1. Deficiencies

(1) For the frequencies 50, 100, 200, and 400 Hz in the angular region $6^{0}<\theta g<15^{0}$, BLUP predictions fall below the data (maximum difference of 16 dB at 50 Hz and a minimum difference of 1 dB for 400 Hz) (problem type 3).

(2) For 1600 Hz, predictions are above the data (maximum difference of 7 dB at 15^{0}) (problem type 1).

(3) In the angular region $40^{0}<\theta g<65^{0}$ for 800 and 1600 Hz, predictions fall below the data (maximum difference of 3 dB at 45^{0}) (problem type 2).

(4) For frequencies 50, 100, 200, and 400 Hz in the angular region $15^{0}<\theta g<40^{0}$, predictions exceed the data by an average of 2 dB (problem type 4).

2. Comments

Even though sediment thickness maps report a thickness of 80 m, a thickness of 39 m is used here. This thickness is consistent with DSDP sites 37 and 38 which report thicknesses of 31 and 48 m, respectively, near location 3.

Surface sediment acoustic velocity maps prepared by the U.S. Naval Oceanographic Office show a surface velocity of 1,495 m/sec. A value of 1,542 m/sec associated with a 0.995 velocity ratio (within the expected range for pelagic clay) was used to produce the fit to the data shown here.

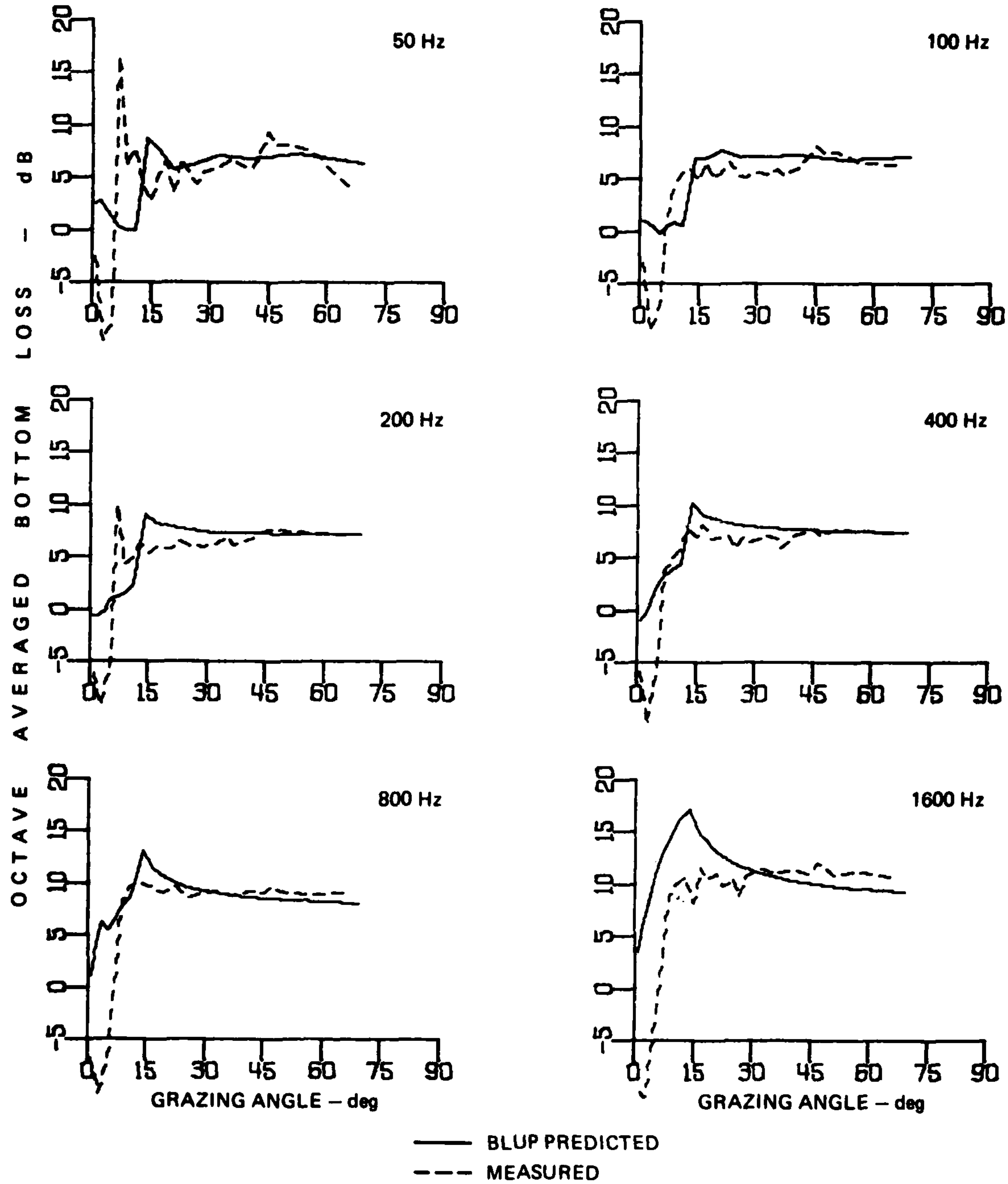

OCTAVE AVERAGED BOTTOM LOSS PREDICTED BY BOTTOM LOSS UPGRADE GEOACOUSTIC PROFILE versus NADC BOTTOM LOSS DATA AT LOCATION 3

ARL:UT
AS-81-1127
DPK - GA
9 - 17 - 81

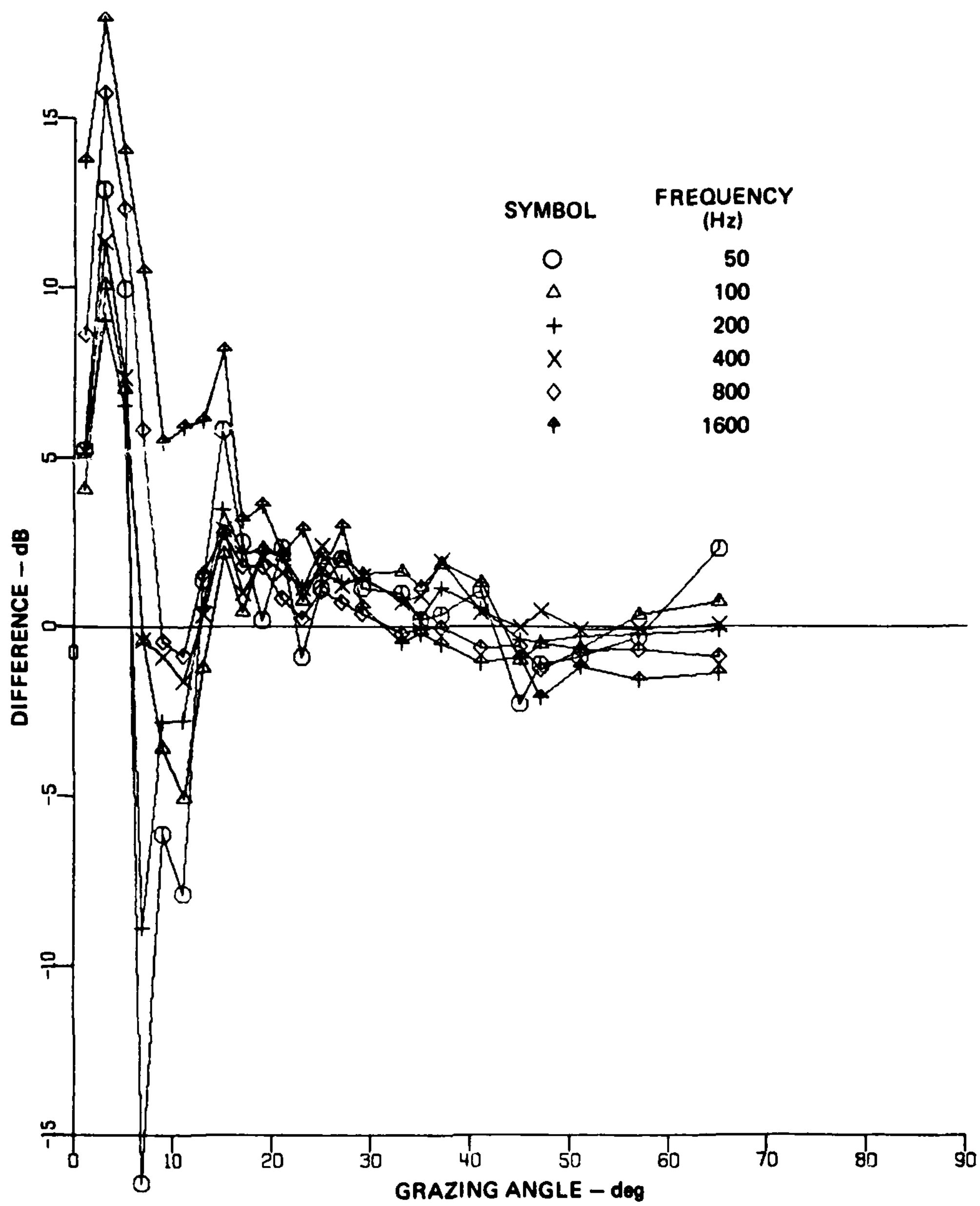

DIFFERENCE BETWEEN BLUP PREDICTED BOTTOM LOSS AND NADC DATA AT LOCATION 3

ARL:UT
AS-81-1158
DPK - GA
9 - 17 - 81

D. Location 4

1. Deficiencies

(1) For the frequencies 50, 100, 200, 400, and 800 Hz in the angular region $3^{0} < \theta g < 12^{0}$, BLUP predictions for bottom loss fall below the data (maximum difference of 6 dB at 100 Hz and a minimum difference of 2 dB for 50 and 800 Hz) (problem type 3).

(2) For 800 and 1600 Hz in the angular region $25^{0} < \theta g < 52^{0}$, predictions fall below the data (maximum difference of 4 dB at 25^{0} for 1600 Hz (problem type 2).

(3) For 1600 Hz, predictions are above the data by 5 dB at 10^{0} (problem type 1).

(4) For the frequencies 50, 100, 200, and 400 Hz in the angular region $16^{0} < \theta g < 45^{0}$, predictions exceed the data by an average value of 2 dB (problem type 4).

2. Comments

Even though sediment thickness maps report a thickness of 80 m, a thickness of 32 m is used here. This thickness is more consistent with DSDP site 38 which reports a thickness of 17 m near location 4.

Surface sediment acoustic velocity maps prepared by the U.S. Naval Oceanographic Office show a surface velocity of 1,500 m/sec. A value of 1,542 m/sec associated with a 0.995 velocity ratio (within the range expected for pelagic clay) was used to produce the fit shown here.

The difference curve shows a crossover at 15^{0} between opposite low angle and high angle frequency dependencies not predicted by BLUP. This crossover also occurs at other locations.

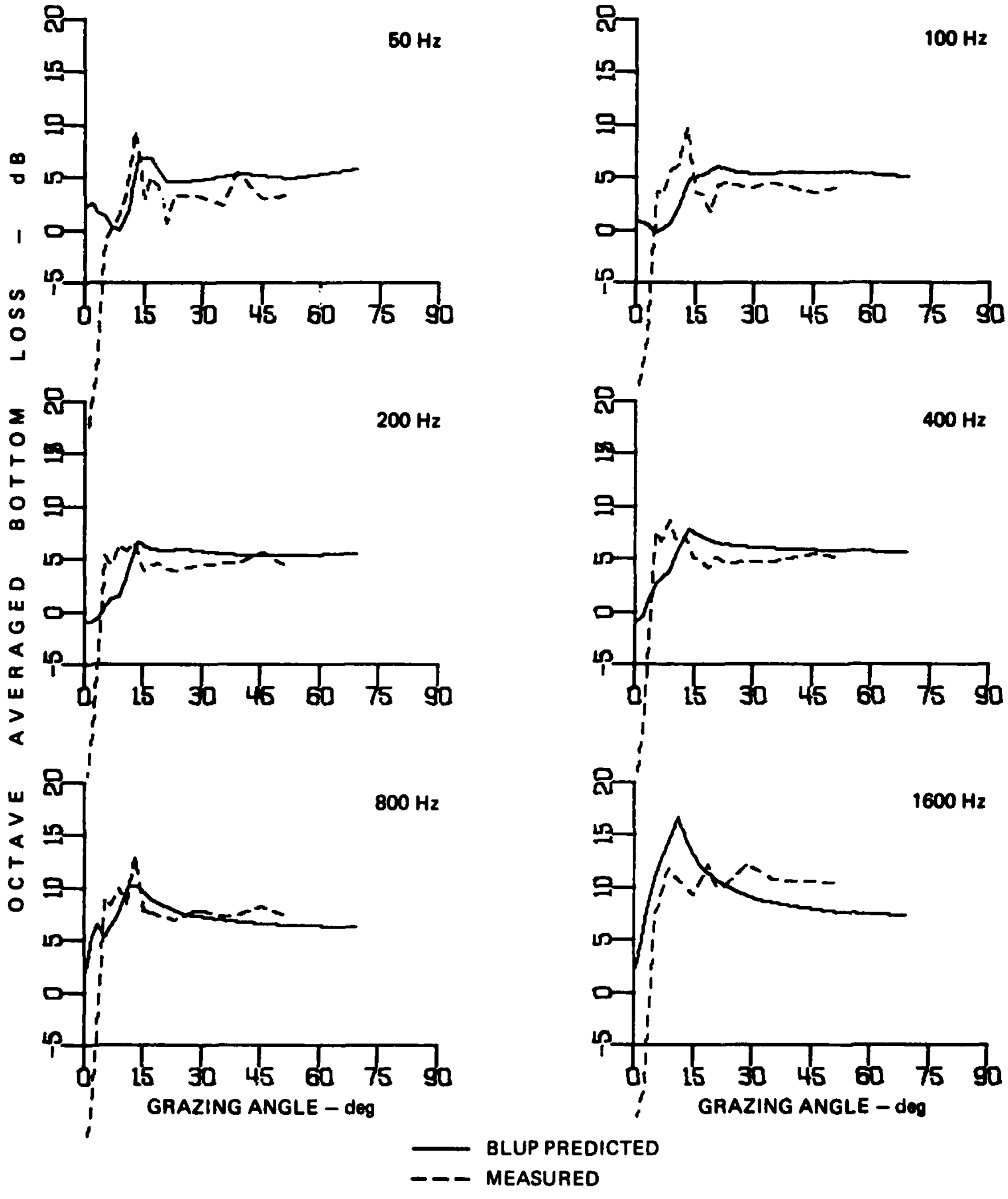

OCTAVE AVERAGED BOTTOM LOSS PREDICTED BY BOTTOM LOSS UPGRADE GEOACOUSTIC PROFILE versus NADC BOTTOM LOSS DATA AT LOCATION 4

ARL:UT
AS-81-1128
DPK - GA
9 - 17 - 81

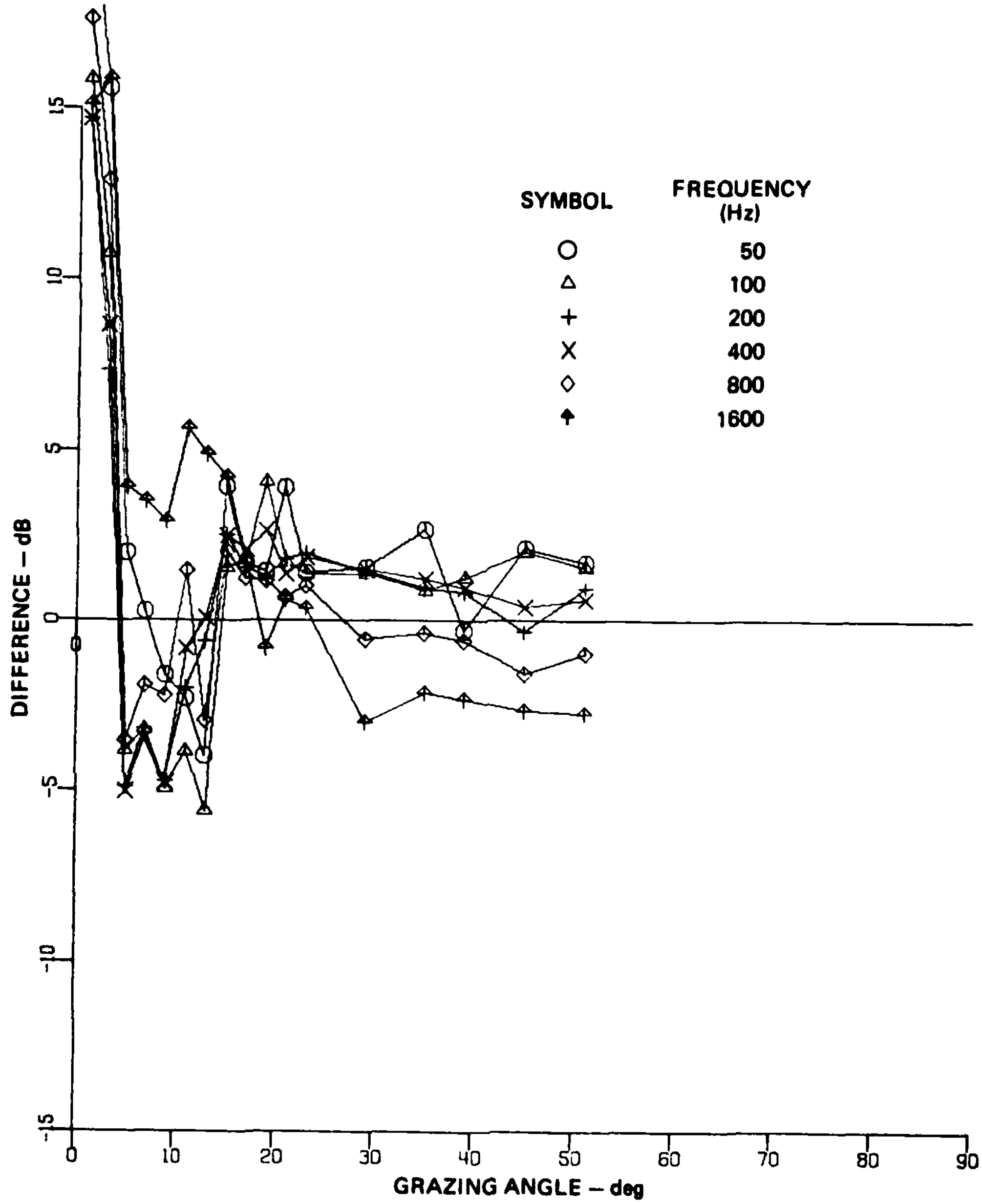

DIFFERENCE BETWEEN BLUP PREDICTED BOTTOM LOSS AND NADC DATA AT LOCATION 4

ARL:UT
AS-81-1159
DPK - GA
9 - 17 - 81

E. Location 5

1. Deficiencies

(1) For the frequencies 50, 100, 200, and 400 Hz in the angular region $5^{o}<\theta g<15^{o}$, BLUP predictions fall below the data (maximum difference of 4 dB at 5^{o} for 400 Hz) (problem type 3).

(2) In the region $30^{o}<\theta g<60^{o}$ for 800 and 1600 Hz, prediction values fall below the data (maximum difference of 5 dB at 45^{o} for 800 Hz) (problem type 2).

(3) Also, for 1600 Hz, predictions exceed the data by 8 dB at 6^{o} (problem type 1).

(4) For 50 Hz in the region $15^{o}<\theta g<30^{o}$, predictions exceed the data by a maximum value of 3.5 dB at 22^{o} (problem type 4).

2. Comments

Even though sediment thickness maps report a sediment thickness of 80 m, a thickness of 40 m is used here. This thickness is consistent with DSDP sites 38 and 39 which report thicknesses of 48 m and 39 m respectively near location 5.

Surface sediment acoustic velocity maps prepared by the U.S. Naval Oceanographic Office show a surface velocity of 1,490 m/sec. A value of 1,542 m/sec associated with a 0.995 velocity ratio (within the expected range for pelagic clay) was used to produce the fit shown here.

The difference curve clearly shows a low angle frequency dependence not predicted by BLUP. This frequency dependence is also observed at other locations.

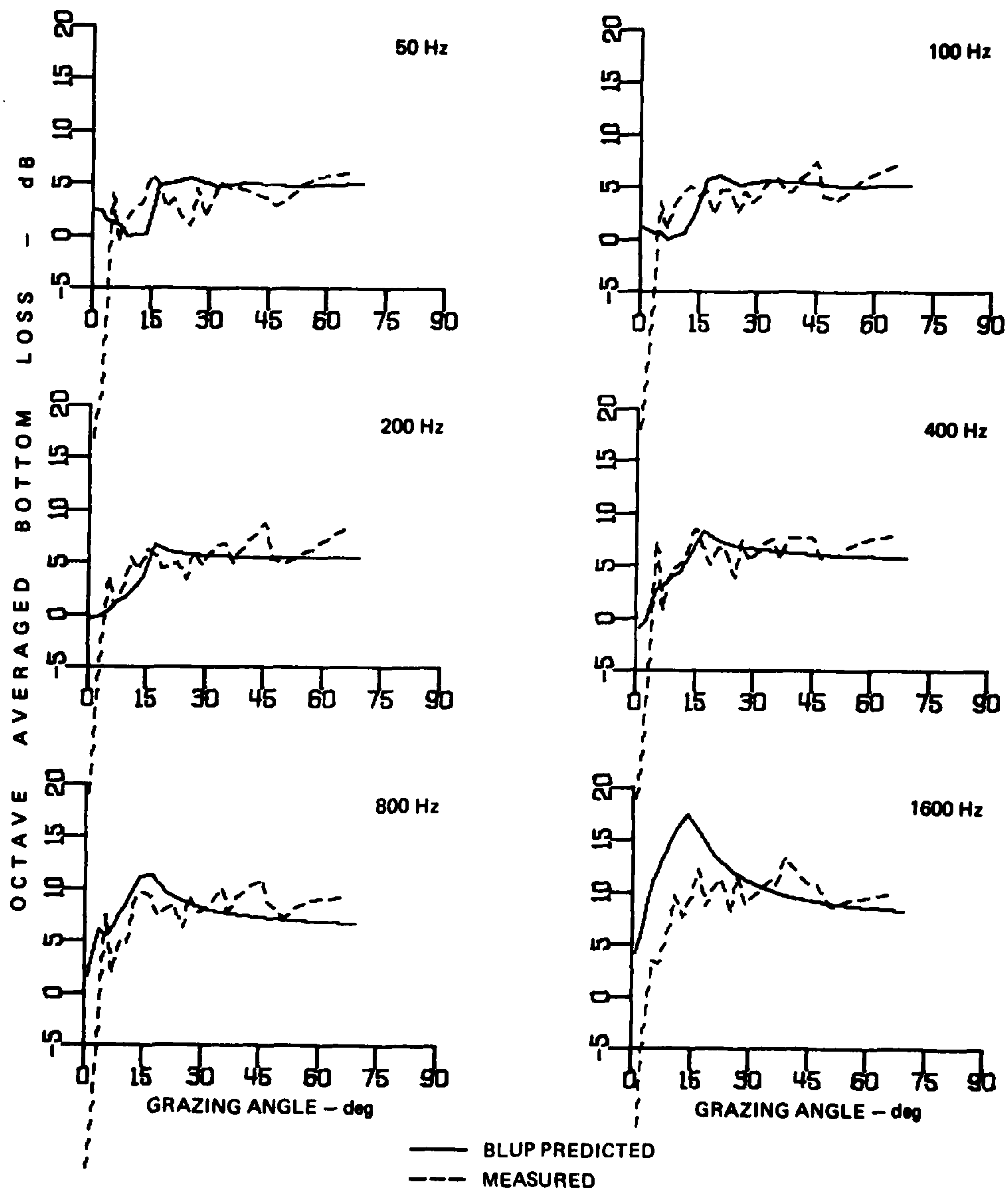

OCTAVE AVERAGED BOTTOM LOSS PREDICTED BY BOTTOM LOSS UPGRADE GEOACOUSTIC PROFILE versus NADC BOTTOM LOSS DATA AT LOCATION 5

ARL:UT
AS-81-1129
DPK - GA
9 - 17 - 81

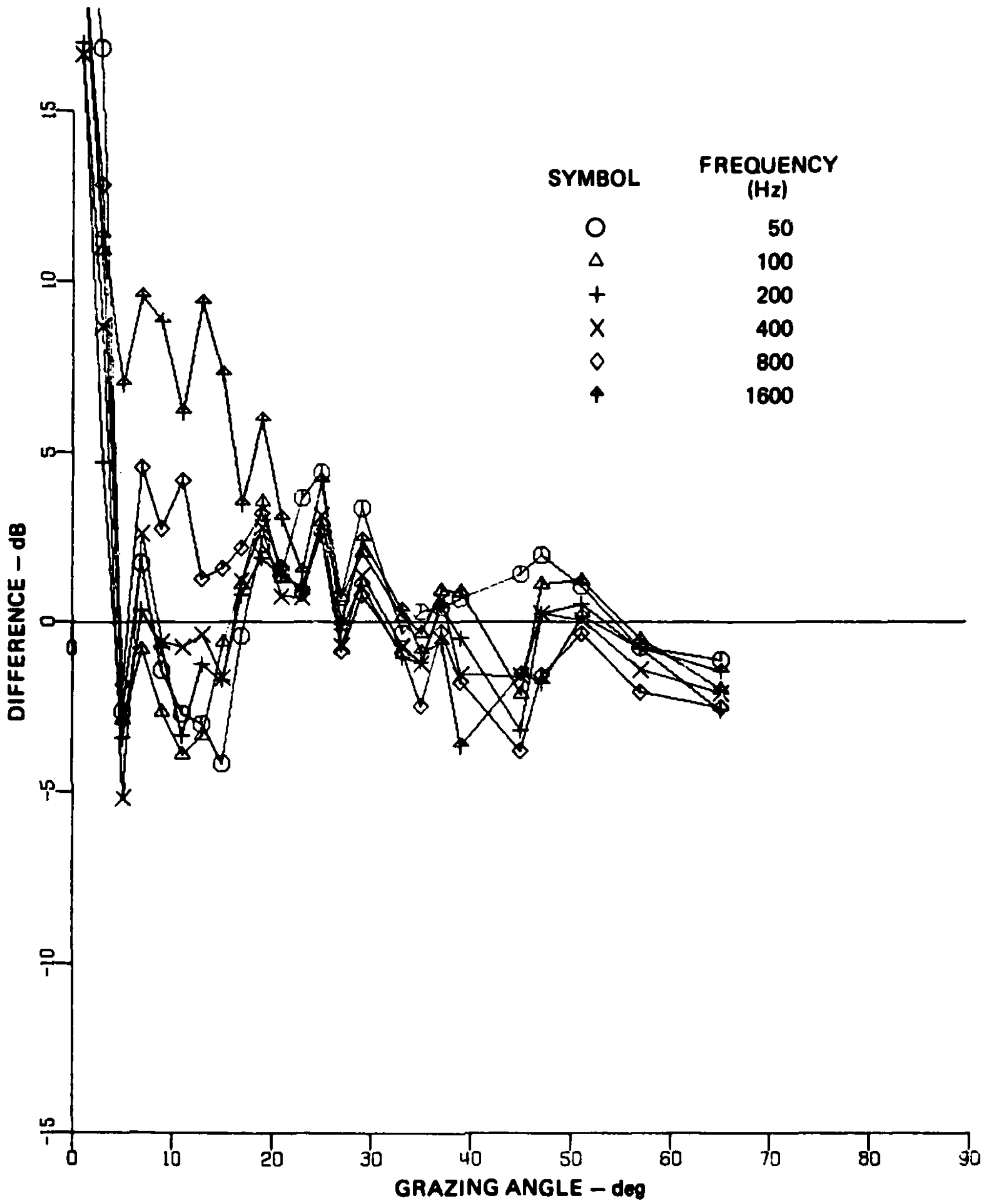

DIFFERENCE BETWEEN BLUP PREDICTED BOTTOM LOSS AND NADC DATA AT LOCATION 5

ARL:UT
AS-81-1160
DPK - GA
9 - 17 - 81

F. Location 6

1. Deficiencies

(1) For frequencies 50, 100, 200, 400 and 800 Hz in the angular region $5^{o}<\theta g<19^{o}$, BLUP predictions for bottom loss fall below the data (maximum difference of 8 dB at 11^{o} for 50 Hz) (problem type 3).

b. In the angular region $20^{o}<\theta g<63^{o}$ for 800 and 1600 Hz, predictions fall below the data by a maximum difference of 6 dB at 35^{o} for 1600 Hz (problem type 2).

(3) For 1600 Hz, predictions are above the data (maximum difference of 5 dB at 12^{o}) (problem type 1).

2. Comments

Even though sediment thickness maps report a thickness of 80 m, a thickness of 49 m is used here. This thickness is consistent with DSDP site 38 which reports a thickness of 48 m near location 6.

Surface sediment acoustic velocity maps prepared by the U.S. Naval Oceanographic Office show a surface velocity of 1,490 m/sec. A value of 1,538 m/sec associated with a 0.995 velocity ratio (within the expected range for pelagic clay) was used to produce the fit shown here.

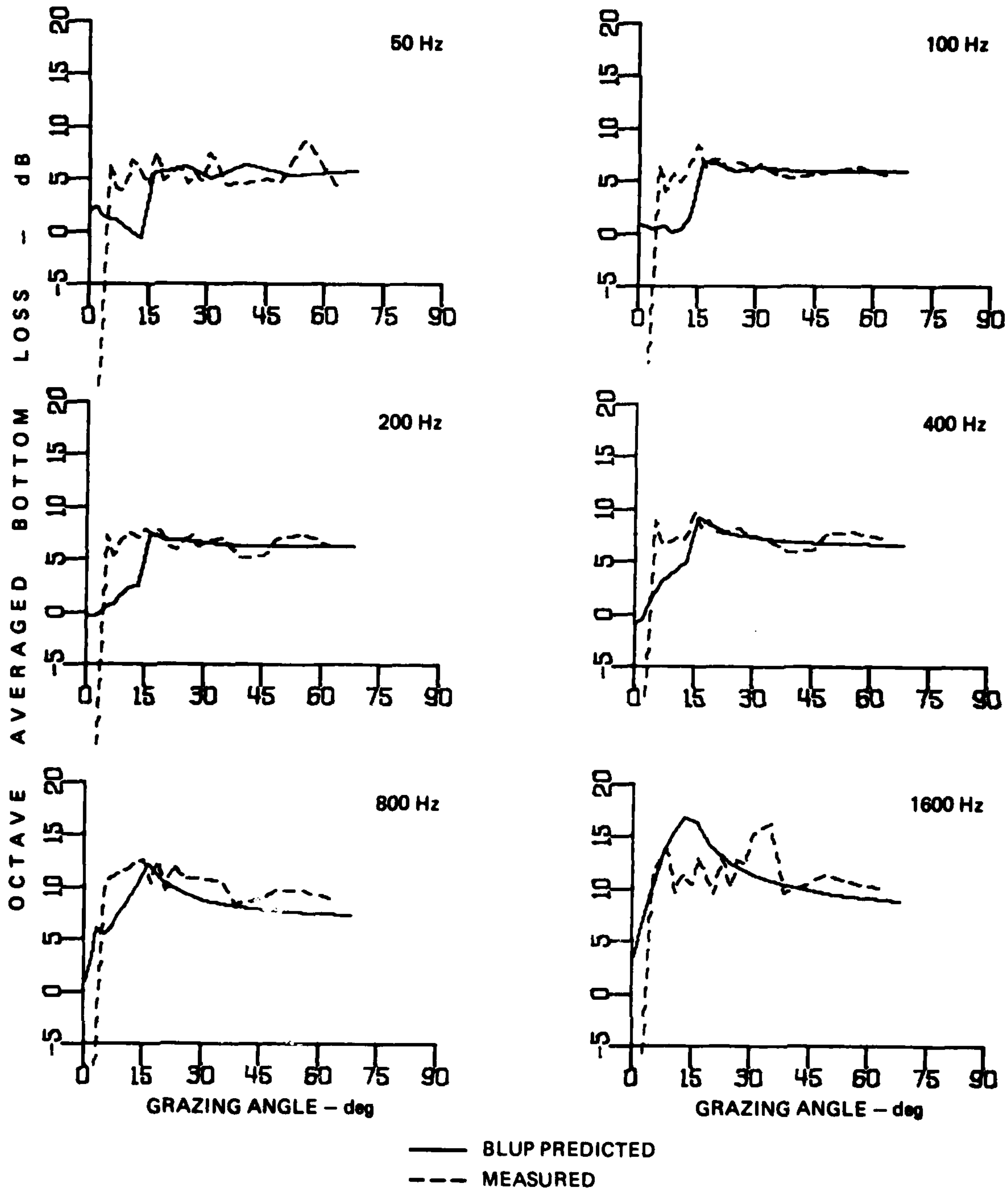

OCTAVE AVERAGED BOTTOM LOSS PREDICTED BY BOTTOM LOSS UPGRADE GEOACOUSTIC PROFILE versus NADC BOTTOM LOSS DATA AT LOCATION 6

ARL:UT
AS-81-1130
DPK - GA
9 - 17 - 81

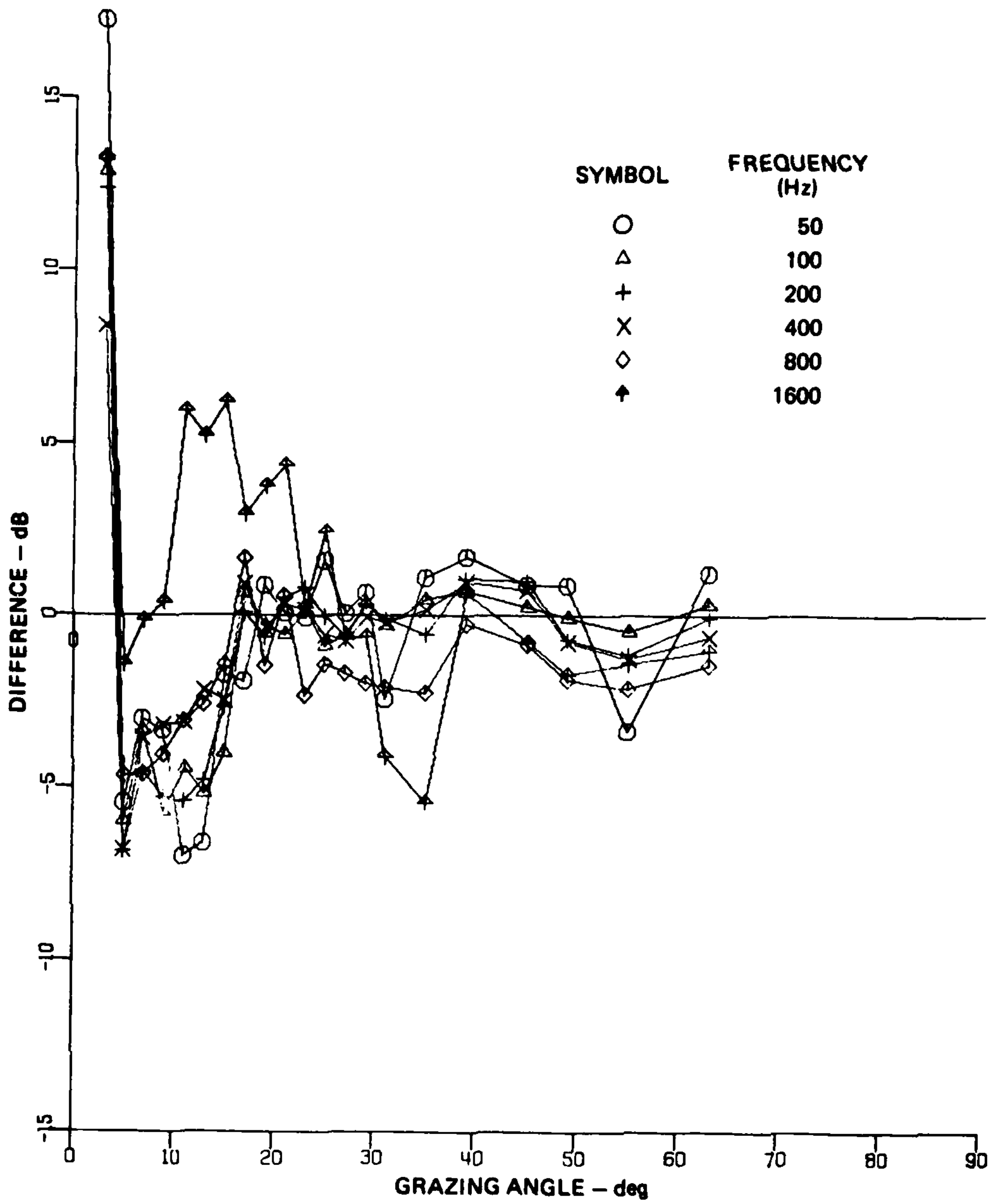

DIFFERENCE BETWEEN BLUP PREDICTED BOTTOM LOSS AND NADC DATA AT LOCATION 6

ARL:UT
AS-81-1161
DPK - GA
9 - 17 - 81

G. Location 7

1. Deficiencies

(1) For the frequencies 100, 200, 400, and 800 Hz in the angular region $5^o<\theta g<28^o$, BLUP predictions fall below the data (maximum difference of 15 dB at 5^o for 100 Hz) (problem type 3).

(2) For 1600 Hz, predictions exceed the data in the region $5^o<\theta g<22^o$ (maximum difference of 7 dB at 15^o) (problem type 1).

(3) For 50 Hz, predictions for bottom loss exceed the data in the region $10^o<\theta g<60^o$ (maximum difference of 9 dB at 11^o) (average difference of 3 dB) (problem type 4).

B. Comments

This location exhibits unusually high bottom loss at the lower grazing angles as compared to the other locations.

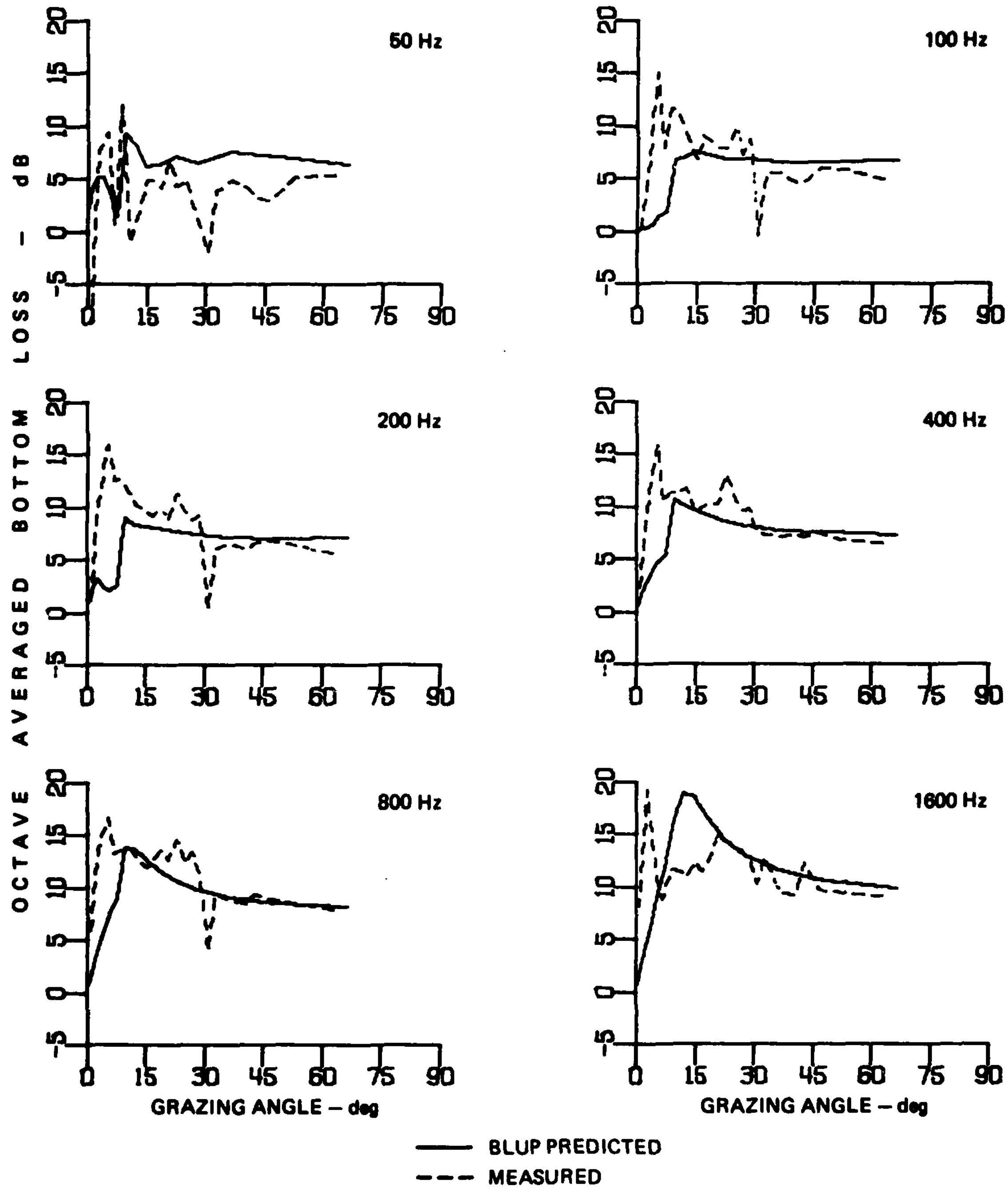

OCTAVE AVERAGED BOTTOM LOSS PREDICTED BY BOTTOM LOSS UPGRADE GEOACOUSTIC PROFILE versus NADC BOTTOM LOSS DATA AT LOCATION 7

ARL:UT
AS-81-1131
DPK - GA
9 - 17 - 81

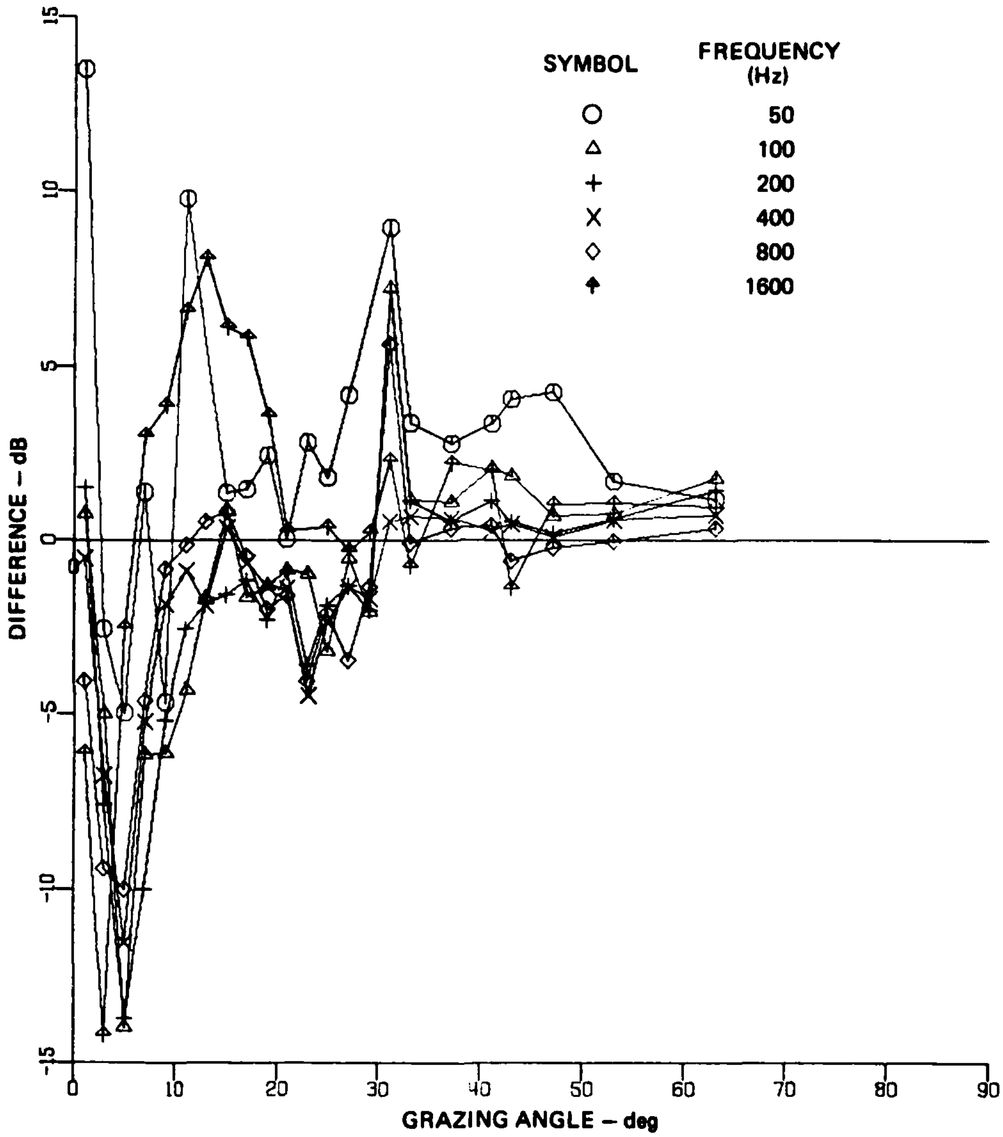

DIFFERENCE BETWEEN BLUP PREDICTED BOTTOM LOSS AND NADC DATA AT LOCATION 7

ARL:UT
AS-81-1162
DPK - GA
9 - 17 - 81

H. Location 8

1. Deficiencies

(1) For 800 and 1600 Hz, BLUP predictions are greater than the data in the angular region $5^{o}<\theta g<20^{o}$ (maximum difference of 4 dB at 12^{o} for 1600 Hz) (problem type 1).

(2) Also for 1600 Hz, the predictions in the angular region $25^{o}<\theta g<65^{o}$ fall below the data by 2 dB (problem type 2).

(3) For 50 Hz, predictions are greater than the data in the angular region $5^{o}<\theta g<55^{o}$ (maximum difference of 5 dB at 48^{o}) (problem type 4).

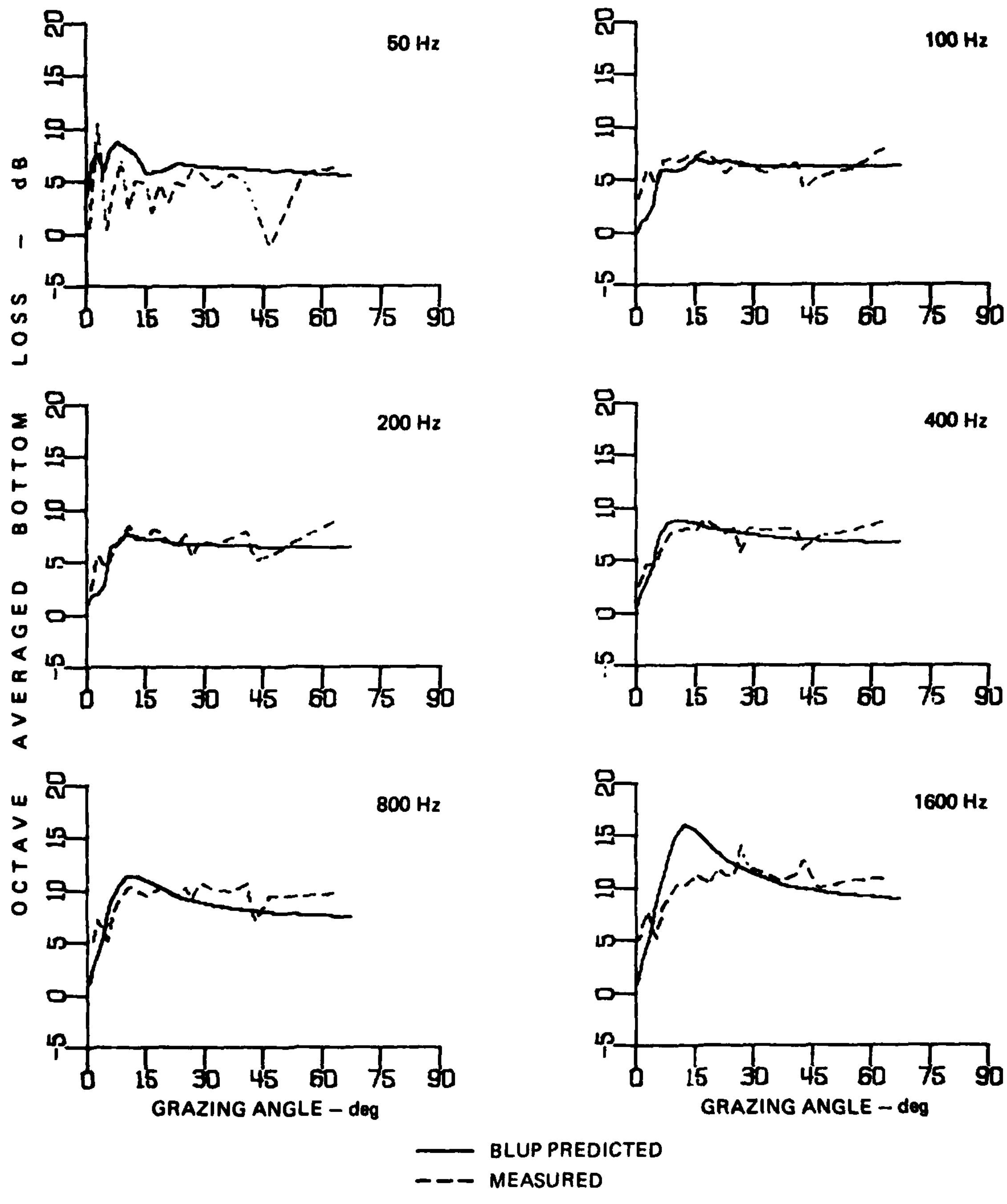

OCTAVE AVERAGED BOTTOM LOSS PREDICTED BY BOTTOM LOSS UPGRADE GEOACOUSTIC PROFILE versus NADC BOTTOM LOSS DATA AT LOCATION 8

ARL:UT
AS-81-1132
DPK - GA
9 - 17 - 81

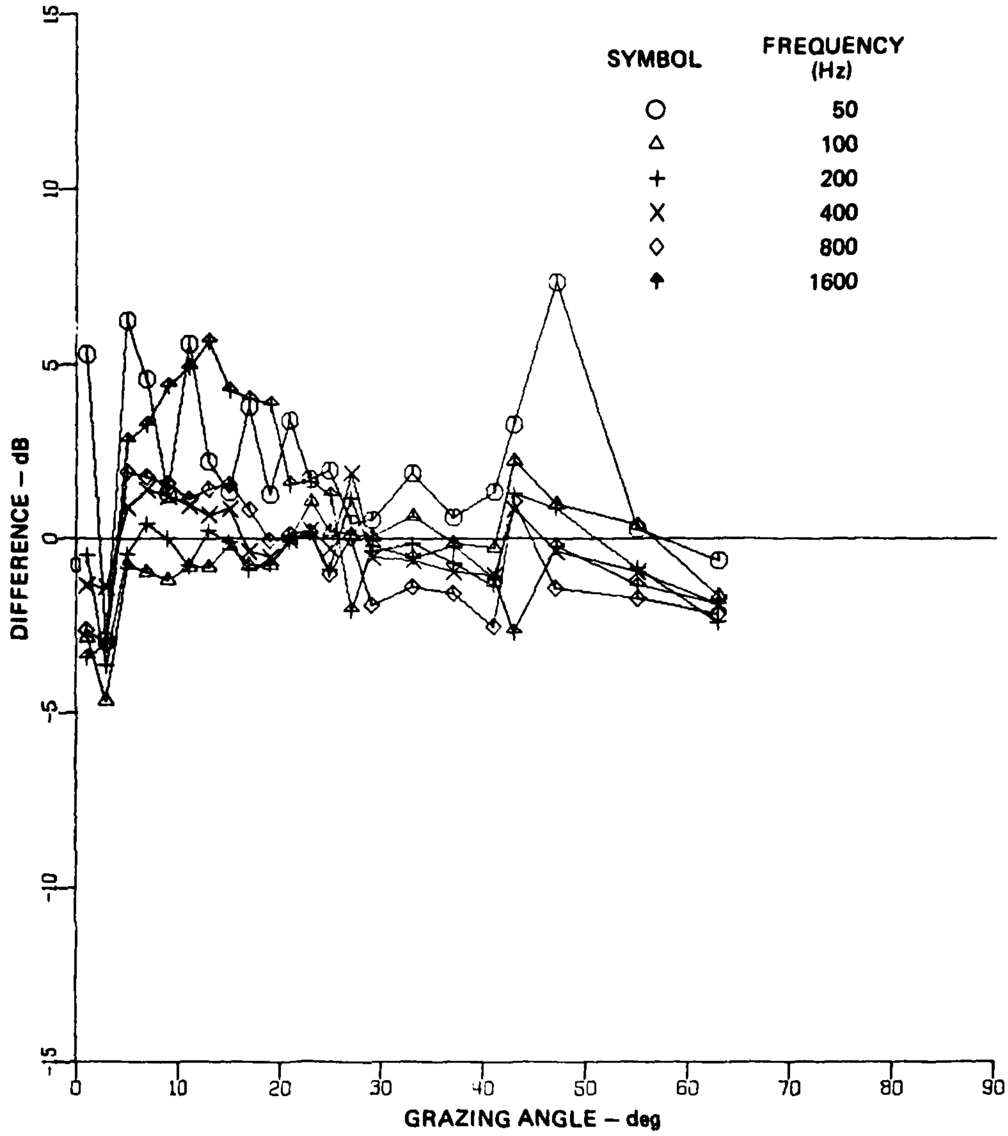

DIFFERENCE BETWEEN BLUP PREDICTED BOTTOM LOSS AND NADC DATA AT LOCATION 8

ARL:UT
AS-81-1163
DPK - GA
9 - 17 - 81

I. Location 9

1. Deficiencies

(1) For the frequencies 100, 200, 400, and 800 Hz in the angular region $0^{o}<\theta g<15^{o}$, BLUP predictions fall below the data (maximum difference of 8 dB at 9^{o} for 200 Hz) (problem type 3).

(2) For 1600 Hz, predictions exceed the data in the region $5^{o}<\theta g<20^{o}$ (maximum difference of 5 dB at 16^{o}) (problem type 1).

(3) For 50 Hz, predictions exceed the data in the region $15^{o}<\theta g<70^{o}$ (average value of 8 dB). Also, for 100 Hz, predictions exceed the data in the region $25^{o}<\theta g<70^{o}$ (maximum difference of 2.5 dB) (problem type 4).

2. Comments

For 50 Hz, an unusually large "dip" in measured bottom loss occurs at 10^{o}. This may be due to a processing error since the rest of the frequencies for this location are well-behaved. Also note the large oscillations in bottom loss at 50 and 1600 Hz, probably due to data collection or analysis problems.

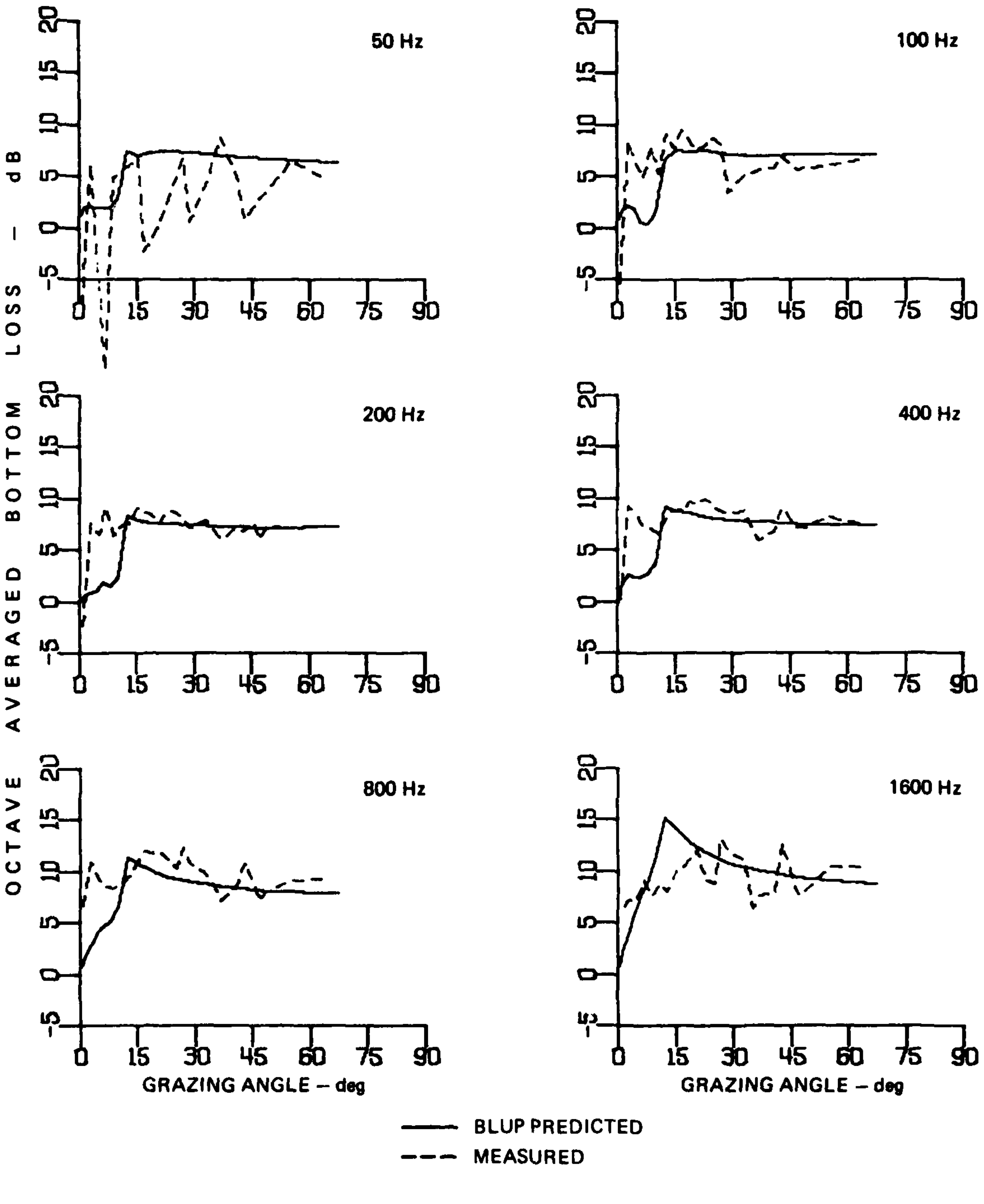

OCTAVE AVERAGED BOTTOM LOSS PREDICTED BY BOTTOM LOSS UPGRADE GEOACOUSTIC PROFILE versus NADC BOTTOM LOSS DATA AT LOCATION 9

ARL:UT
AS-81-1133
DPK - GA
9 - 17 - 81

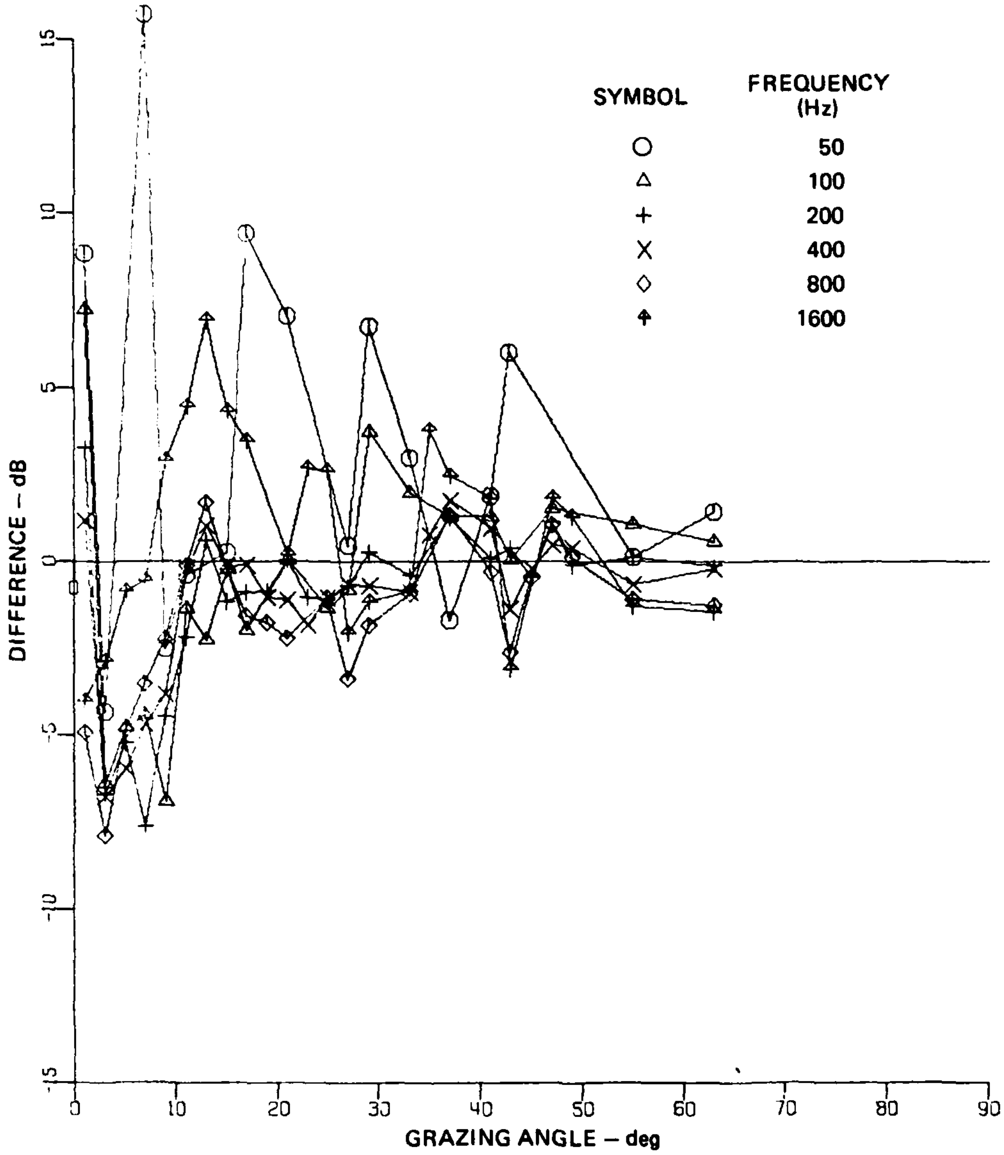

DIFFERENCE BETWEEN BLUP PREDICTED BOTTOM LOSS AND NADC DATA AT LOCATION 9

ARL:UT
AS-81-1164
DPK - GA
9 - 17 - 81

J. Location 10

1. Deficiencies

(1) For the 800 and 1600 Hz in the angular region $10^o < \theta g < 20^o$, BLUP predictions exceed the data (5 dB for 1600 Hz and 1.5 dB for 800 Hz) (problem type 1).

(2) For 800 Hz, predictions fall below the data in the angular region $20^o < \theta g < 70^o$ (average value of 2 dB) (problem type 2).

(3) For 50 Hz, predictions exceed the data in the angular region $10^o < \theta g < 70^o$ (maximum difference 8 dB at 20^o) (problem type 3).

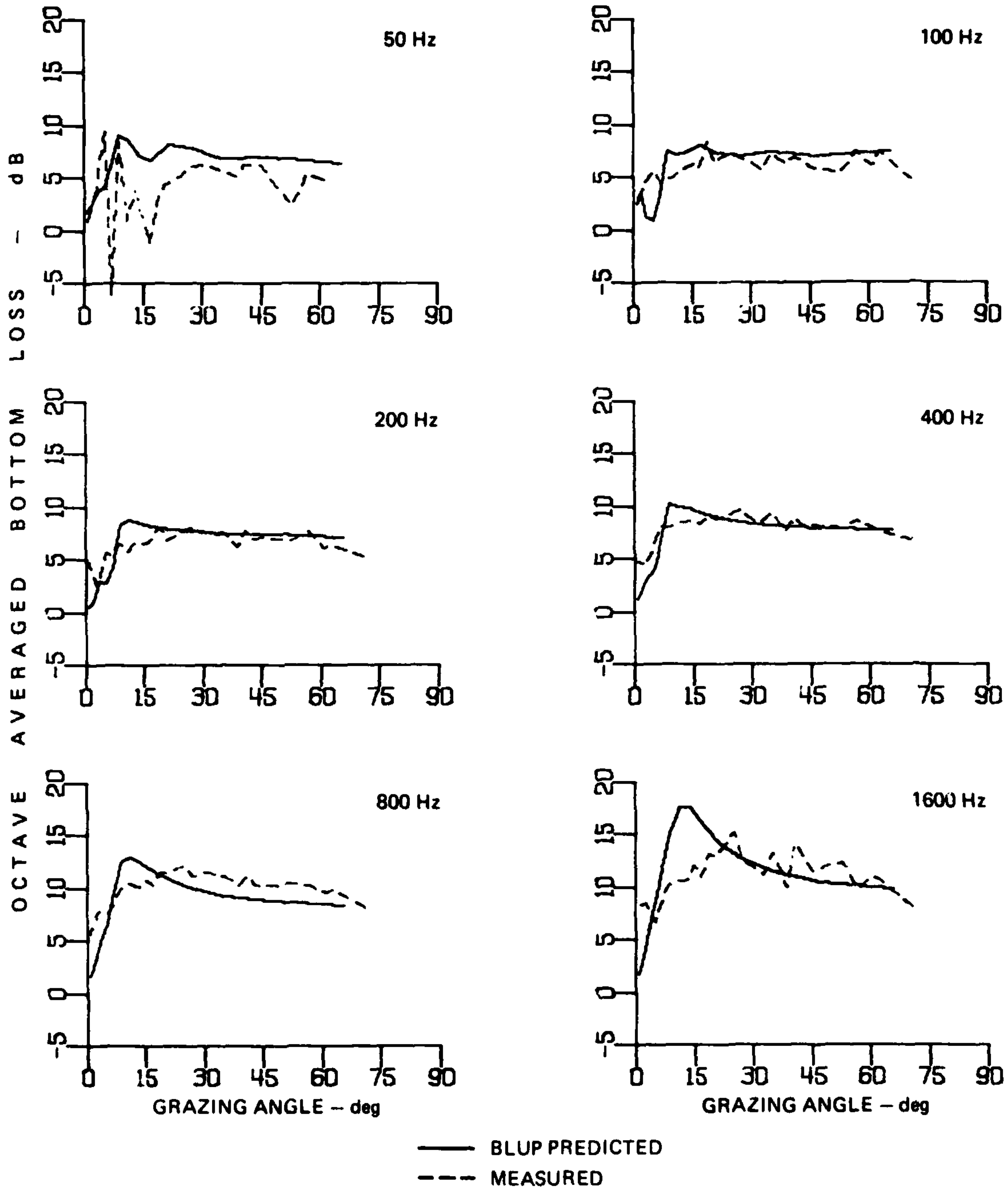

OCTAVE AVERAGED BOTTOM LOSS PREDICTED BY BOTTOM LOSS UPGRADE GEOACOUSTIC PROFILE versus NADC BOTTOM LOSS DATA AT LOCATION 10

ARL:UT
AS-81-1134
DPK - GA
9 - 17 - 81

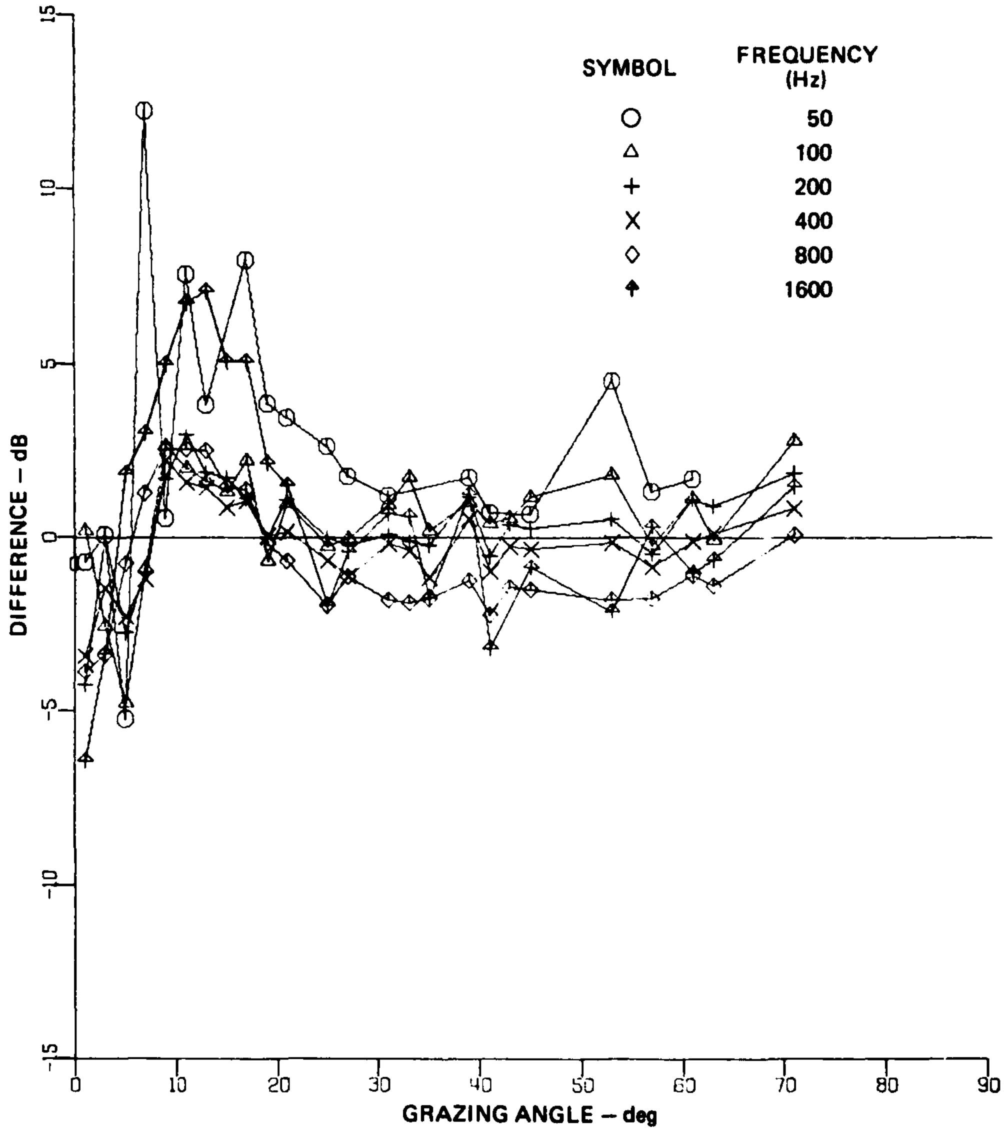

DIFFERENCE BETWEEN BLUP PREDICTED BOTTOM LOSS AND NADC DATA AT LOCATION 10

ARL:UT
AS-81-1165
DPK - GA
9 - 17 - 81

K. Location 11

1. Deficiencies

(1) For 50, 100, 200 and 400 Hz in the angular region $0^{o}<\theta g<16^{o}$, BLUP predictions fall below the data (maximum difference of 6 dB at 10^{o} for 200 Hz). Also, for 800 Hz in the region $0^{o}<\theta g<12^{o}$, predictions fall below the data by approximately 6 dB (problem type 3).

(2) For 800 Hz at 15^{o}, predictions exceed the data by 2 dB. Also for 1600 Hz in the region $5^{o}<\theta g<25^{o}$, predictions exceed the data (maximum difference of 8 dB at 15^{o}) (problem type 1).

(3) For 50 Hz in the region $20^{o}<\theta g<70^{o}$, predictions exceed the data (maximum difference of 4 dB at 70^{o}) (problem type 4).

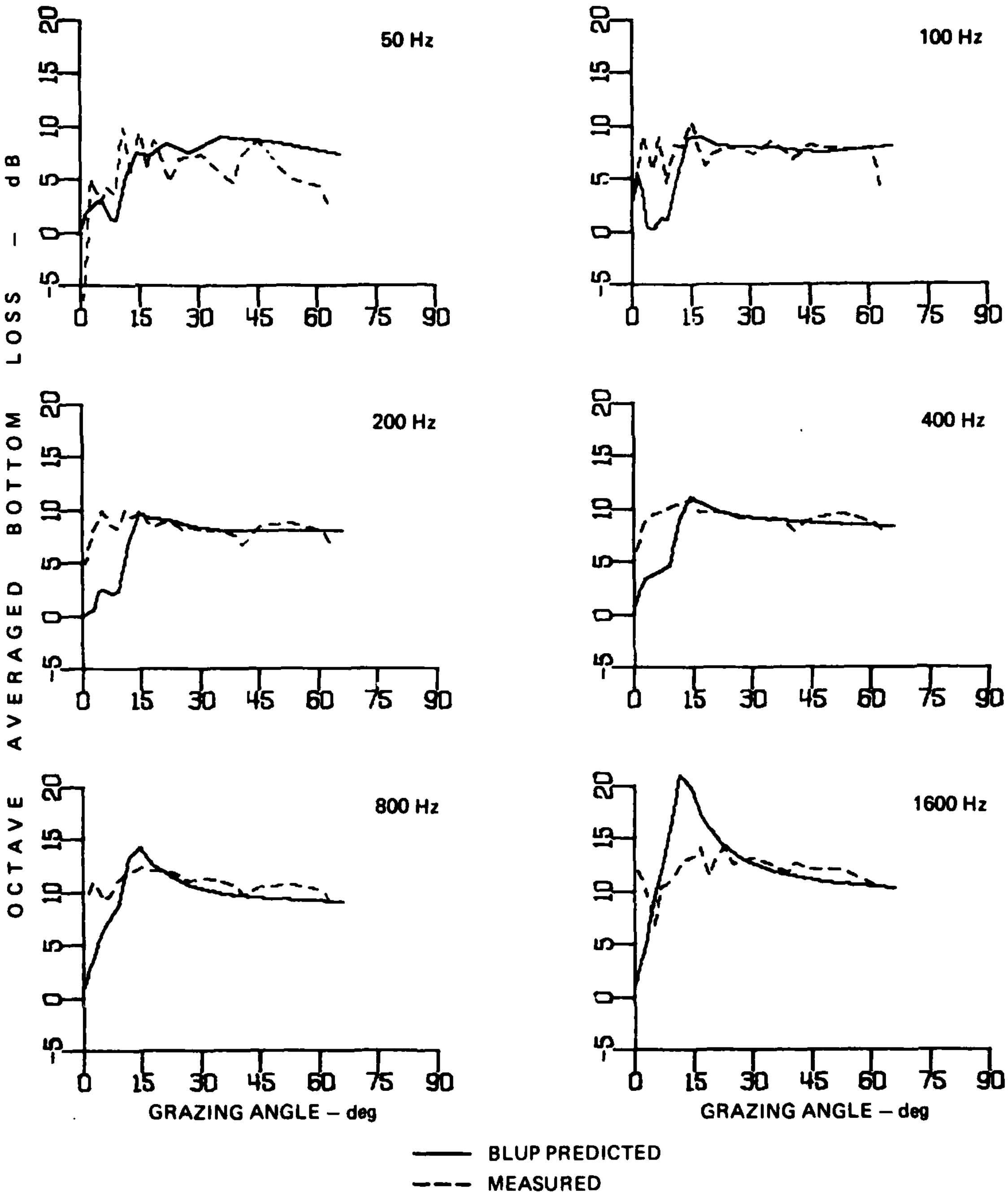

OCTAVE AVERAGED BOTTOM LOSS PREDICTED BY BOTTOM LOSS UPGRADE GEOACOUSTIC PROFILE versus NADC BOTTOM LOSS DATA AT LOCATION 11

ARL:UT
AS-81-1135
DPK - GA
9 - 17 - 81

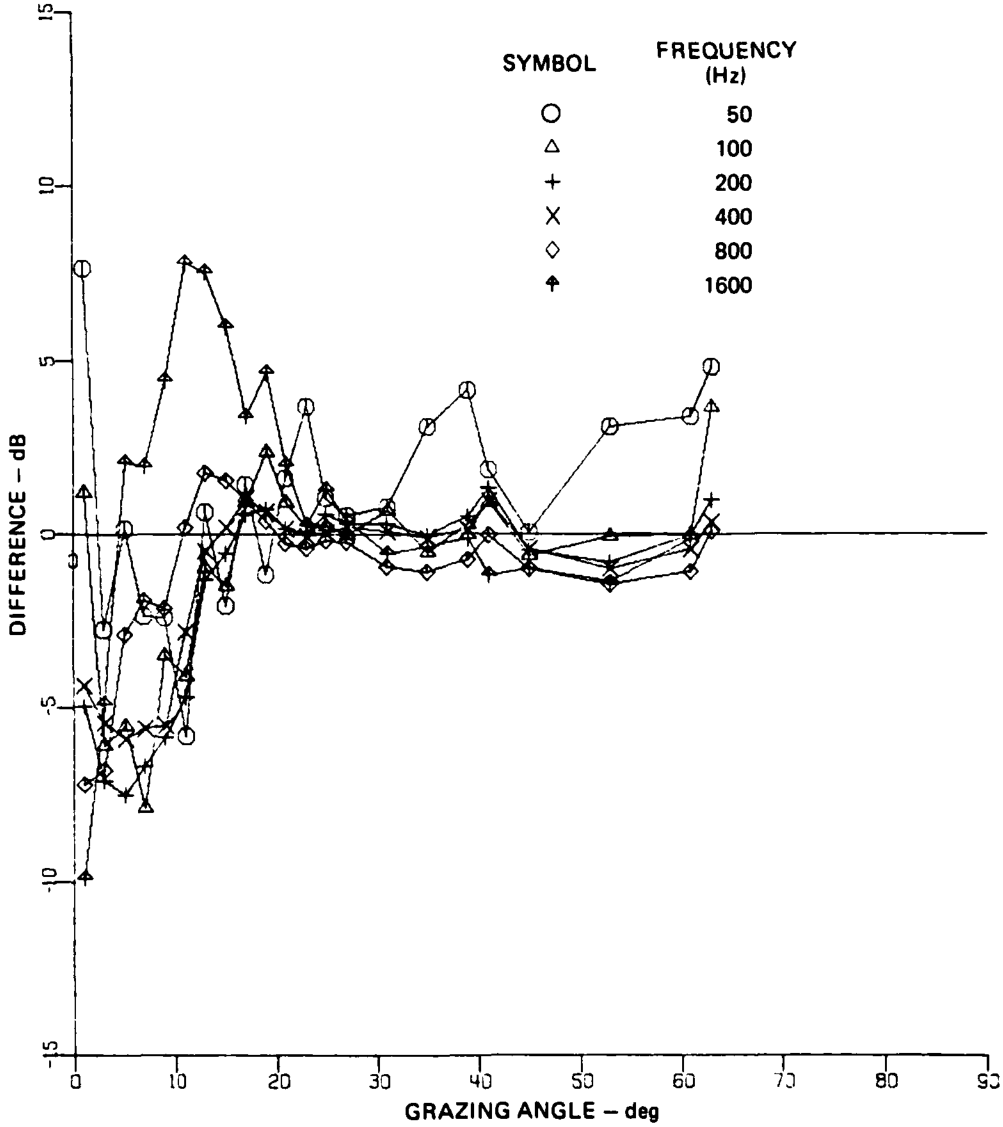

DIFFERENCE BETWEEN BLUP PREDICTED BOTTOM LOSS AND NADC DATA AT LOCATION 11

ARL:UT
AS-81-1166
DPK - GA
9-17-81

L. Location 12

1. Deficiencies

(1) For 100 Hz in the angular region $0^{o} < \theta g < 10^{o}$, BLUP predictions fall below the data by a maximum of 5 dB at 1^{o} (problem type 3).

(2) For 100 Hz in the region $30^{o} < \theta g < 60^{o}$, BLUP predictions exceed the data by 1 dB. For 50 Hz in the region $20^{o} < \theta g < 55$, predictions exceed the data (maximum difference of 3 dB at 30^{o}) (problem type 4).

(3) For 1600 Hz in the region $2^{o} < \theta g < 20^{o}$, predictions exceed the data (maximum difference of 8 dB at 13^{o}) (problem type 1).

(4) For 800 Hz in the region $16^{o} < \theta g < 70^{o}$, predictions fall below the data (maximum difference of 2 dB at 30^{o}) (problem type 2).

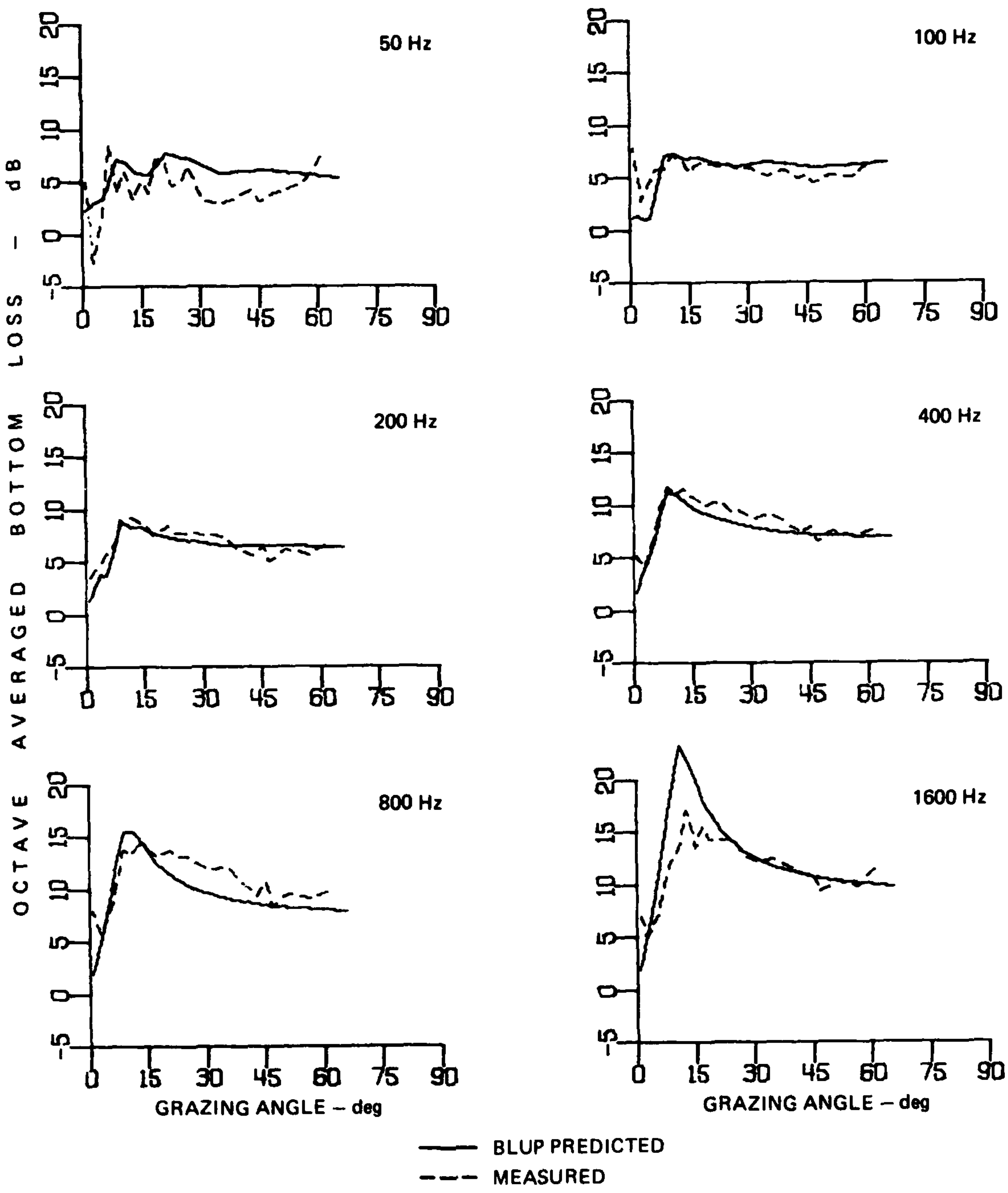

OCTAVE AVERAGED BOTTOM LOSS PREDICTED BY BOTTOM LOSS UPGRADE GEOACOUSTIC PROFILE versus NADC BOTTOM LOSS DATA AT LOCATION 12

ARL:UT
AS-81-1136
DPK - GA
9 - 17 - 81

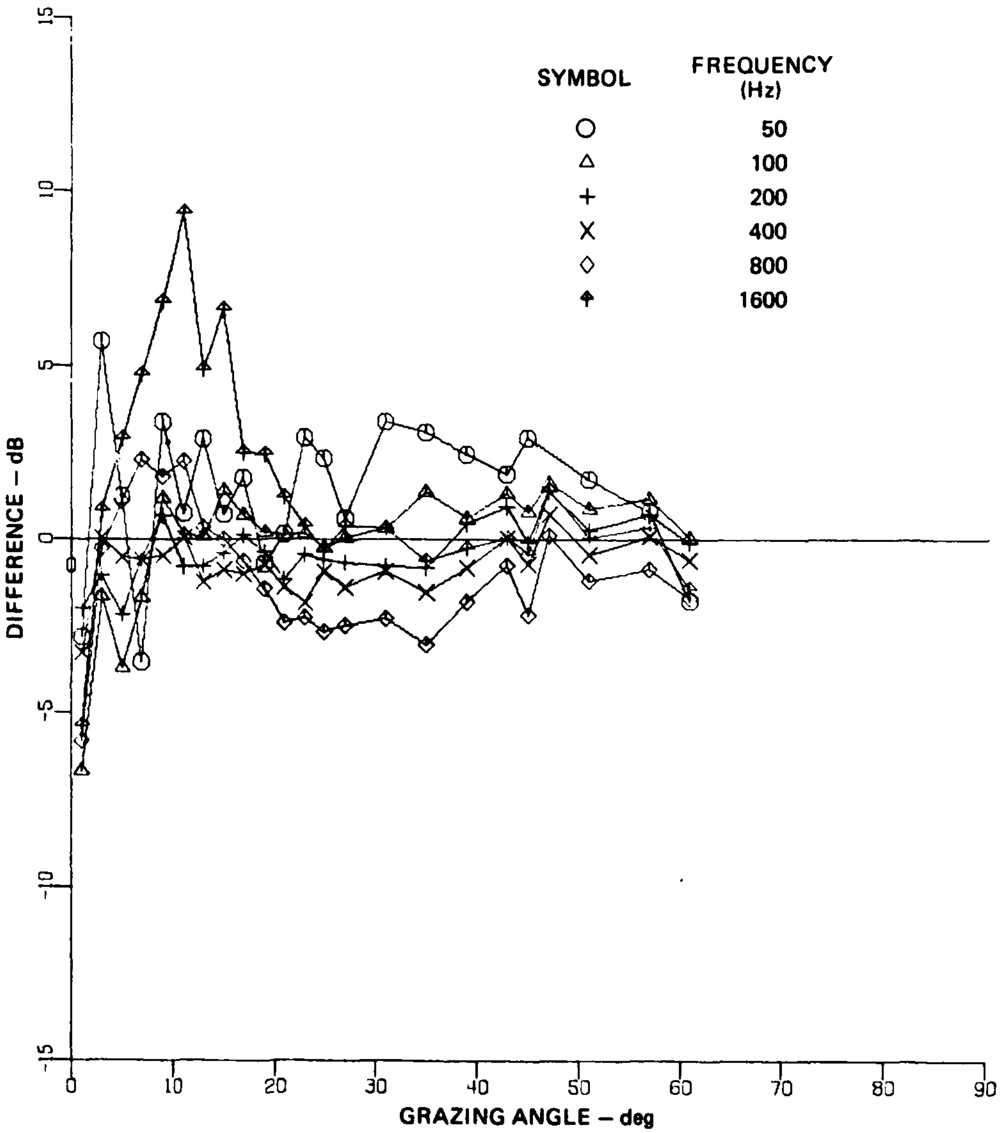

DIFFERENCE BETWEEN BLUP PREDICTED BOTTOM LOSS AND NADC DATA AT LOCATION 12

ARL:UT
AS-81-1167
DPK - GA
9 - 17 - 81

M. Location 13

1. Deficiencies

(1) For all frequencies in the angular region $0^{o}<\theta g<13^{o}$, BLUP predictions fall below the data (maximum difference of 9 dB for 50 Hz, 8 dB for 200 Hz, 7 dB for 400, and 800 Hz at 5^{o}) (problem type 3).

(2) For 50 Hz in the region $13^{o}<\theta g<50^{o}$, predictions exceed the data (maximum difference of 4 dB at 12^{o}). Also, for 100 Hz in the region $13^{o}<\theta g<30^{o}$, predictions exceed the data (maximum difference of 3 dB at 16^{o}) (problem type 4).

(3) For 400 Hz in the region $15^{o}<\theta g<65^{o}$, predictions fall below the data (maximum difference of 2 dB at 25^{o}). Also, for 800 Hz in the same region, predictions fall below the data (maximum difference of 7 dB at 30^{o}) (problem type 2).

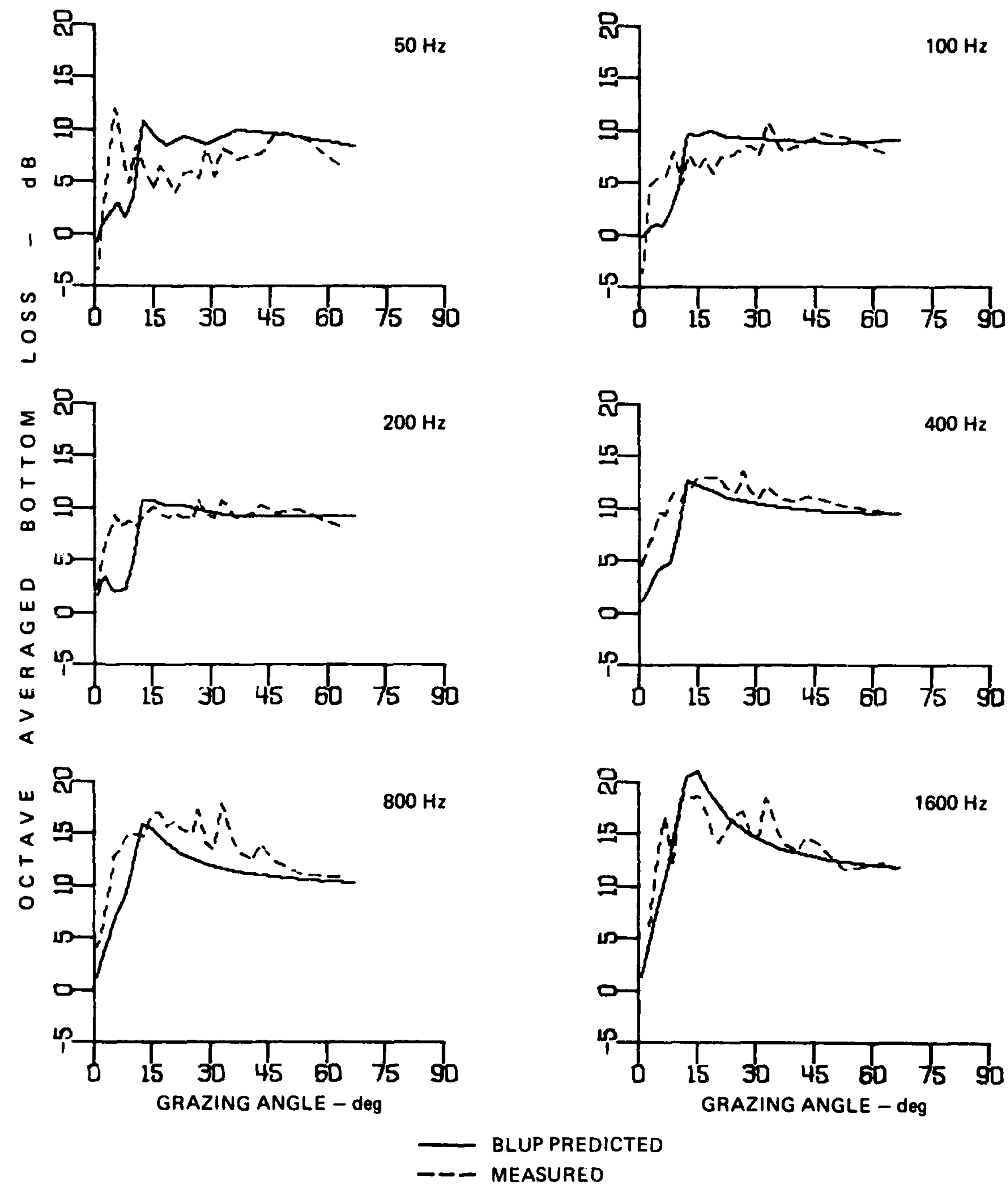

OCTAVE AVERAGED BOTTOM LOSS PREDICTED BY BOTTOM LOSS UPGRADE GEOACOUSTIC PROFILE *versus* NADC BOTTOM LOSS DATA AT LOCATION 13

ARL:UT
AS-81-1137
DPK - GA
9 - 17 - 81

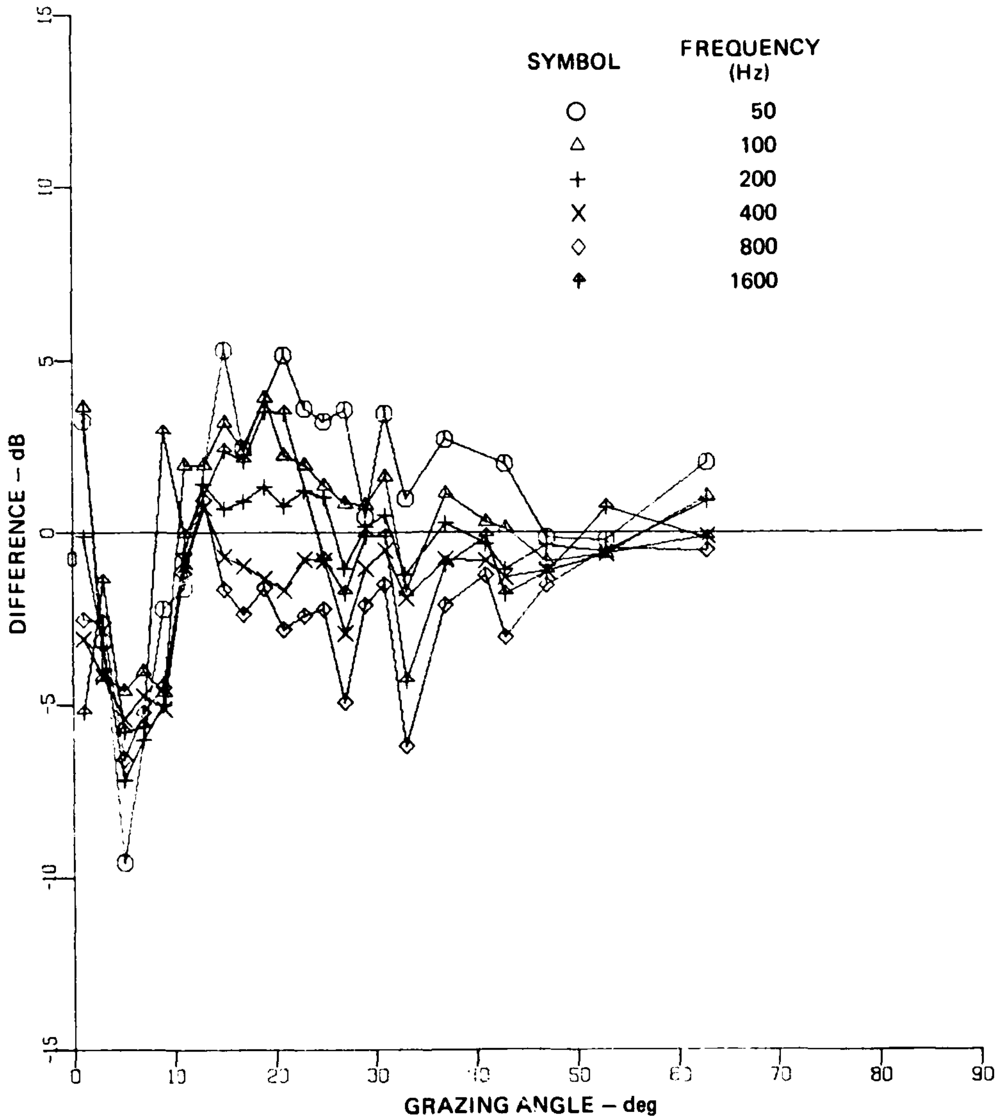

DIFFERENCE BETWEEN BLUP PREDICTED BOTTOM LOSS AND NADC DATA AT LOCATION 13

ARL:UT
AS-81-1168
DPK - GA
9 - 17 - 81

N. Location 14

1. Deficiencies

(1) For 50 Hz in the angular region $0^{o}<\theta g<55^{o}$, BLUP predictions exceed the data (maximum difference of 4 dB at 17^{o}) (problem type 4).

(2) For 100 Hz in the region $0^{o}<\theta g<15^{o}$, predictions fall below the data (maximum difference of 6 dB at 2^{o}) (problem type 3).

(3) For 200, 400, 800, and 1600 Hz in the region $30^{o}<\theta g<60^{o}$, prediction fall below the data by an average value of 7 dB at 45^{o} (problem type 2).

(4) For 1600 Hz in the region $5^{o}<\theta g<25^{o}$, predictions exceed the data (maximum difference of 7 dB at 10^{o}). Also, for 800 Hz in the region $5^{o}<\theta g<15^{o}$, predictions fall below the data (maximum difference of 5 dB at 10^{o}) (problem type 1).

2. Comments

The BLUP model fit to the data for this location was exceptionally poor.

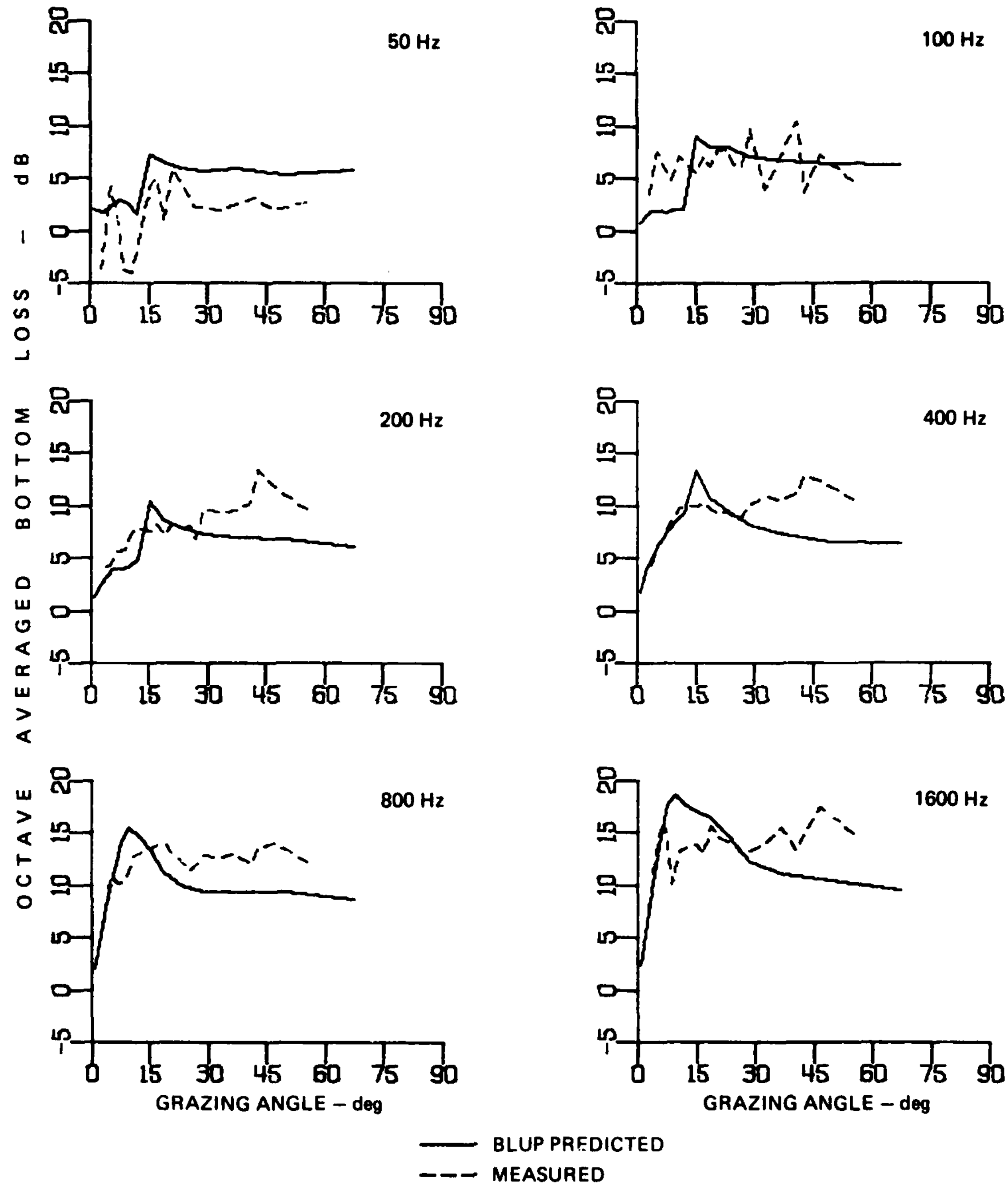

OCTAVE AVERAGED BOTTOM LOSS PREDICTED BY BOTTOM LOSS UPGRADE GEOACOUSTIC PROFILE versus NADC BOTTOM LOSS DATA AT LOCATION 14

ARL:UT
AS-81-1138
DPK - GA
9 - 17 - 81

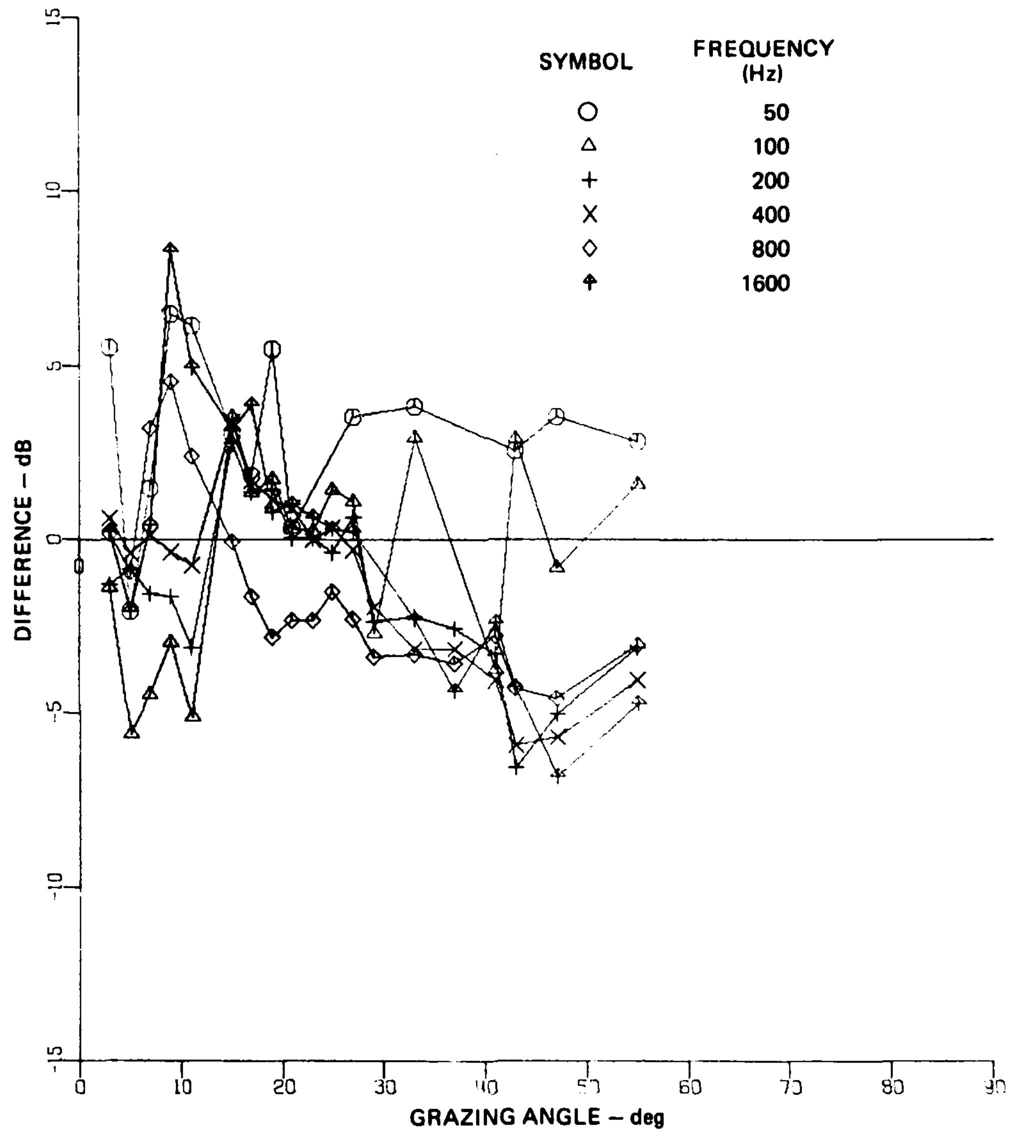

DIFFERENCE BETWEEN BLUP PREDICTED BOTTOM LOSS AND NADC DATA AT LOCATION 14

ARL:UT
AS-81-1169
DPK - GA
9 - 17 - 81

O. Location 15

1. Deficiencies

(1) For 50 Hz in the angular region $13^{0}<\theta g<27^{0}$ and $30^{0}<\theta g<60^{0}$, the BLUP model exceeds the data (maximum difference of 3 dB at 50^{0}). For 100 Hz in the region $15^{0}<\theta g<19^{0}$ and $20^{0}<\theta g<35^{0}$, predictions fall below the data by a maximum value of 3 dB at 15^{0}. Also, for 100 Hz in the region $35^{0}<\theta g<60^{0}$, predictions exceed the data (maximum difference of 4 dB at 55^{0}) (problem type 4).

(2) For 200 and 400 Hz in the region $0^{0}<\theta g<14^{0}$, predictions fall below the data (maximum difference of 5.5 dB at 10^{0} for 200 Hz) (problem type 3).

(3) For 400, 800, and 1600 Hz in the region $15^{0}<\theta g<45^{0}$, predictions fall below the data (maximum difference of 4 dB at 30^{0} for 800 Hz) (a combination of problem types 2 and 4).

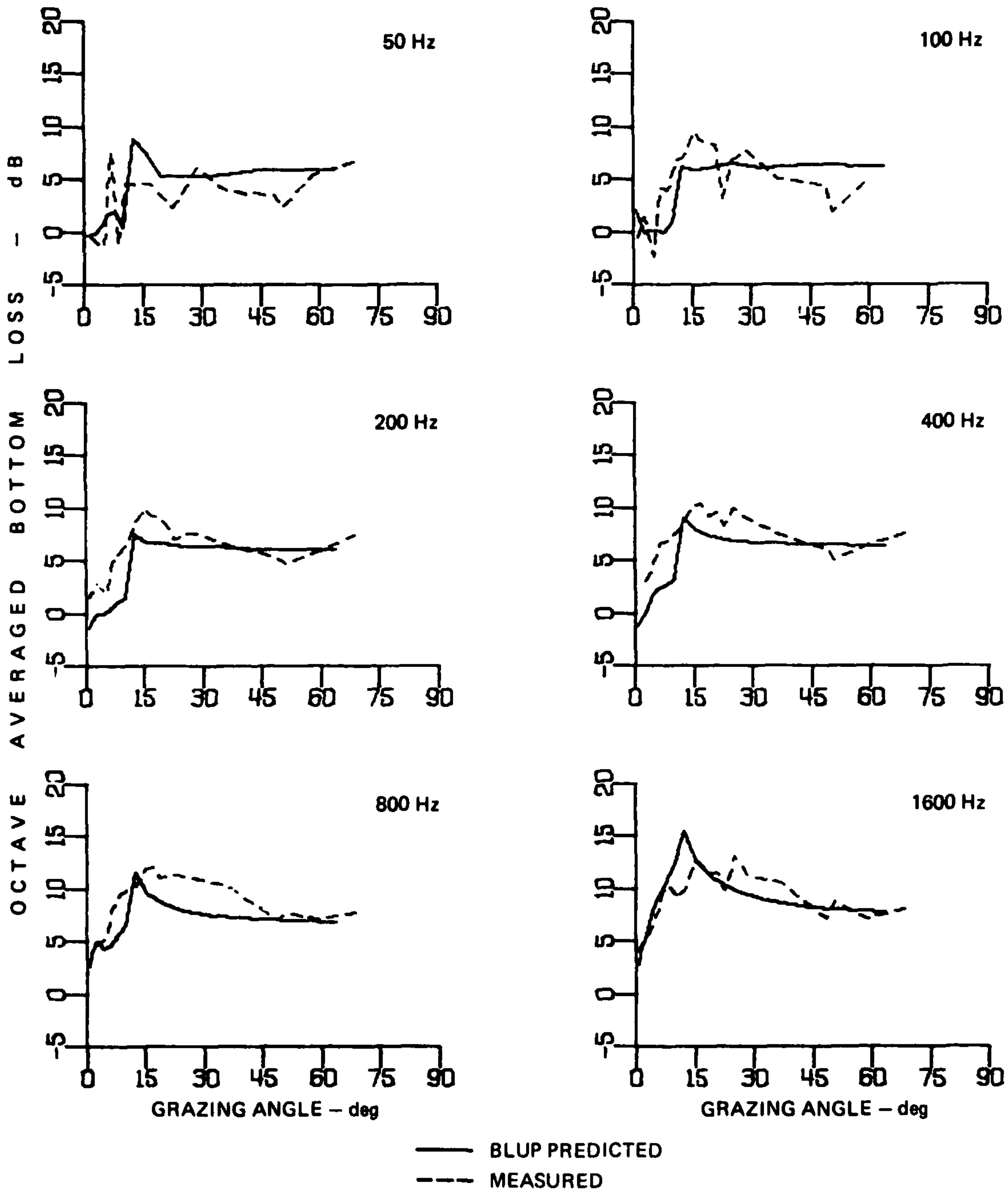

OCTAVE AVERAGED BOTTOM LOSS PREDICTED BY BOTTOM LOSS UPGRADE GEOACOUSTIC PROFILE versus NADC BOTTOM LOSS DATA AT LOCATION 15

ARL:UT
AS-81-1139
DPK - GA
9 - 17 - 81

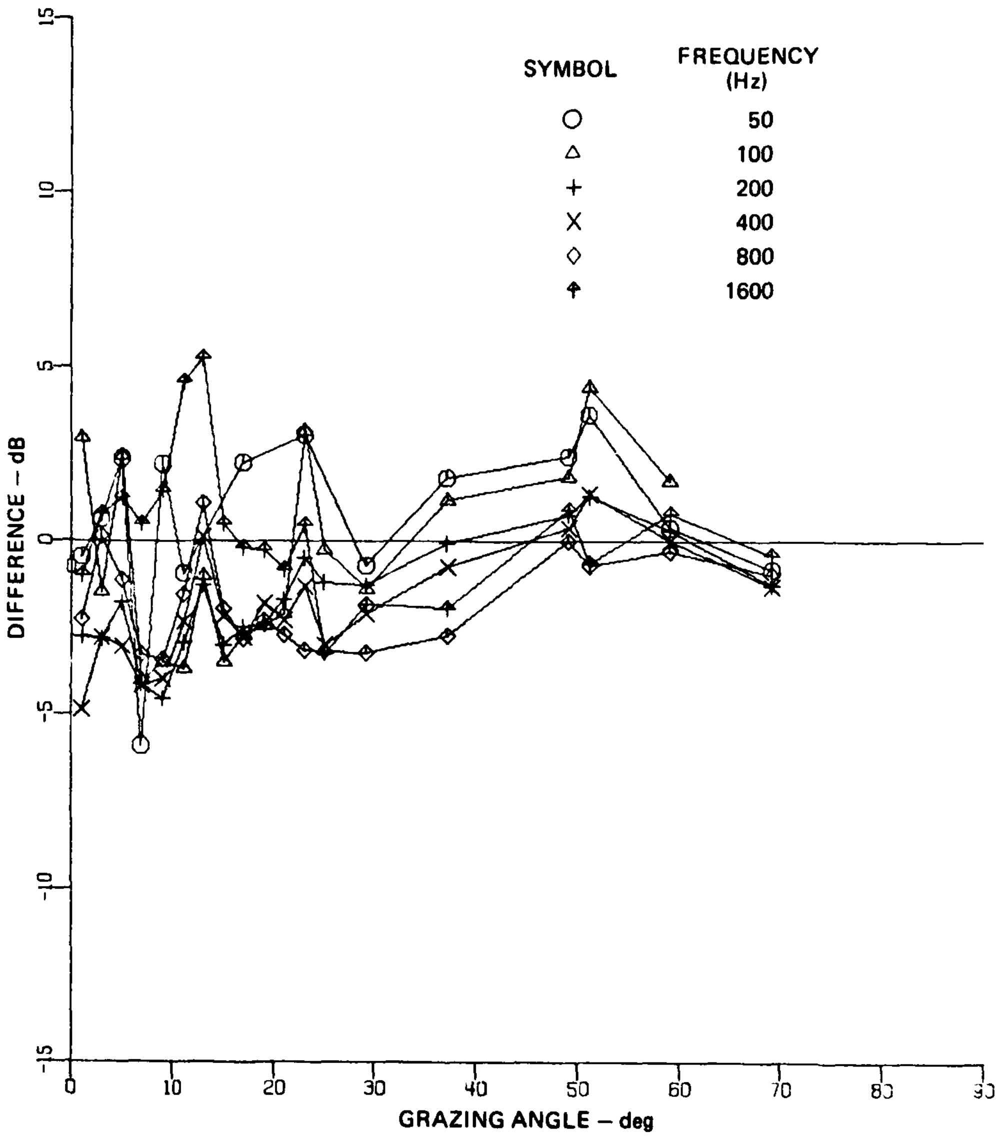

DIFFERENCE BETWEEN BLUP PREDICTED BOTTOM LOSS AND NADC DATA AT LOCATION 15

ARL:UT
AS-81-1170
DPK - GA
9 - 17 - 81

P. Location 16

1. Deficiencies

(1) For 50, 100, 200, 400, and 800 Hz in the region $0^{\circ} < \theta g < 12^{\circ}$, BLUP predictions fall below the data (maximum difference of 6 dB at 8° for 50 Hz) (problem type 3).

(2) For 50, 100, 200, and 400 Hz in the region $45^{\circ} < \theta g < 70^{\circ}$, predictions exceed the data (maximum difference of 6 dB at 50° for 50 Hz) (problem type 4).

(4) As problem type 4 diminishes with increasing frequency, predictions centered about 40° exceed the data by greater amounts with increasing frequency up to 800 Hz (maximum difference of 5 dB).

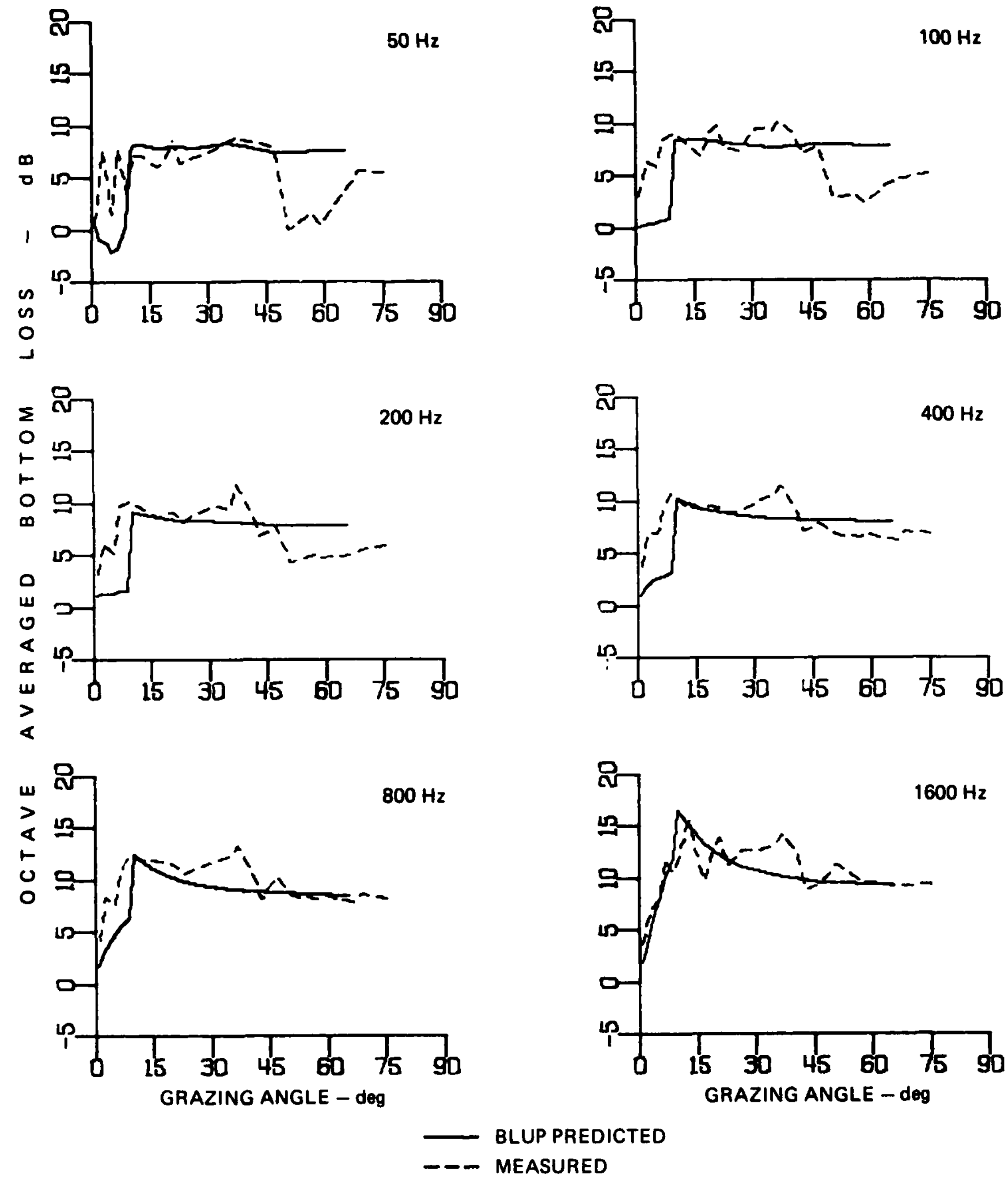

OCTAVE AVERAGED BOTTOM LOSS PREDICTED BY BOTTOM LOSS UPGRADE GEOACOUSTIC PROFILE versus NADC BOTTOM LOSS DATA AT LOCATION 16

ARL:UT
AS-81-1140
DPK - GA
9 - 17 - 81

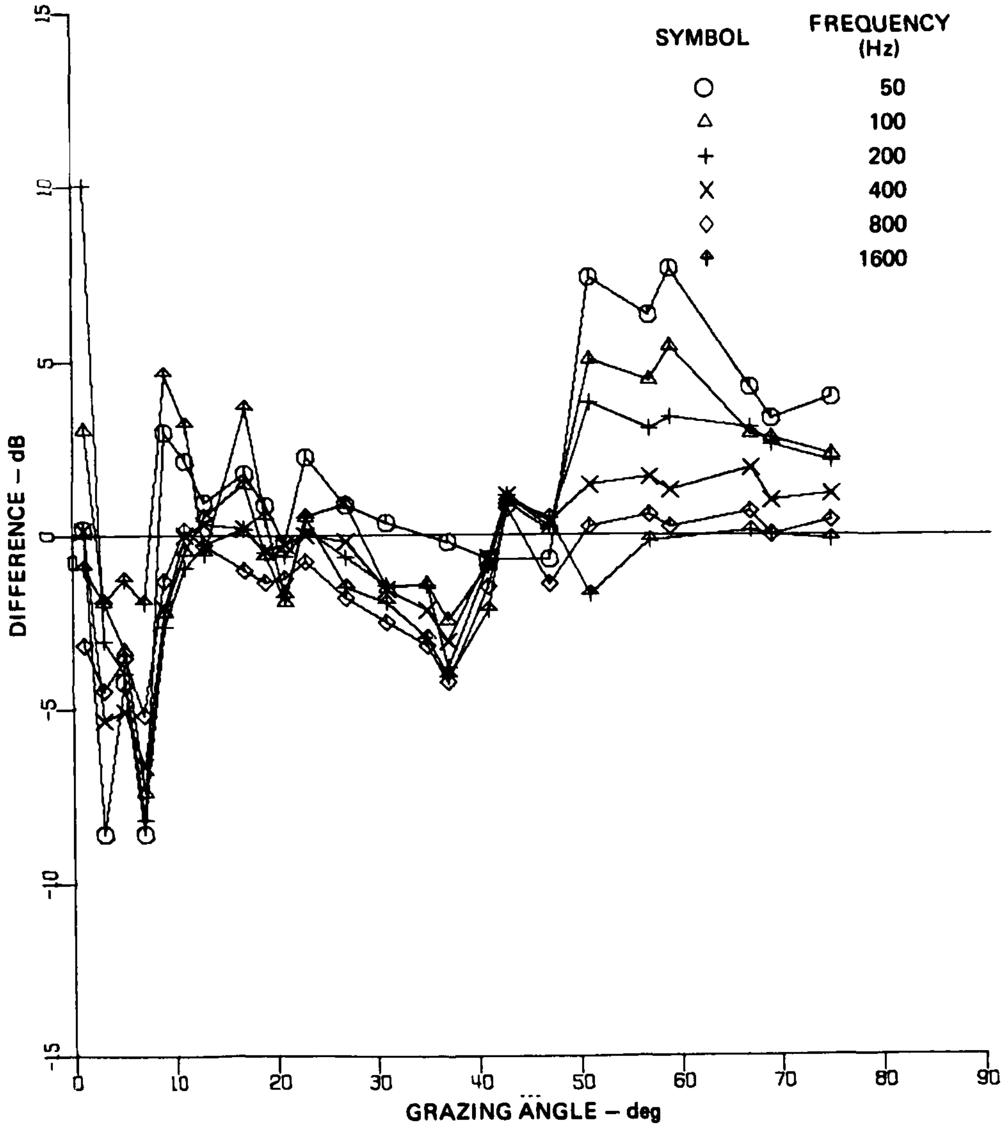

DIFFERENCE BETWEEN BLUP PREDICTED BOTTOM LOSS AND NADC DATA AT LOCATION 16

ARL:UT
AS-81-1171
DPK - GA
9 - 17 - 81

Q. Location 17

1. Deficiencies

(1) In the angular region $0^{o} < \theta g < 12^{o}$, BLUP predictions fall below the data for all frequencies. The data in this region exhibits extraordinary high bottom loss. One can only speculate as to the physical mechanisms causing this high bottom loss.

2. Comments

The data shows a consistent rise at low angles that is not seen in the rest of the data.

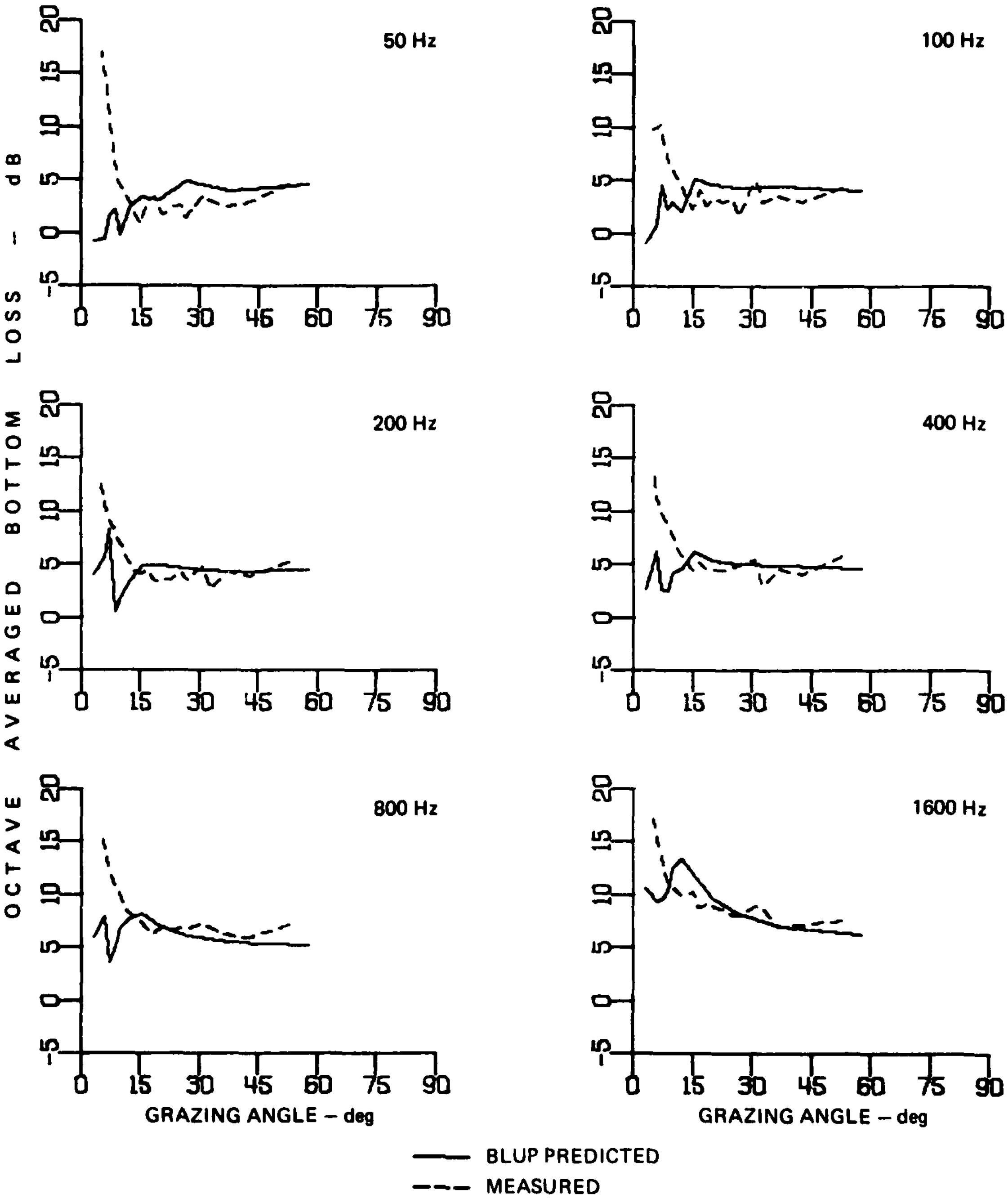

OCTAVE AVERAGED BOTTOM LOSS PREDICTED BY BOTTOM LOSS UPGRADE GEOACOUSTIC PROFILE versus NADC BOTTOM LOSS DATA AT LOCATION 17

ARL:UT
AS-81-1141
DPK - GA
9 - 17 - 81

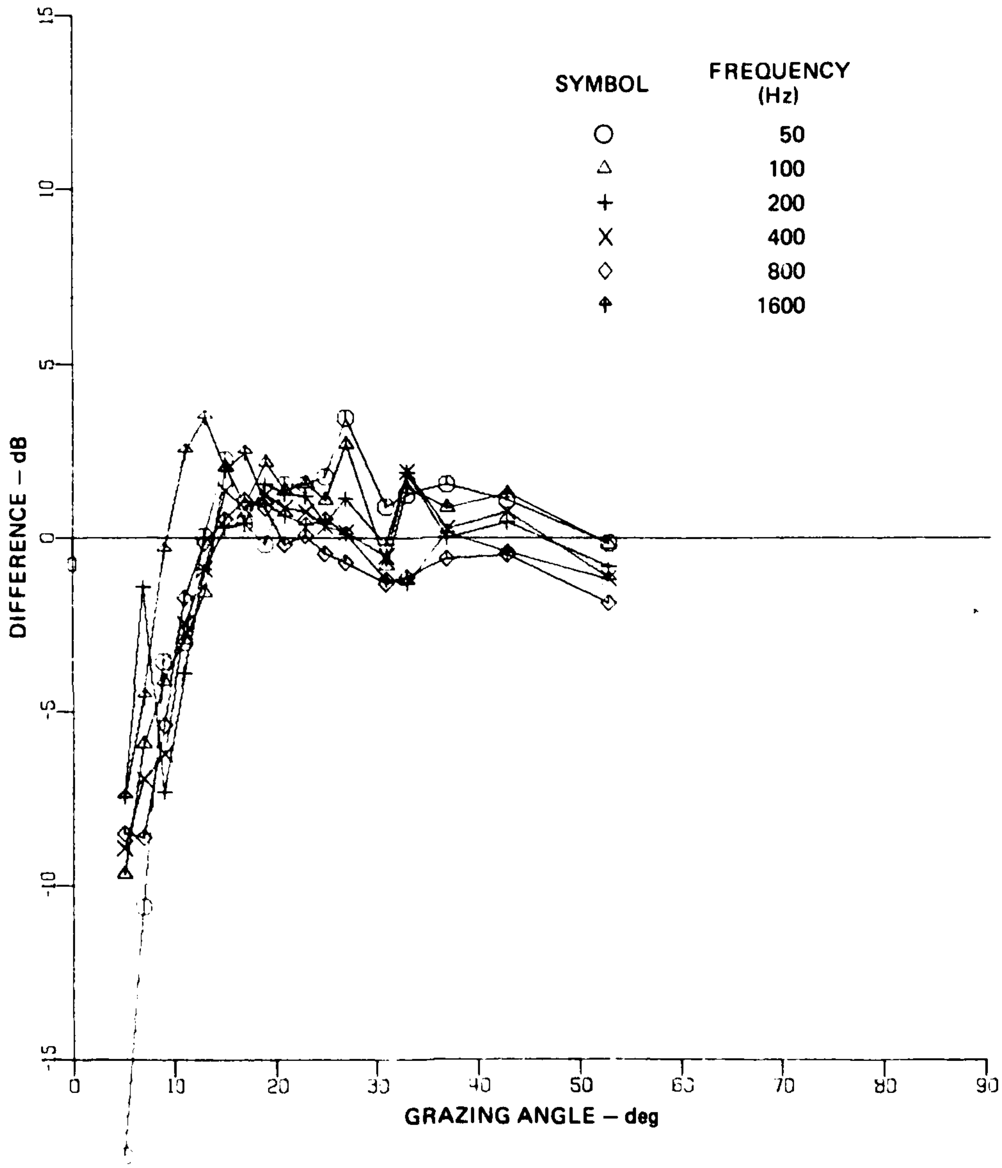

DIFFERENCE BETWEEN BLUP PREDICTED BOTTOM LOSS AND NADC DATA AT LOCATION 17

ARL:UT
AS-81-1172
DPK - GA
9 - 17 - 81

AD-A120 077 TEXAS UNIV AT AUSTIN APPLIED RESEARCH LABS F/G 20/1
GENERATION AND ANALYSIS OF BOTTOM LOSS UPGRADE GEOACOUSTIC PARA--ETC(U)
AUG 82 D P KNOBLES, P J VIDMAR N00014-82-C-0049
UNCLASSIFIED ARL-TR-82-17 NL

2 OF 2
AD A
120077

END
DATE
FILMED
1-83
DTIC

R. Location 18

1. Deficiencies

(1) For 50, 100, 200, 400, and 800 Hz in the angular region $5^{0}<\theta g<15^{0}$, BLUP predictions fall below the data (maximum difference of 7 dB at 5^{0} for 200 Hz) (problem type 3).

(2) For 50 Hz in the region $20^{0}<\theta g<60^{0}$, predictions exceed the data (maximum difference of 4 dB at 35^{0}) (problem type 4).

(3) Starting with 200 Hz at 16^{0}, predictions begin to fall below the data. This condition becomes more severe for the higher frequencies (maximum difference of 7 dB at 35^{0} for 1600 Hz) (problem type 2).

2. Comments

The difference curve clearly illustrates a frequency dependence at high angles not predicted by BLUP. This frequency dependence also occurs at other locations.

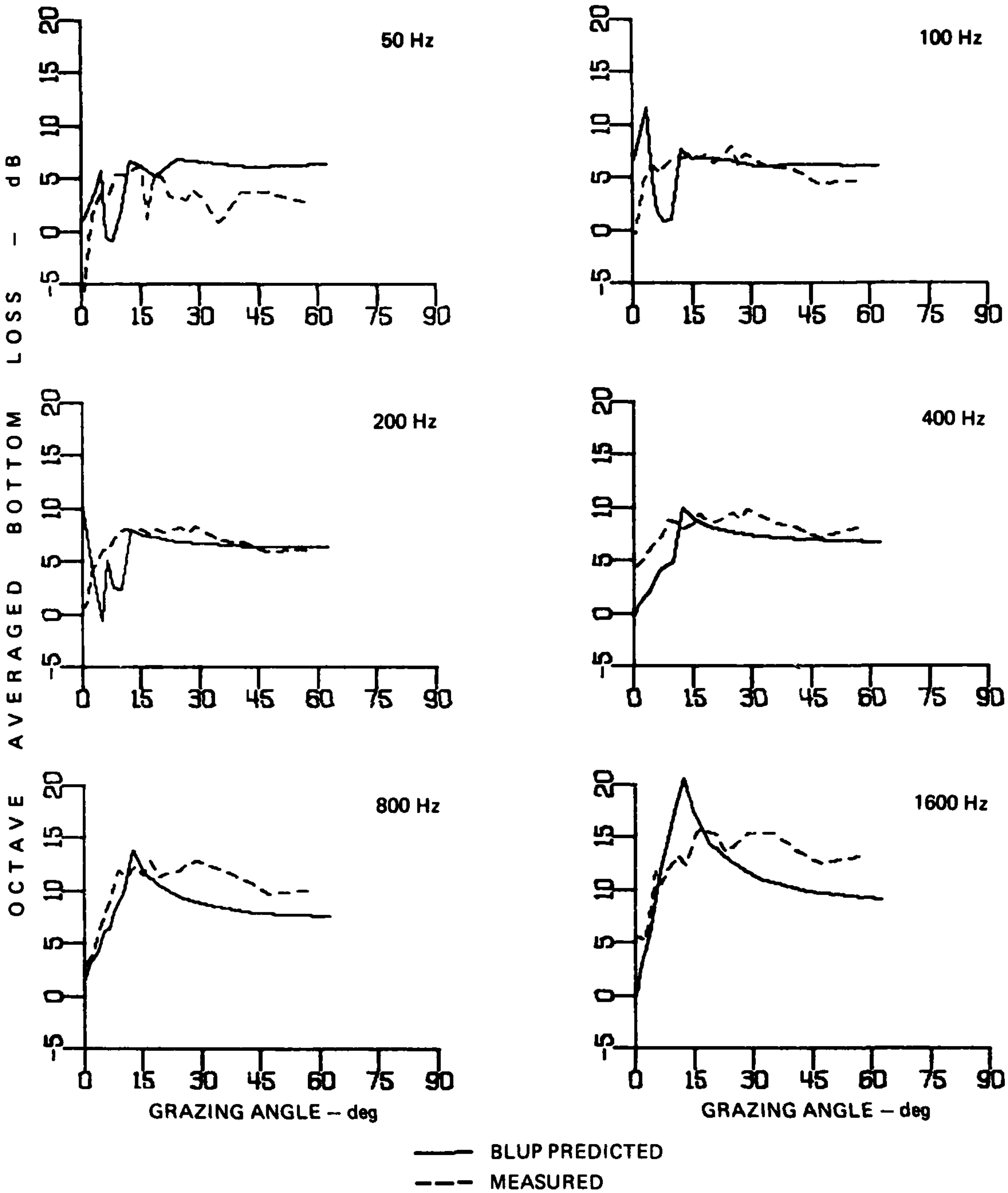

OCTAVE AVERAGED BOTTOM LOSS PREDICTED BY BOTTOM LOSS UPGRADE GEOACOUSTIC PROFILE versus NADC BOTTOM LOSS DATA AT LOCATION 18

ARL:UT
AS-81-1142
DPK - GA
9 - 17 - 81

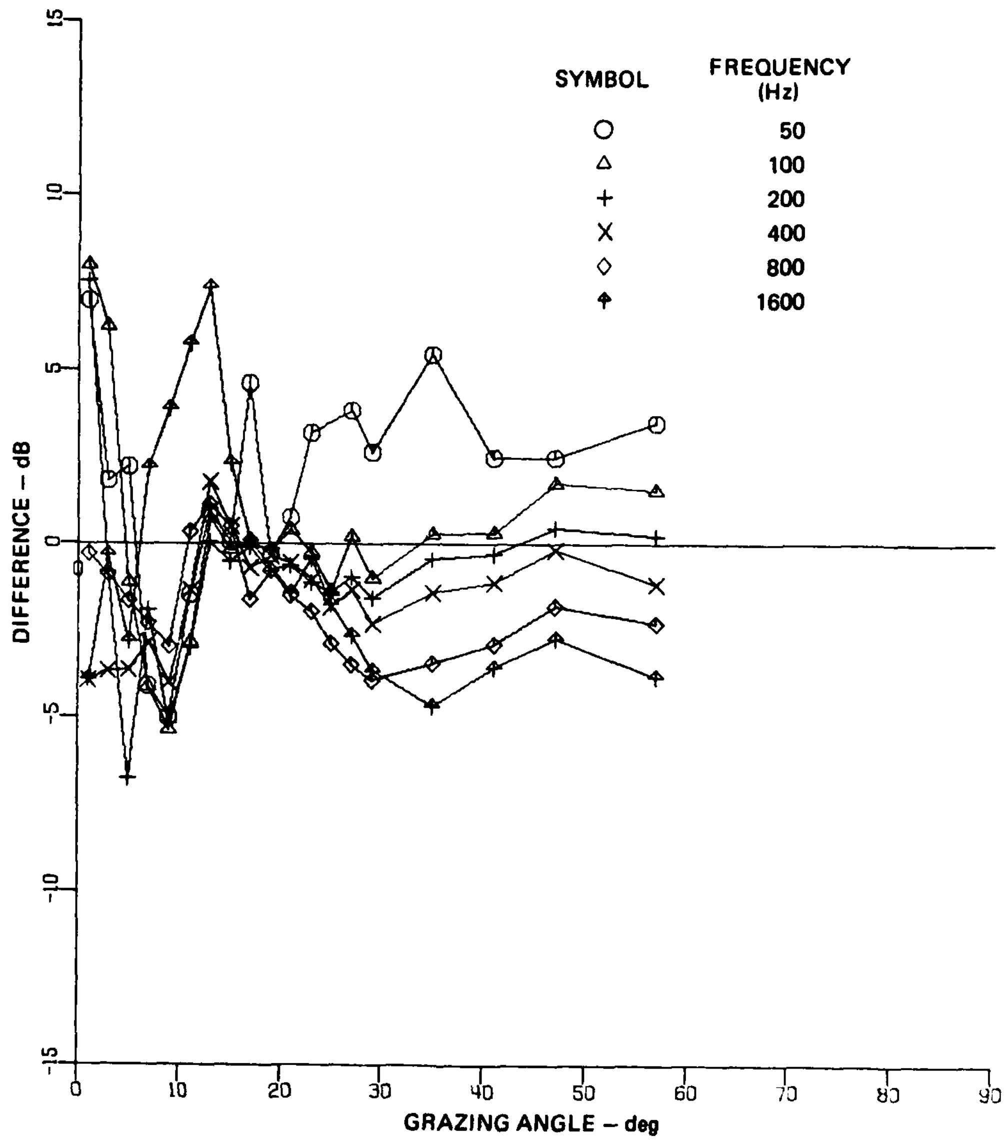

DIFFERENCE BETWEEN BLUP PREDICTED BOTTOM LOSS AND NADC DATA AT LOCATION 18

ARL:UT
AS-81-1173
DPK - GA
9 - 17 - 81

S. Location 19

1. Deficiencies

(1) For all frequencies in the angular region $5^{o}<\theta g<11^{o}$, BLUP predictions fall below the data (maximum difference of 12 dB at 8^{o} for 200 Hz) (problem type 3).

(2) For all frequencies in the region $20^{o}<\theta g<35^{o}$, predictions fall below the data (maximum difference of 6 dB at 21^{o} for 50 Hz) (problem type 4).

(3) For 100, 200, 400, and 800 Hz in the region $40^{o}<\theta g<70^{o}$, predictions fall below the data (maximum difference of 5 dB at 48^{o} for 800 Hz) (problem type 2).

(4) For 800 and 1600 Hz in the region $10^{o}<\theta g<22^{o}$, predictions exceed the data (maximum difference of 11 dB at 11^{o} for 1600 Hz) (problem typè 1).

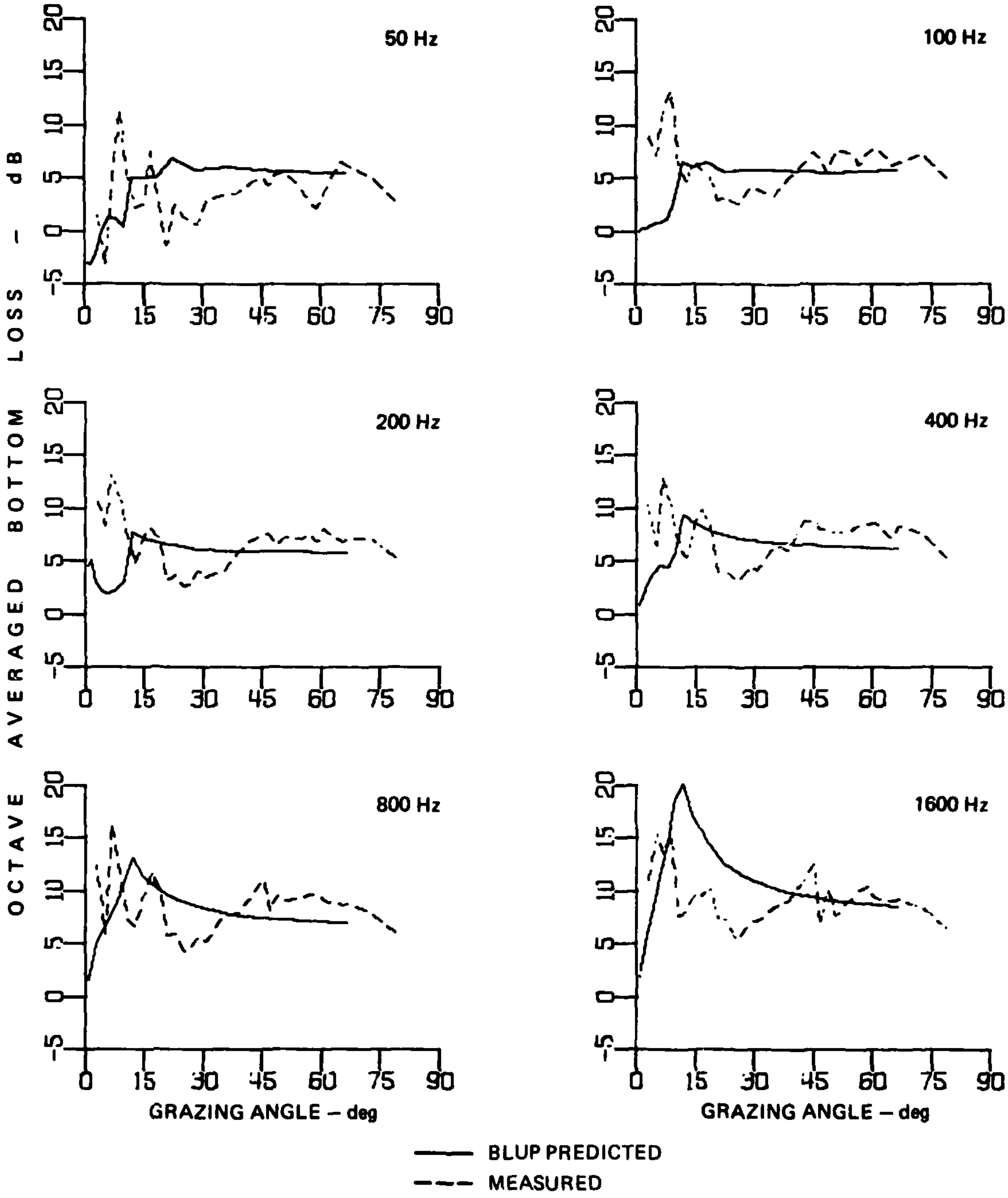

OCTAVE AVERAGED BOTTOM LOSS PREDICTED BY BOTTOM LOSS UPGRADE GEOACOUSTIC PROFILE versus NADC BOTTOM LOSS DATA AT LOCATION 19

ARL:UT
AS-81-1143
DPK - GA
9 - 17 - 81

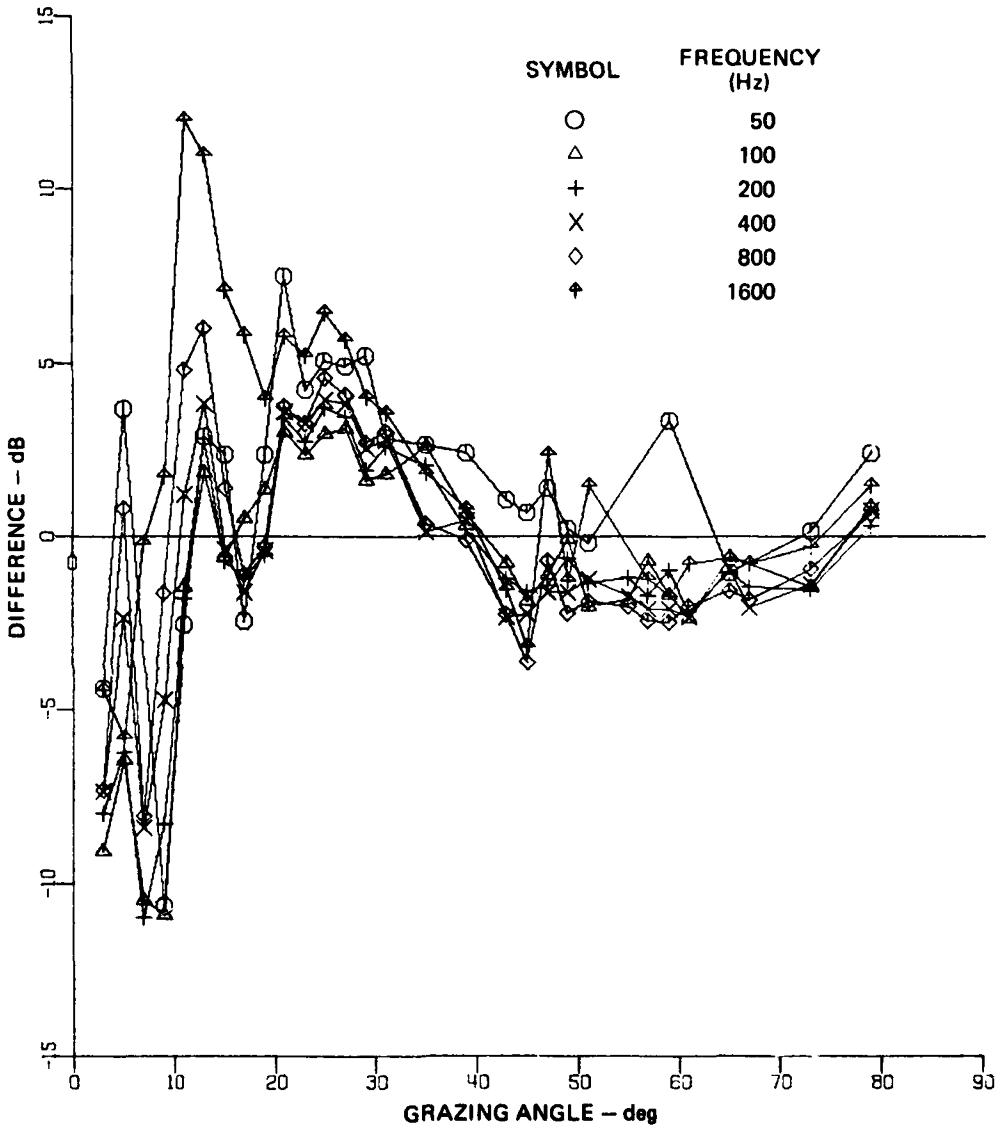

DIFFERENCE BETWEEN BLUP PREDICTED BOTTOM LOSS AND NADC DATA AT LOCATION 19

ARL:UT
AS-81-1174
DPK - GA
9 - 17 - 81

T. Locations 20-24 and 26-29

All of the above locations were given the same BLUP parameters (except for some minor differences in substrate reflectivity) since the locations are separated by small distances and the data for each location exhibit similar characteristics.

1. Deficiencies

50 Hz Deficiencies

(1) In the angular region $5^{o}<\theta g<15^{o}$, BLUP predictions fall below the data by an average of 4 dB (problem type 3).

(2) In the region $15^{o}<\theta g<45^{o}$, predictions exceed the data (average maximum value of 2.5 dB).

100 Hz Deficiencies

(1) In the region $5^{o}<\theta g<15^{o}$, predictions fall below the data by a maximum average of 2 dB (problem type 3).

(2) In the region $15^{o}<\theta g<40^{o}$, predictions exceed the data by a maximum average of 2 dB (problem type 4).

(3) Locations 20, 23, 26, 27, 28, and 29 in the region $45^{o}<\theta g<70^{o}$, predictions fall below the data by a maximum average of 1.5 dB (problem type 2).

200 Hz Deficiencies

(1) Except for locations 20, 21, and 29 in the region $5^{o}<\theta g<15^{o}$, predictions fall below the data by an average maximum of 3 dB (problem type 3).

(2) In the region $15^{o}<\theta g<40^{o}$, predictions exceed the data by an average maximum of 3 dB (problem type 4).

(3) Except for location 21, predictions in the region $45^{o}<\theta g<70^{o}$ fall below the data by an average maximum of 2.5 dB (problem type 2).

400 Hz Deficiencies

(1) Except for locations 20, 21, and 29, predictions in the region $5^{o}<\theta g<10^{o}$ fall below the data by a maximum average of 3 dB (problem type 3).

(2) In the region $10^{o}<\theta g<30^{o}$, predictions exceed the data by an average maximum of 3 dB (problem types 1 and 4).

(4) In the region $30^{o}<\theta g<70^{o}$, predictions fall below the data by an average maximum of 2.5 dB (problem type 2).

800 Hz Deficiencies

(1) In the region $10^{o}<\theta g<30^{o}$, predictions exceed the data by an average maximum value of 2 dB (problem types 1 and 4).

(2) Except for location 26 in the region $30^{o}<\theta g<70^{o}$, predictions fall below the data by an average maximum of 2 dB (problem type 2).

<u>1600 Hz Deficiencies</u>

(1) In the region $5^{o}<\theta g<30^{o}$, predictions exceed the data by an average maximum of 5 dB (problem types 1 and 4).

(2) For locations 23, 24, 27, 28, and 29 in the region $45^{o}<\theta g<70^{o}$, predictions fall below the data by an average maximum of 2 dB (problem type 2).

2. <u>Comments</u>

It was found that a surface layer for these locations helped reduce the magnitude of problem type 1. For the higher frequencies the wavelength is on the order of the thickness of the surface layer. This causes less energy to be transmitted into the sediment due to reflection, decreasing the bottom loss about θ_c.

The worst fits are those of 200 and 400 Hz. No combination of BLUP parameters can give a bottom loss increasing with angle for these frequencies.

The difference curves for many of these locations show an angular dependence not predicted by BLUP. Location 22 particularly illustrates this dependence on angle.

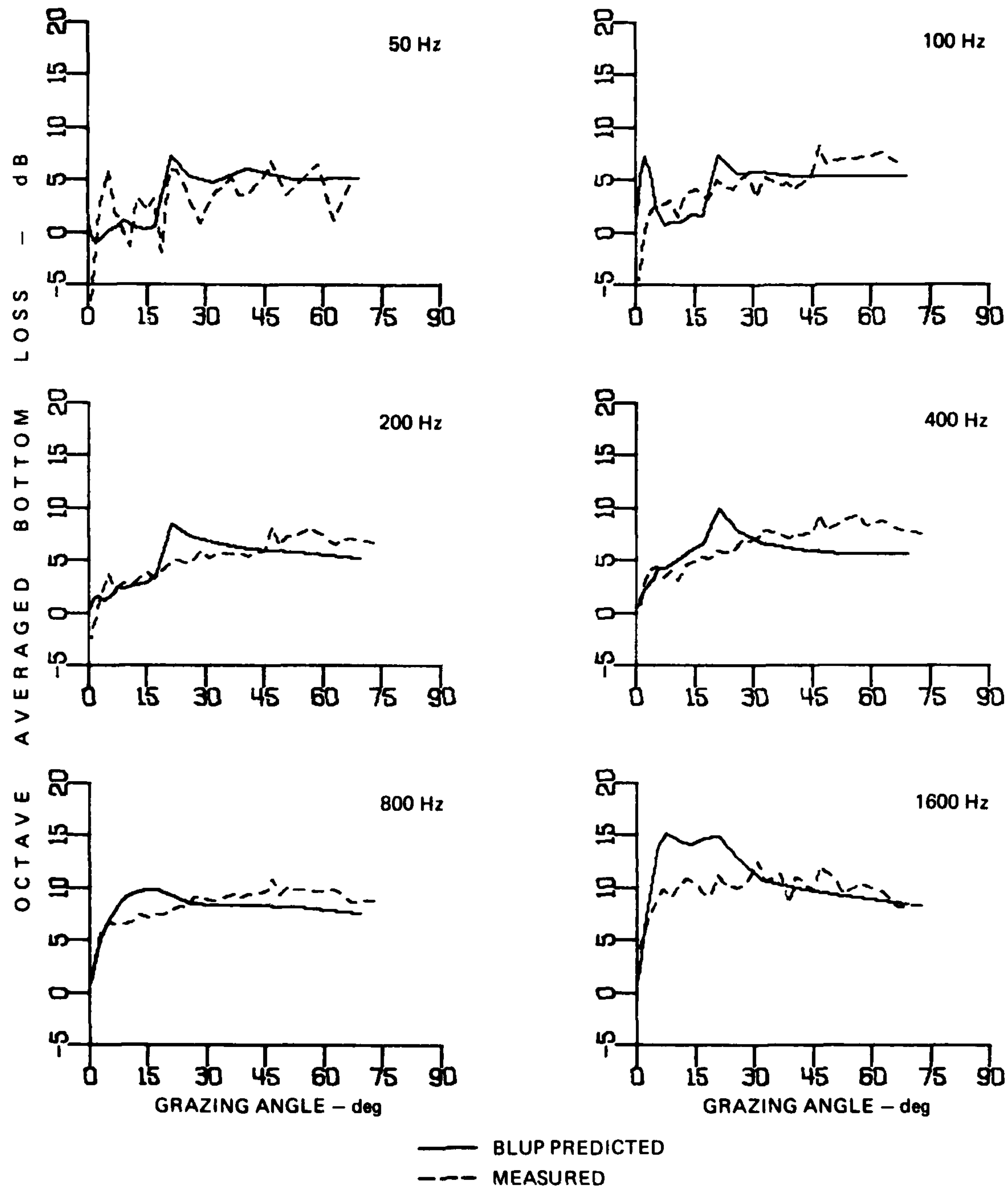

OCTAVE AVERAGED BOTTOM LOSS PREDICTED BY BOTTOM LOSS UPGRADE GEOACOUSTIC PROFILE versus NADC BOTTOM LOSS DATA AT LOCATION 20

ARL:UT
AS-81-1144
DPK - GA
9 - 17 - 81

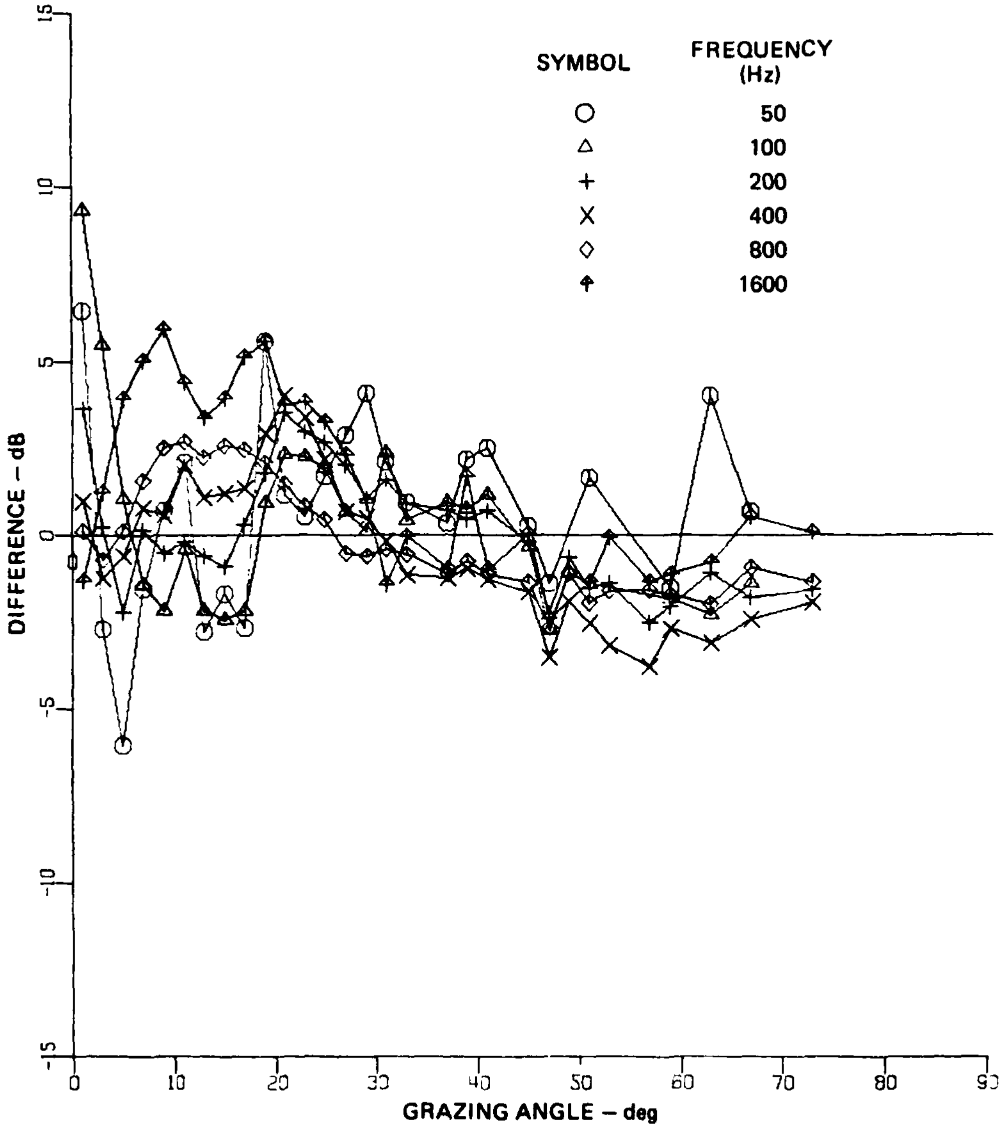

DIFFERENCE BETWEEN BLUP PREDICTED BOTTOM LOSS AND NADC DATA AT LOCATION 20

ARL:UT
AS-81-1175
DPK - GA
9 - 17 - 81

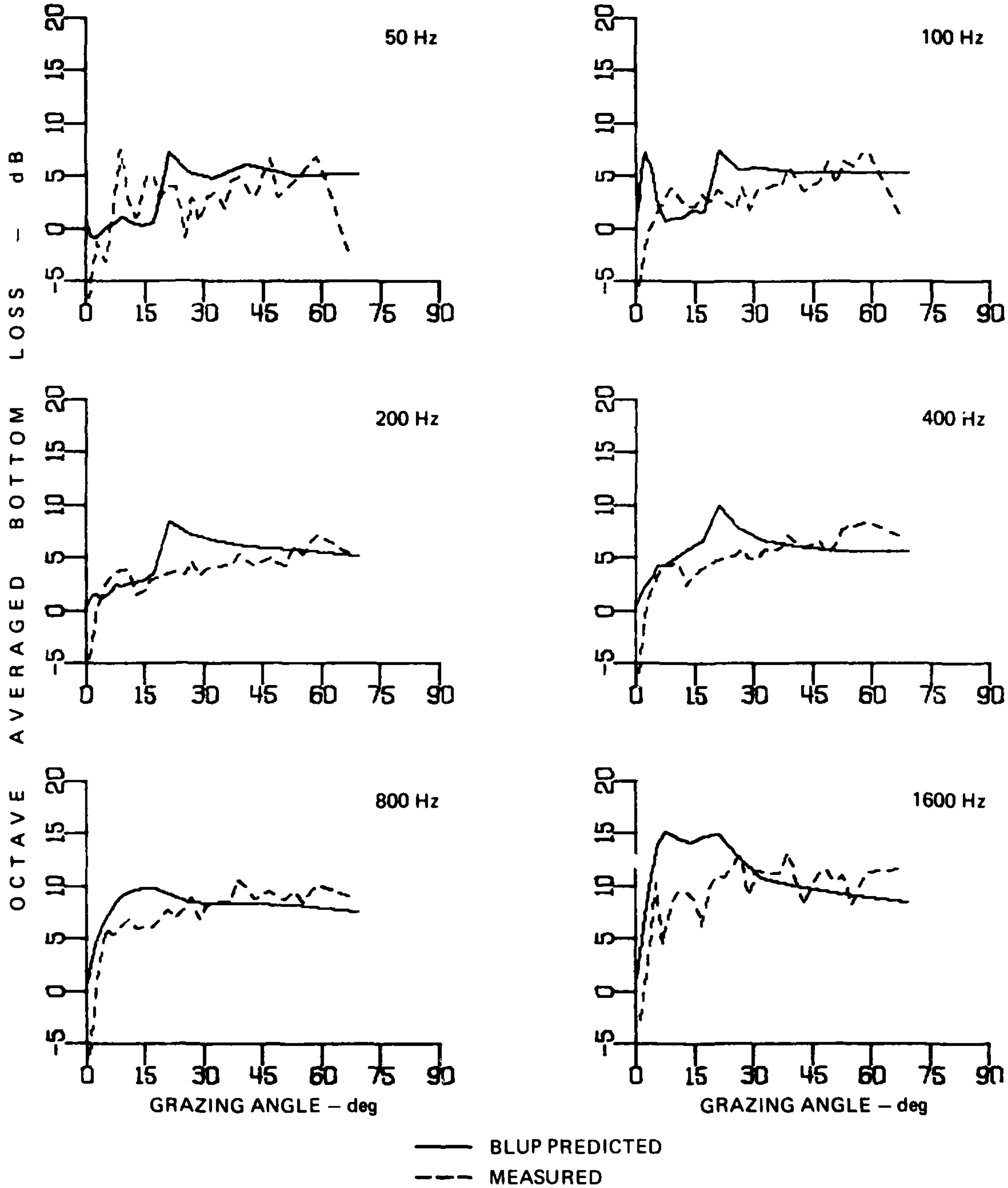

OCTAVE AVERAGED BOTTOM LOSS PREDICTED BY BOTTOM LOSS UPGRADE GEOACOUSTIC PROFILE versus NADC BOTTOM LOSS DATA AT LOCATION 21

ARL:UT
AS-81-1145
DPK - GA
9 - 17 - 81

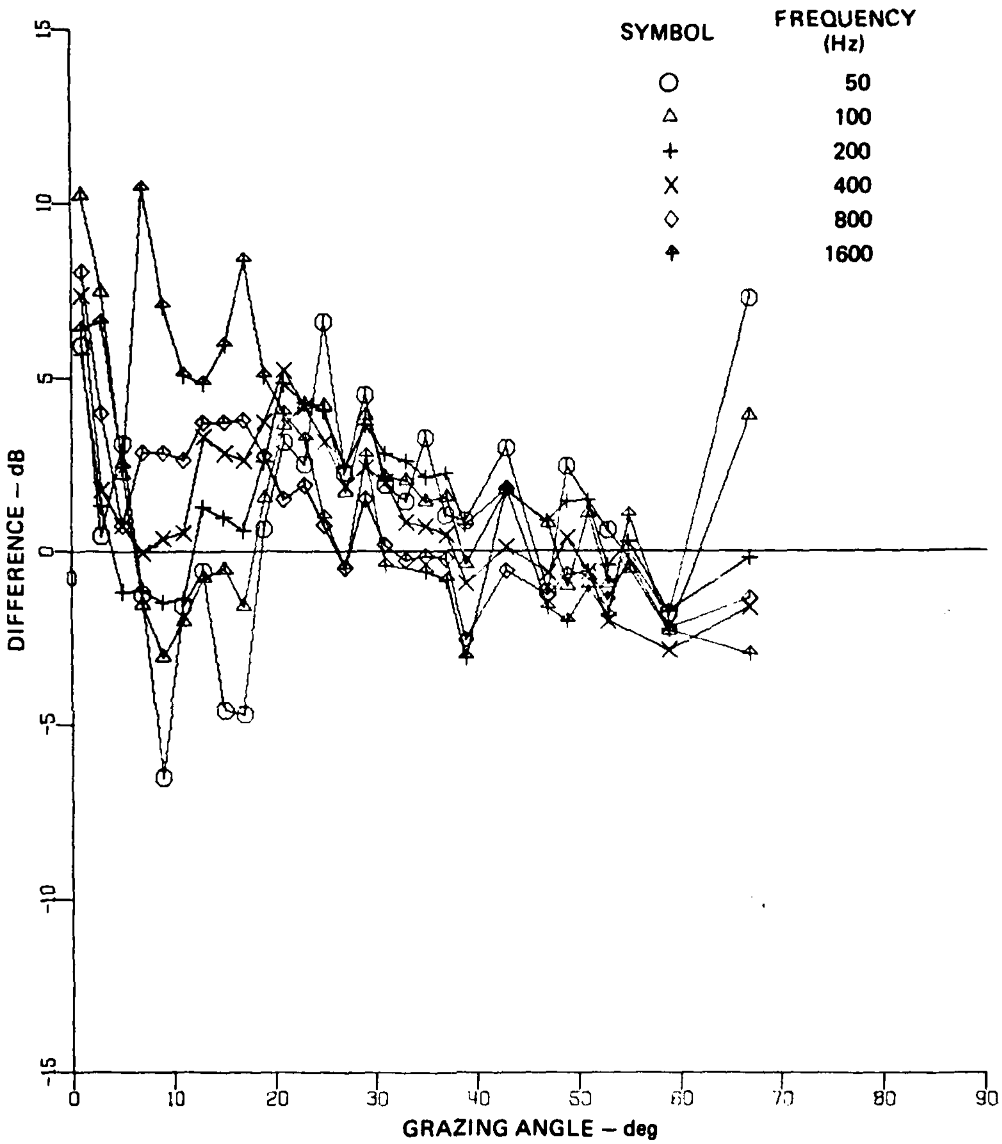

DIFFERENCE BETWEEN BLUP PREDICTED BOTTOM LOSS
AND NADC DATA AT LOCATION 21

ARL:UT
AS-81-1176
DPK - GA
9 - 17 - 81

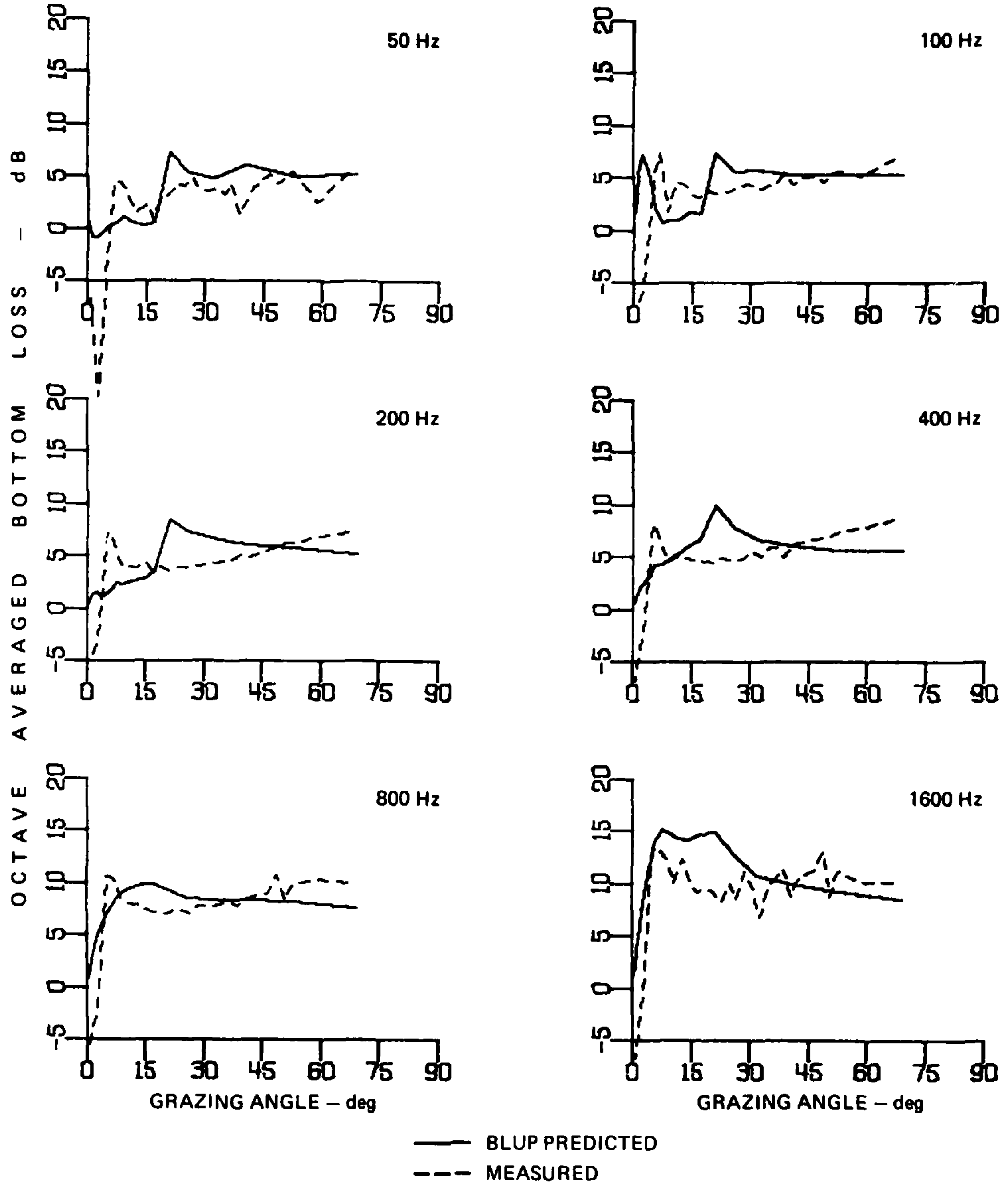

OCTAVE AVERAGED BOTTOM LOSS PREDICTED BY BOTTOM LOSS UPGRADE GEOACOUSTIC PROFILE versus NADC BOTTOM LOSS DATA AT LOCATION 22

ARL:UT
AS-81-1146
DPK - GA
9 - 17 - 81

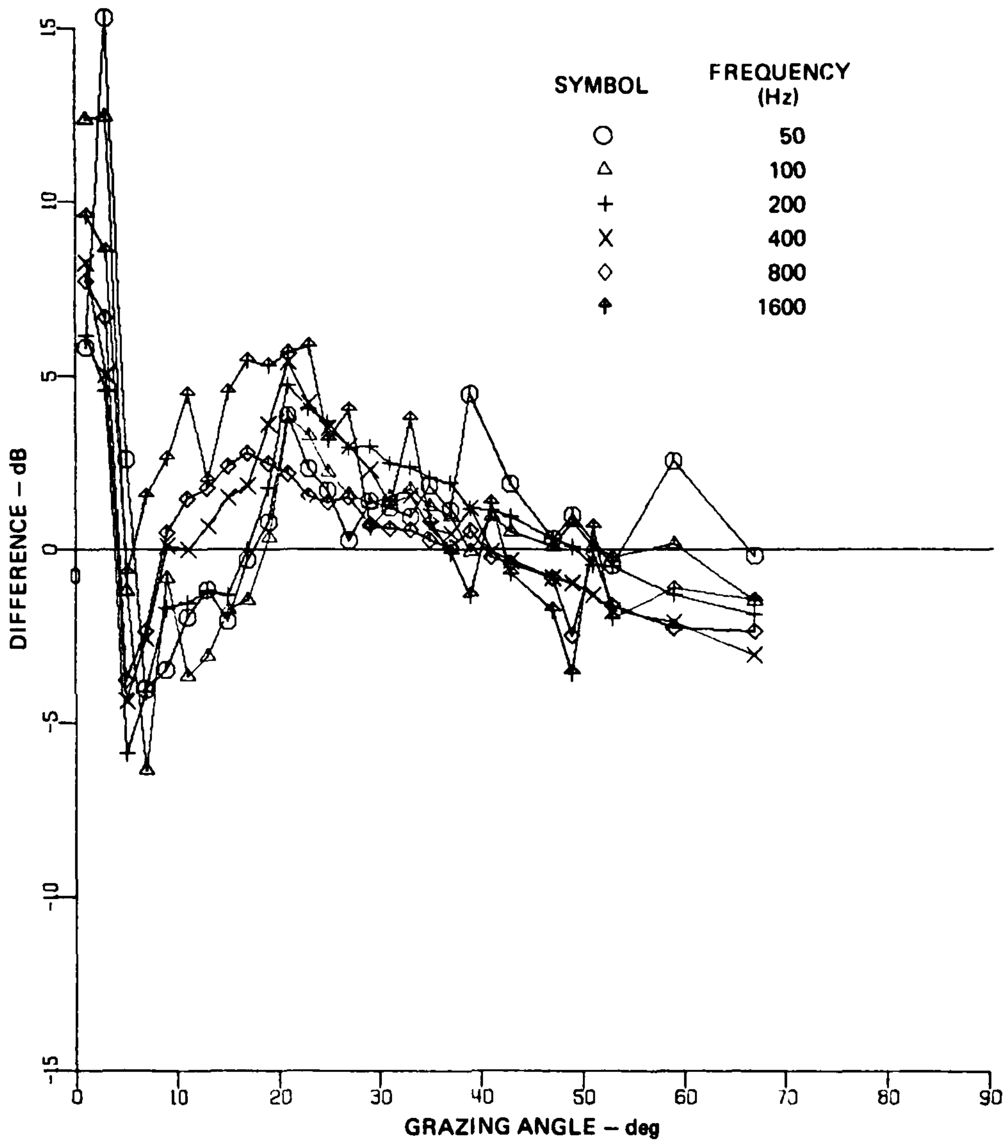

DIFFERENCE BETWEEN BLUP PREDICTED BOTTOM LOSS AND NADC DATA AT LOCATION 22

ARL:UT
AS-81-1177
DPK - GA
9 - 17 - 81

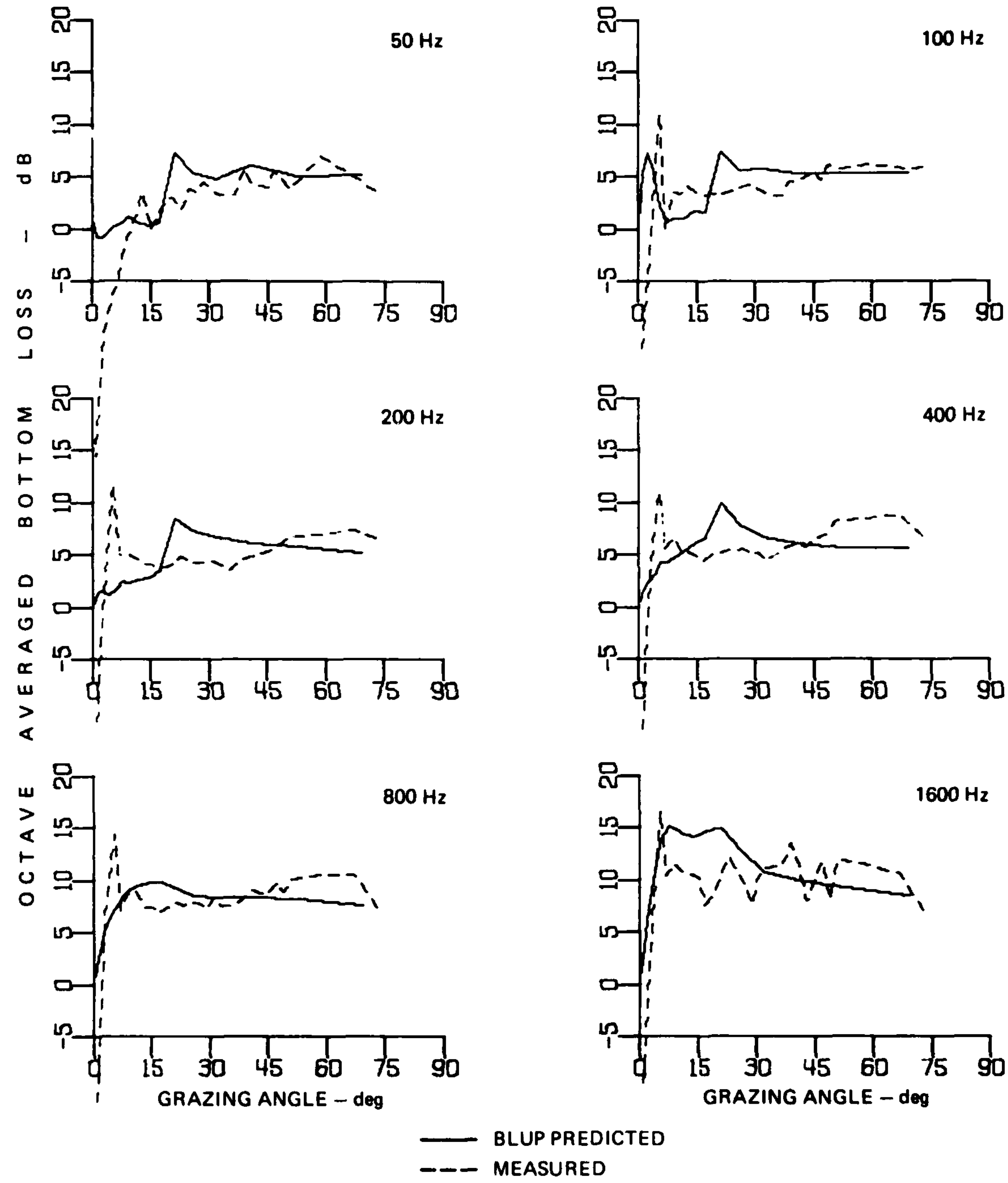

OCTAVE AVERAGED BOTTOM LOSS PREDICTED BY BOTTOM LOSS UPGRADE GEOACOUSTIC PROFILE versus NADC BOTTOM LOSS DATA AT LOCATION 23

ARL:UT
AS-81-1147
DPK - GA
9 - 17 - 81

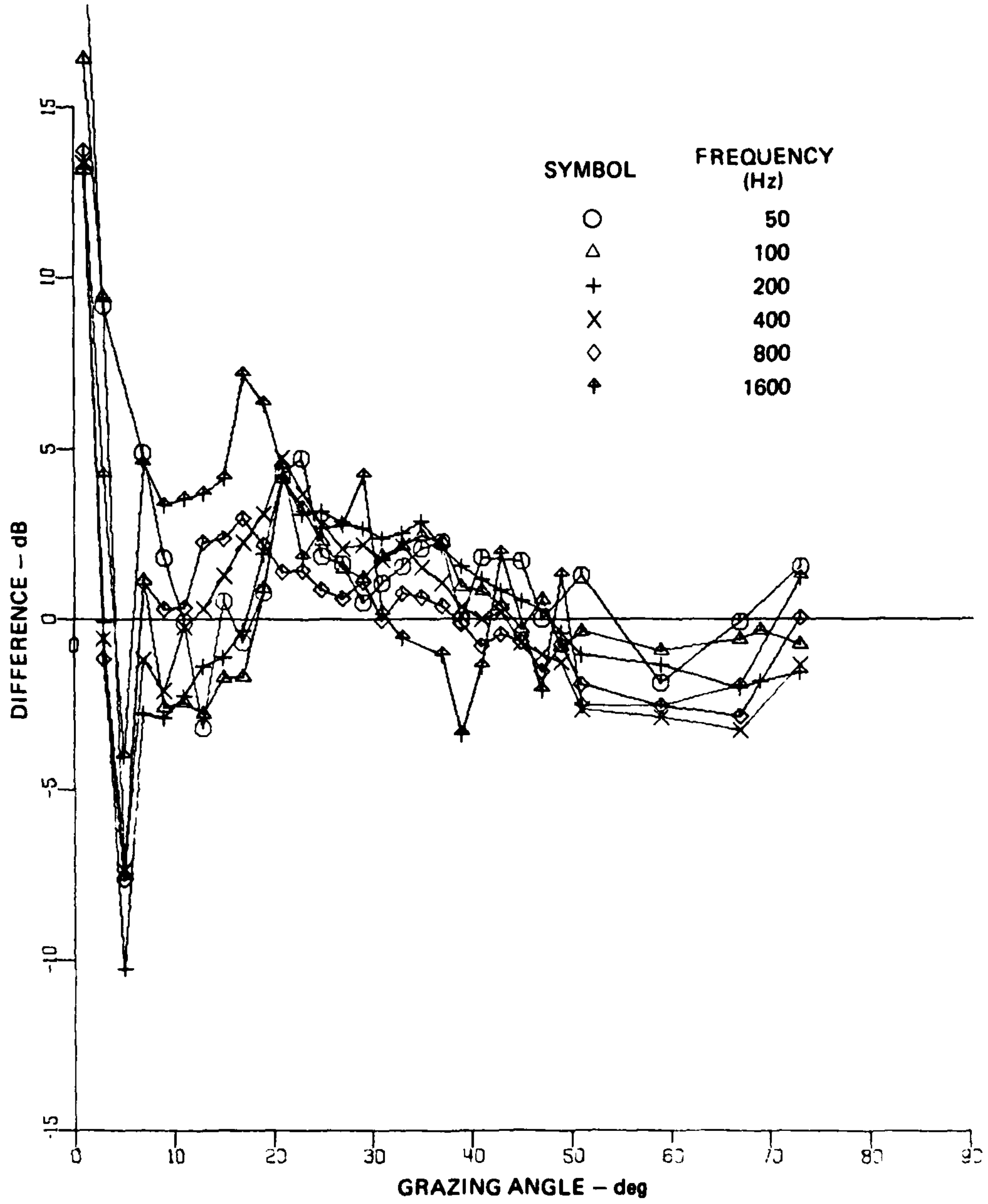

DIFFERENCE BETWEEN BLUP PREDICTED BOTTOM LOSS AND NADC DATA AT LOCATION 23

ARL:UT
AS-81-1178
DPK - GA
9 - 17 - 81

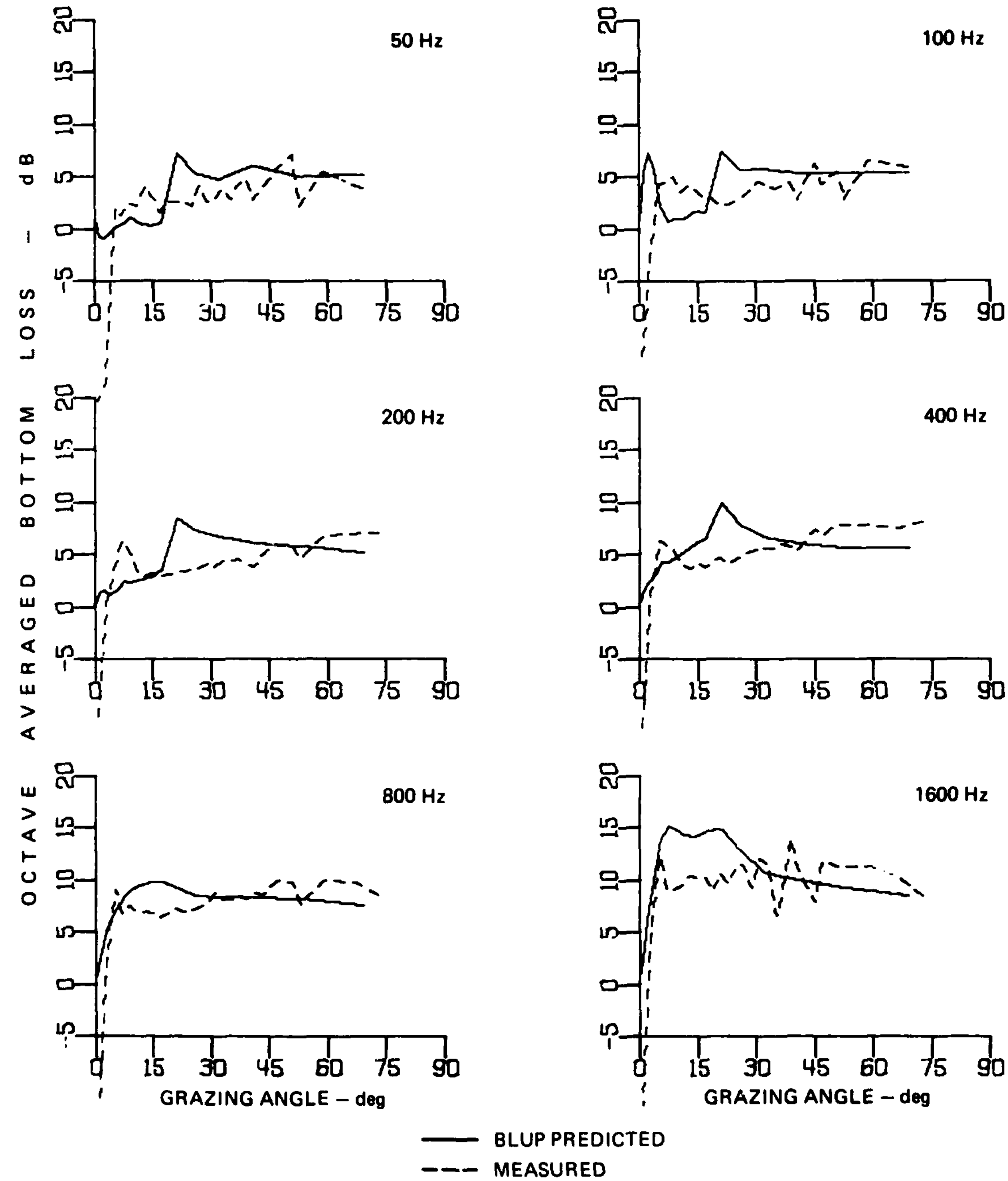

OCTAVE AVERAGED BOTTOM LOSS PREDICTED BY BOTTOM LOSS UPGRADE GEOACOUSTIC PROFILE versus NADC BOTTOM LOSS DATA AT LOCATION 24

ARL:UT
AS-81-1148
DPK - GA
9 - 17 - 81

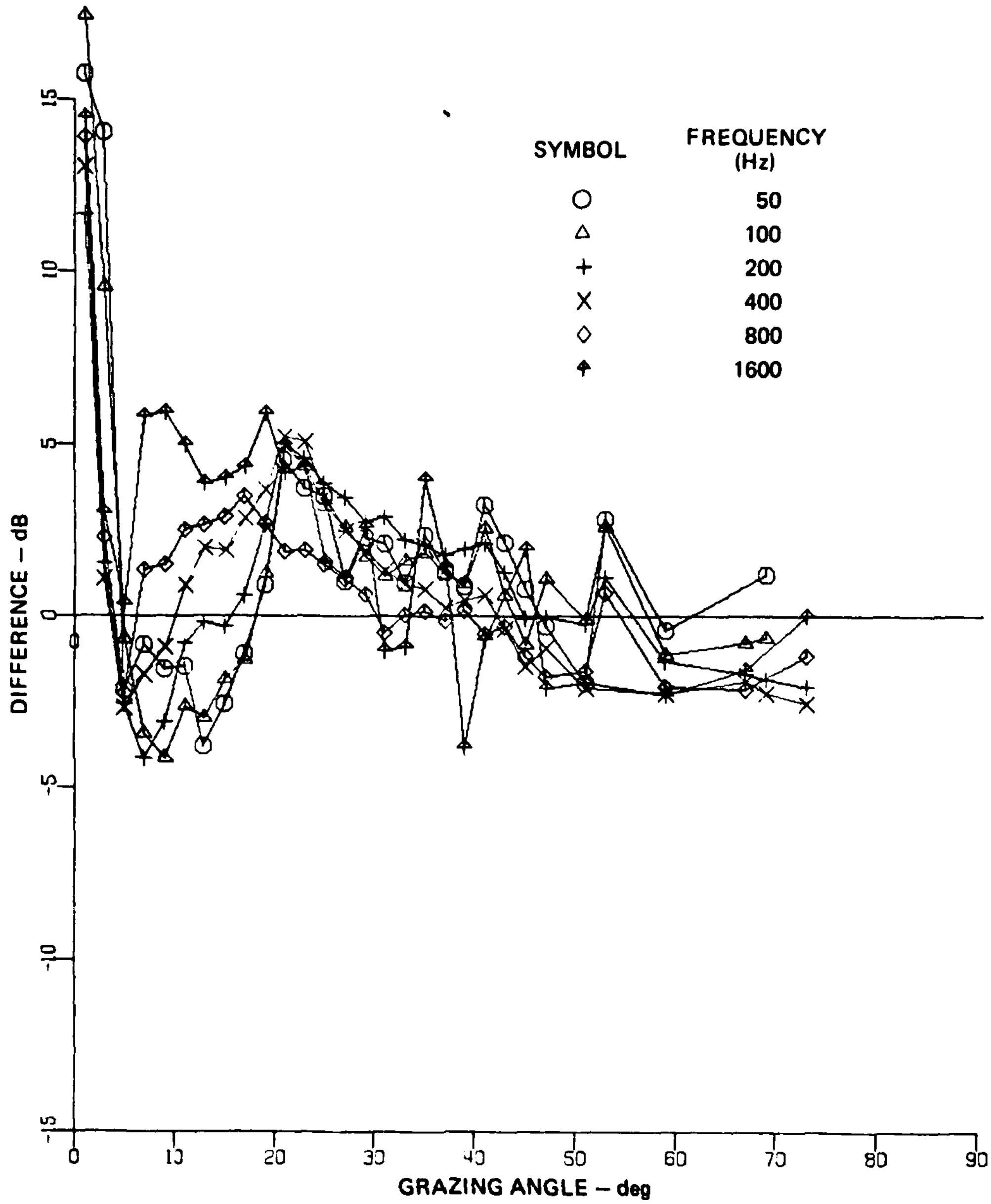

DIFFERENCE BETWEEN BLUP PREDICTED BOTTOM LOSS AND NADC DATA AT LOCATION 24

ARL:UT
AS-81-1179
DPK - GA
9 - 17 - 81

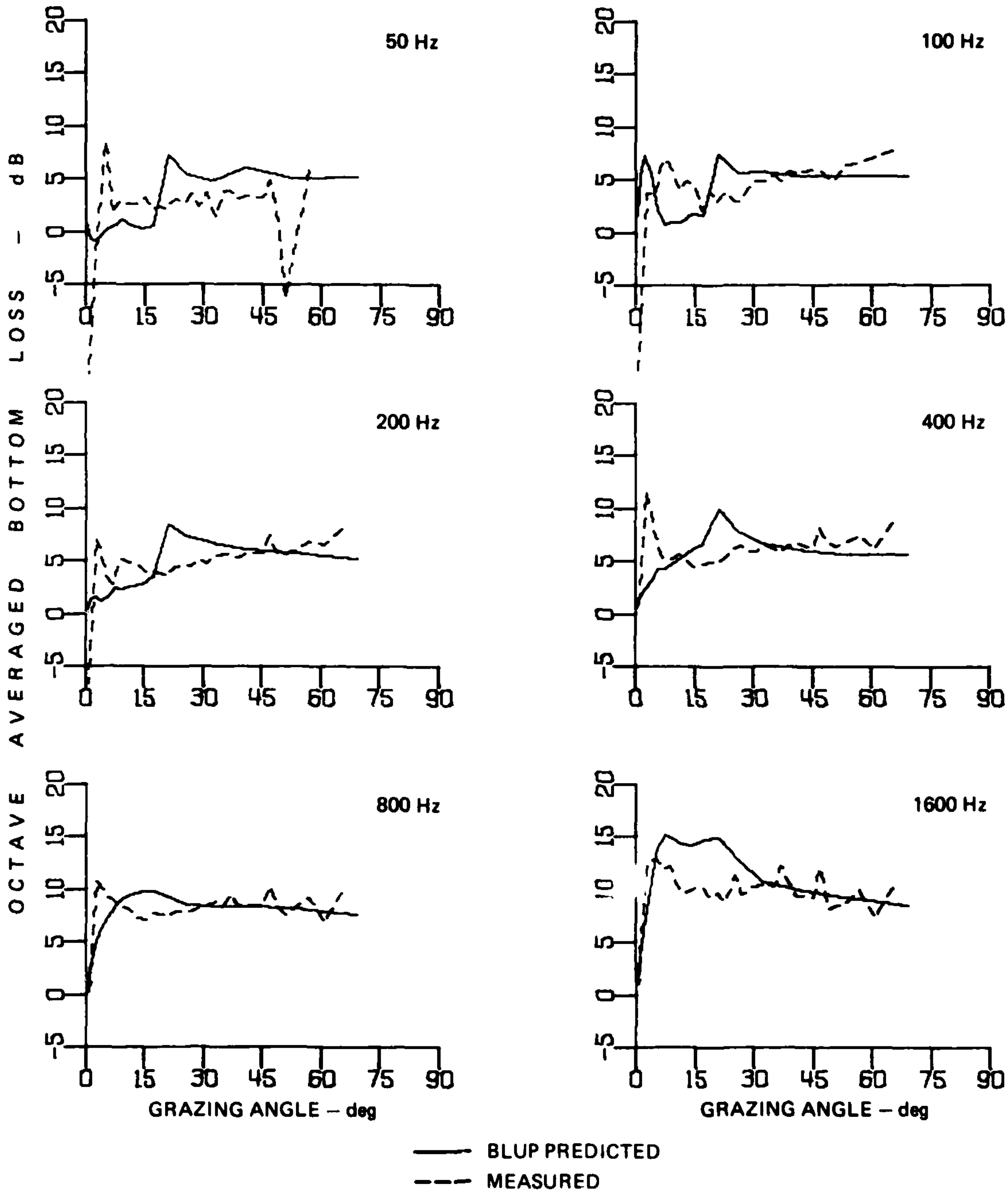

OCTAVE AVERAGED BOTTOM LOSS PREDICTED BY BOTTOM LOSS UPGRADE GEOACOUSTIC PROFILE versus NADC BOTTOM LOSS DATA AT LOCATION 26

ARL:UT
AS-81-1150
DPK - GA
9 - 17 - 81

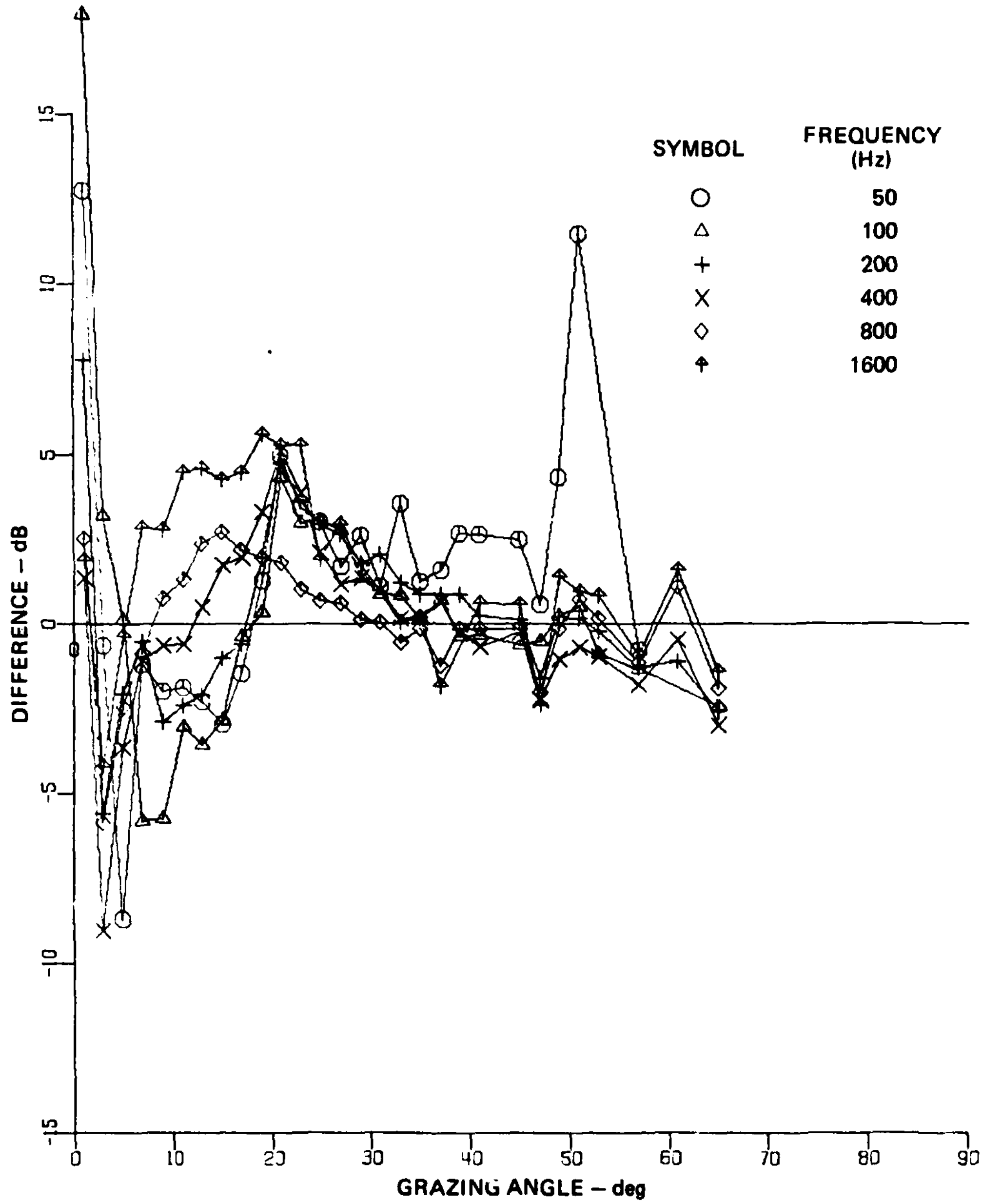

DIFFERENCE BETWEEN BLUP PREDICTED BOTTOM LOSS AND NADC DATA AT LOCATION 26

ARL:UT
AS-81-1181
DPK - GA
9 - 17 - 81

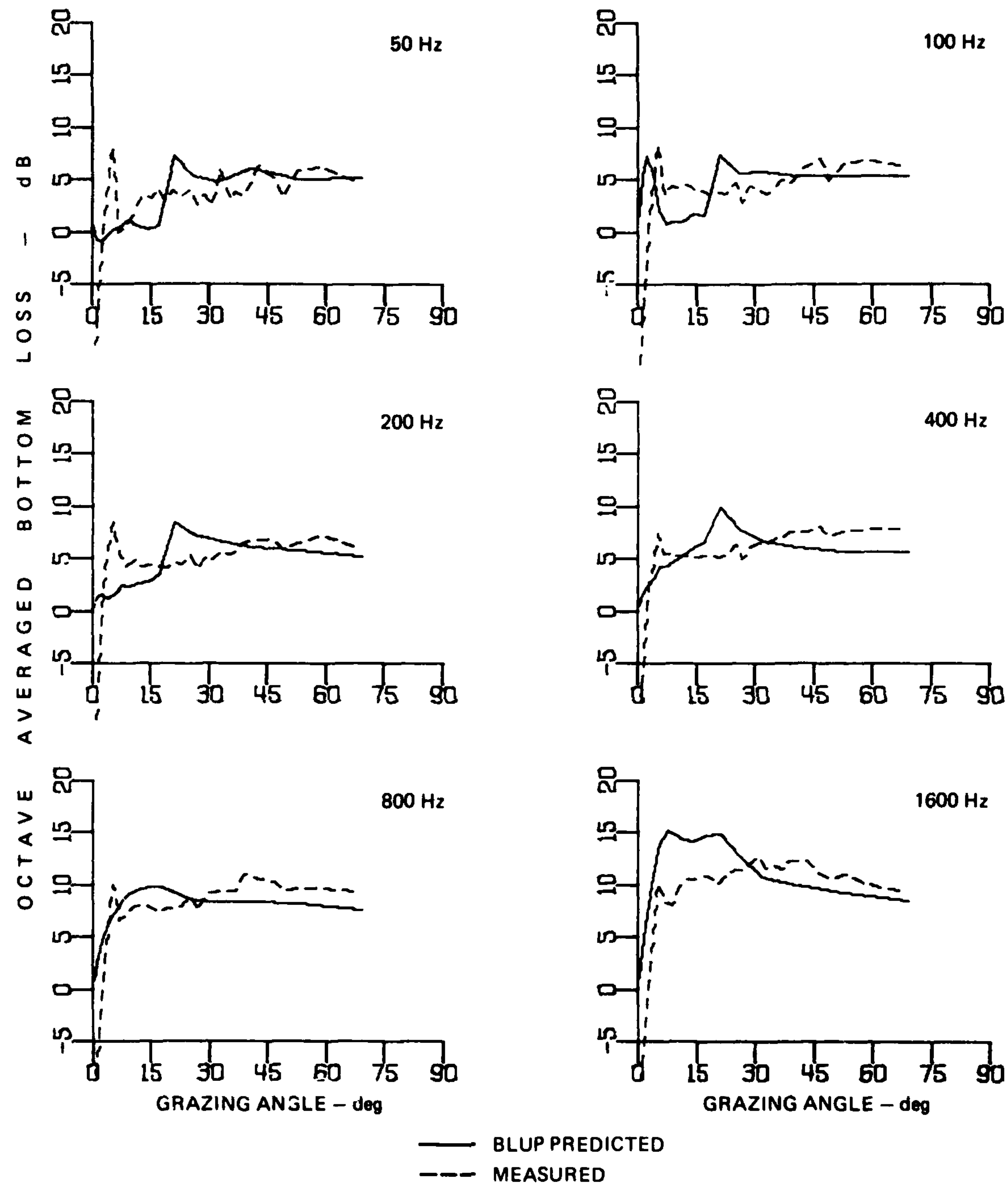

OCTAVE AVERAGED BOTTOM LOSS PREDICTED BY BOTTOM LOSS UPGRADE GEOACOUSTIC PROFILE *versus* NADC BOTTOM LOSS DATA AT LOCATION 27

ARL:UT
AS-81-1151
DPK - GA
9 - 17 - 81

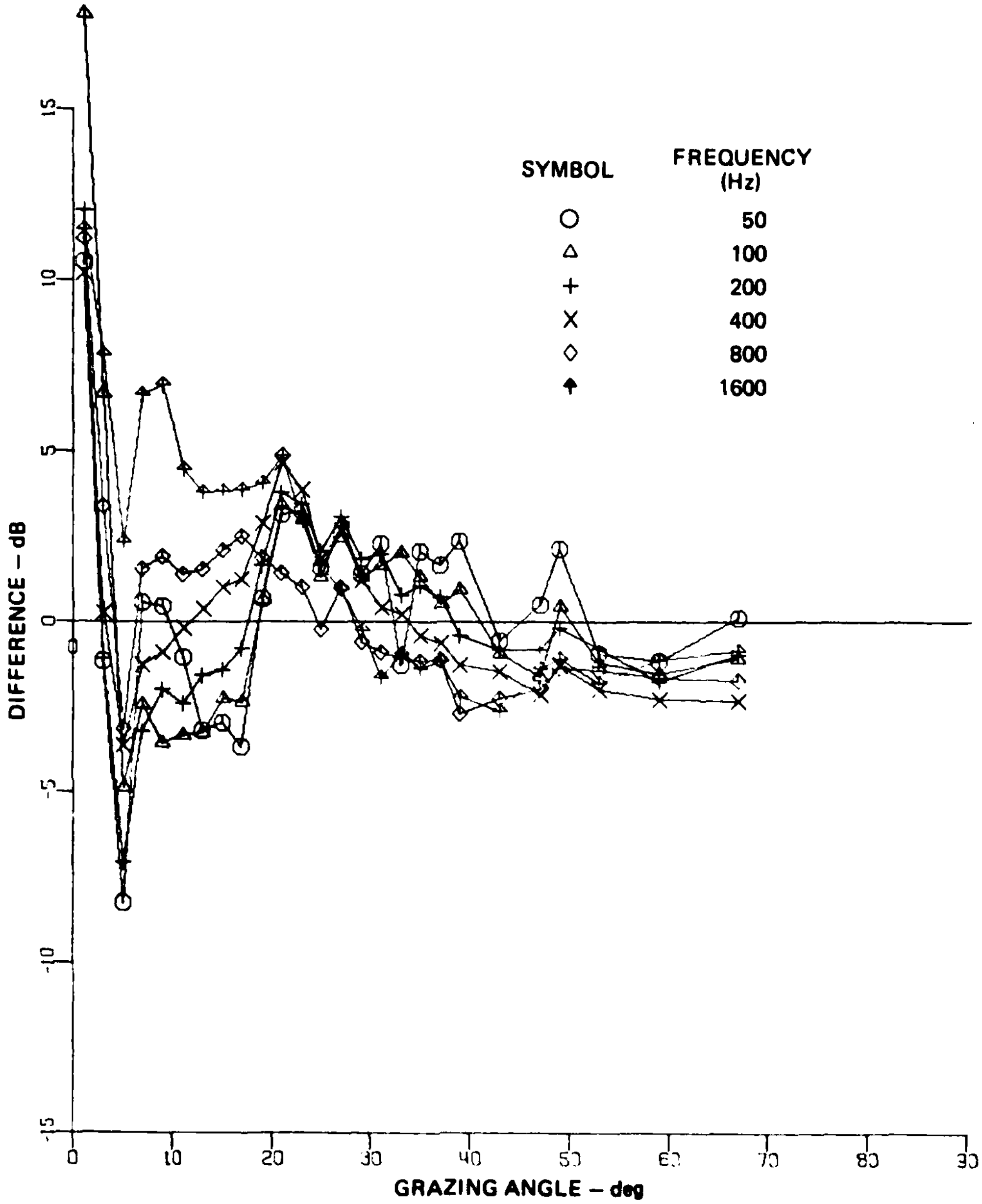

DIFFERENCE BETWEEN BLUP PREDICTED BOTTOM LOSS AND NADC DATA AT LOCATION 27

ARL:UT
AS-81-1182
DPK - GA
9 - 17 - 81

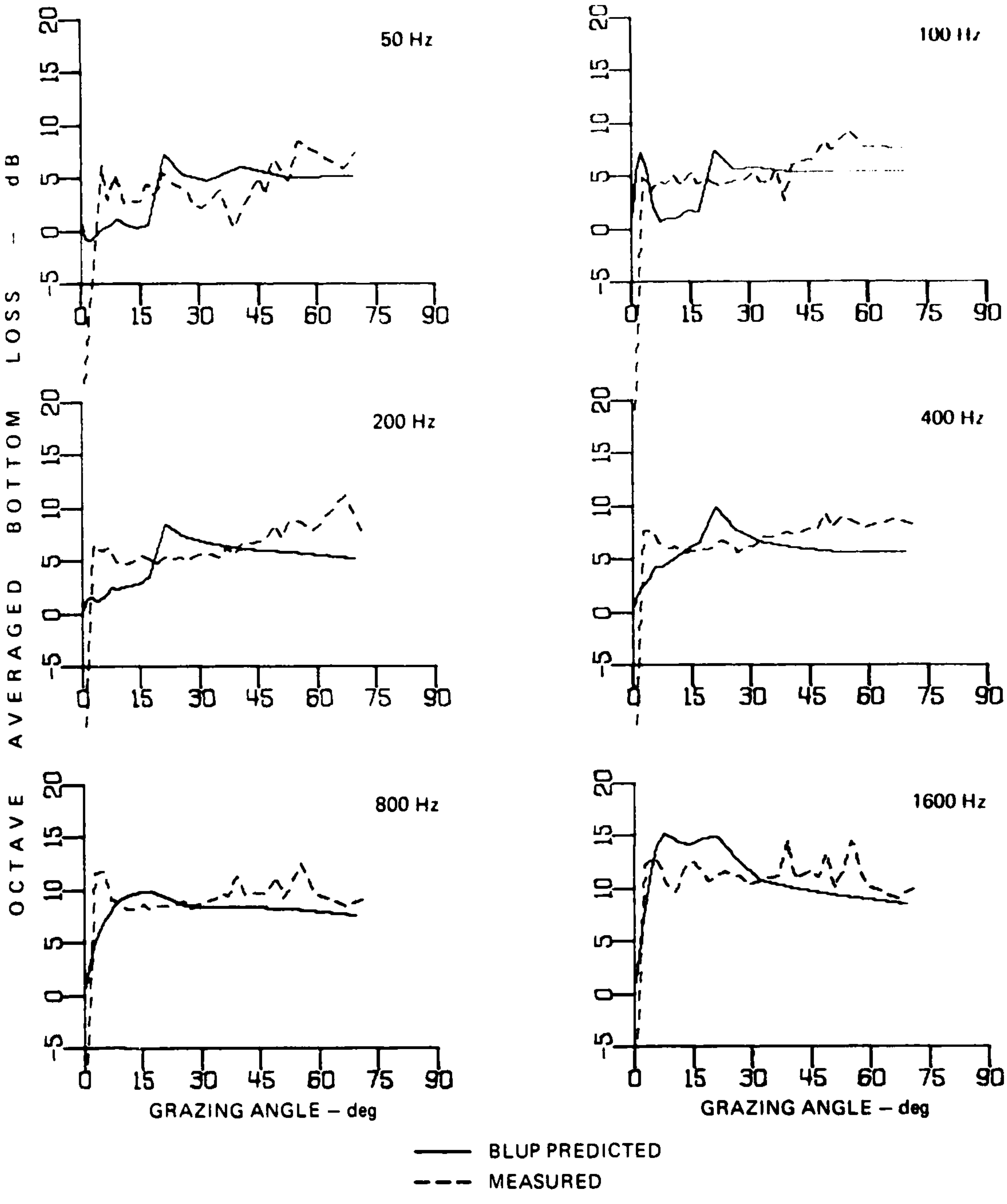

OCTAVE AVERAGED BOTTOM LOSS PREDICTED BY BOTTOM LOSS UPGRADE GEOACOUSTIC PROFILE versus NADC BOTTOM LOSS DATA AT LOCATION 28

ARL:UT
AS-81-1152
DPK - GA
9 - 17 - 81

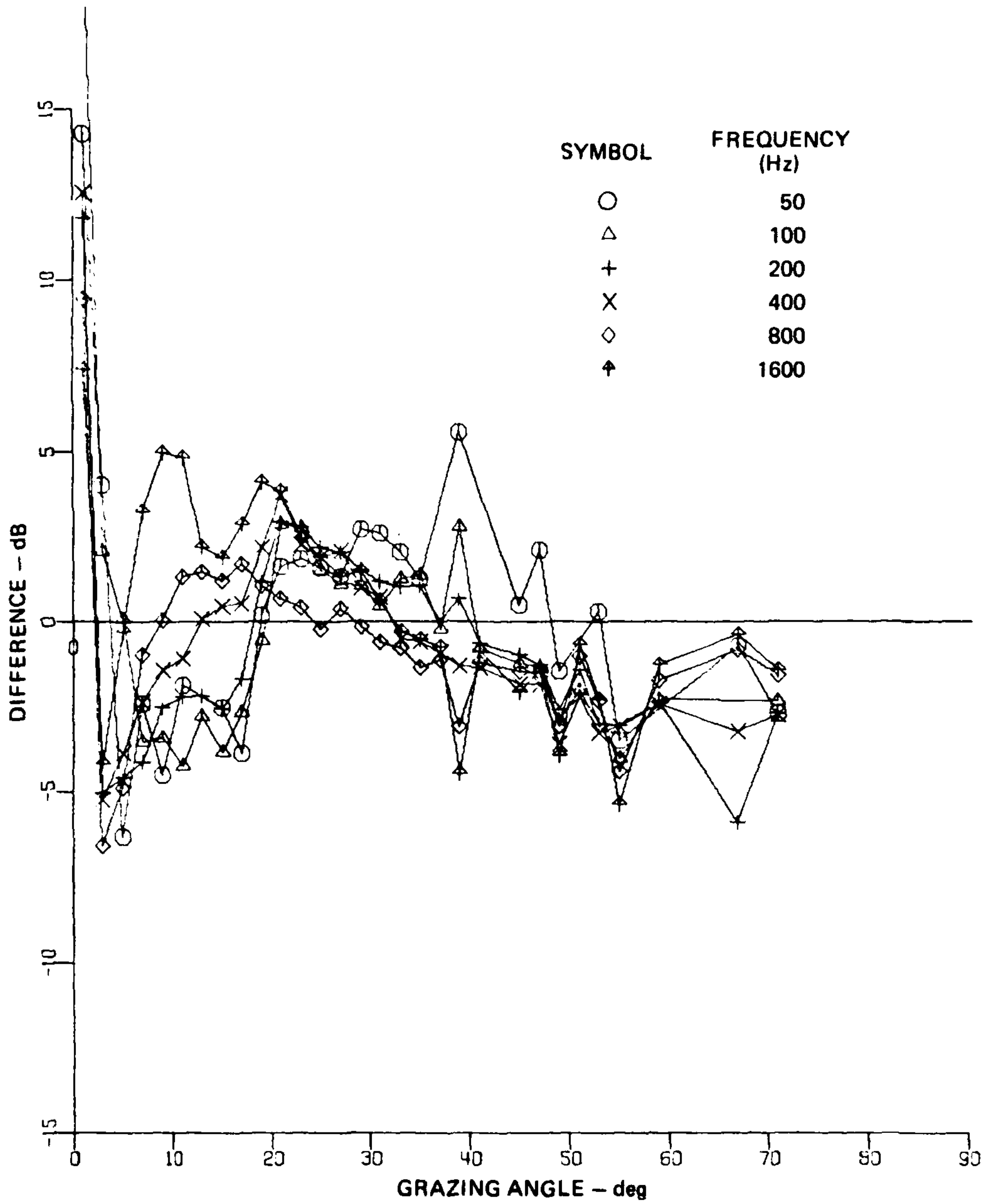

DIFFERENCE BETWEEN BLUP PREDICTED BOTTOM LOSS AND NADC DATA AT LOCATION 28

ARL:UT
AS-81-1183
DPK - GA
9 - 17 - 81

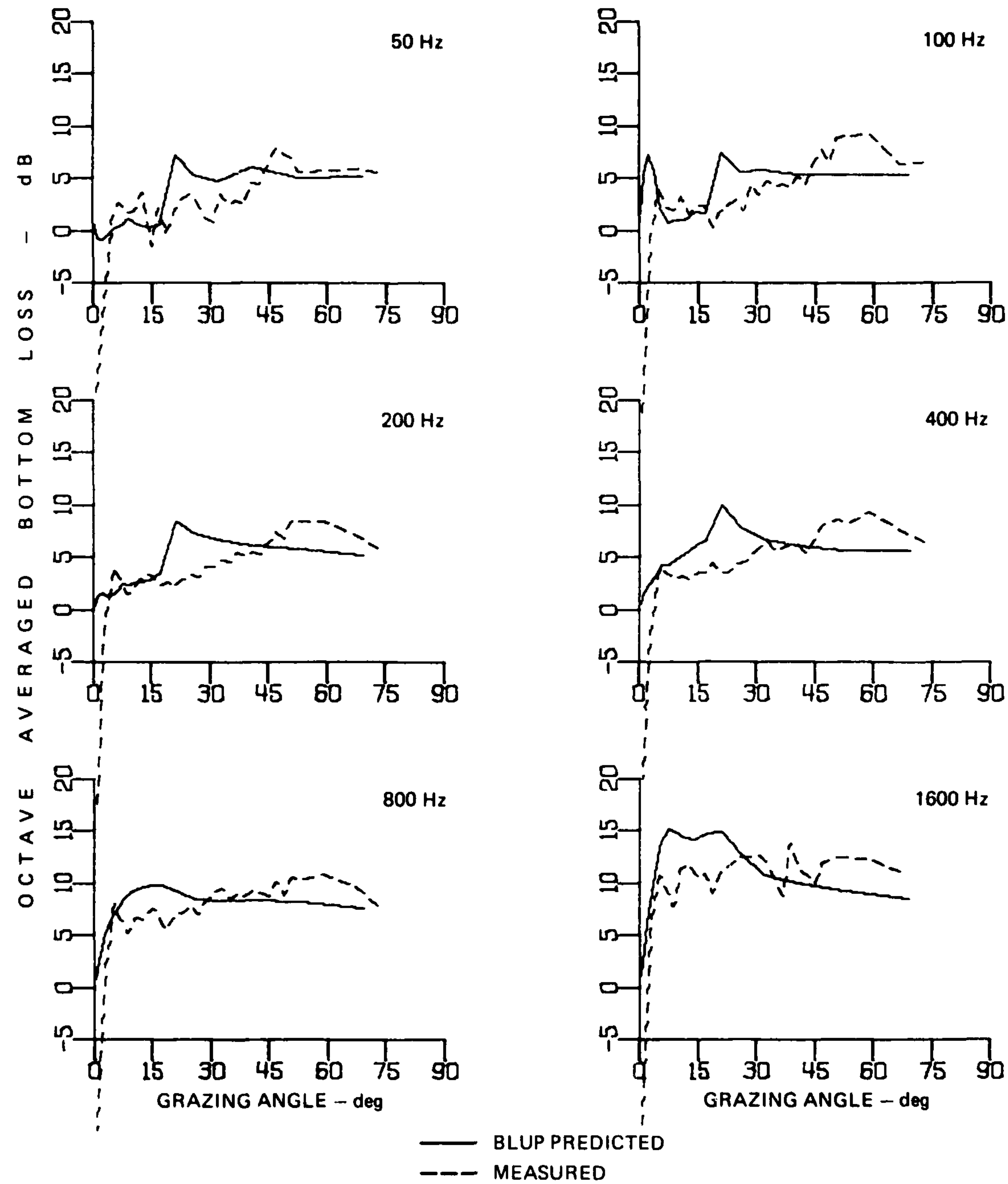

OCTAVE AVERAGED BOTTOM LOSS PREDICTED BY BOTTOM LOSS UPGRADE GEOACOUSTIC PROFILE versus NADC BOTTOM LOSS DATA AT LOCATION 29

ARL:UT
AS-81-1153
DPK - GA
9 - 17 - 81

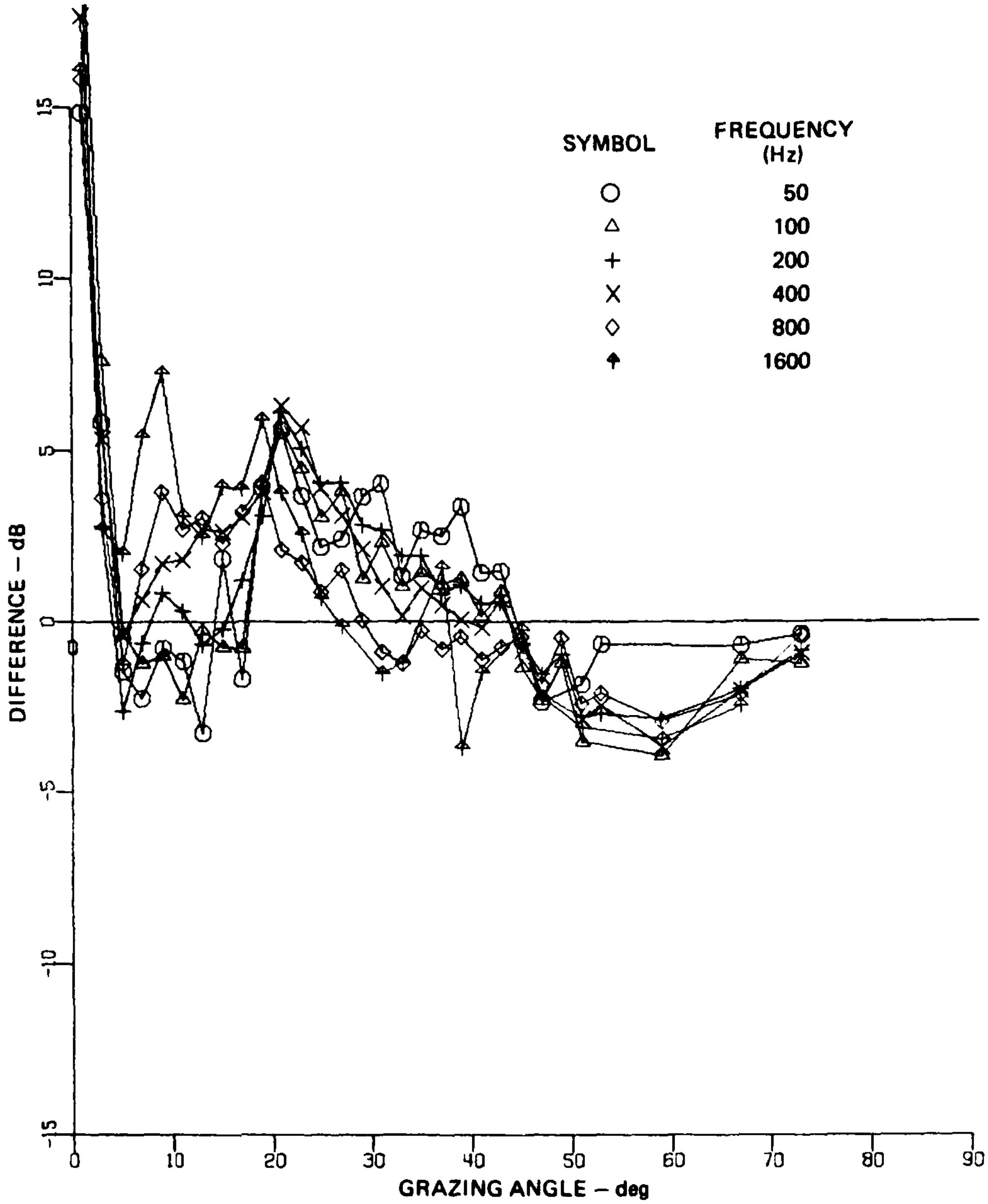

DIFFERENCE BETWEEN BLUP PREDICTED BOTTOM LOSS AND NADC DATA AT LOCATION 29

ARL:UT
AS-81-1184
DPK - GA
9 - 17 - 81

U. Location 25

1. Deficiencies

(1) For 100-1600 Hz, BLUP predictions fall below the data in the angular region $30^{o} < \theta g < 60^{o}$ (problem type 2).

2. Comments

Even though sediment thickness maps report a thickness of greater than 80 m, a thickness of 20 m is used here.

The data shows an increase at 50 Hz between 45^{o} and 65^{o} that is not seen in the other data.

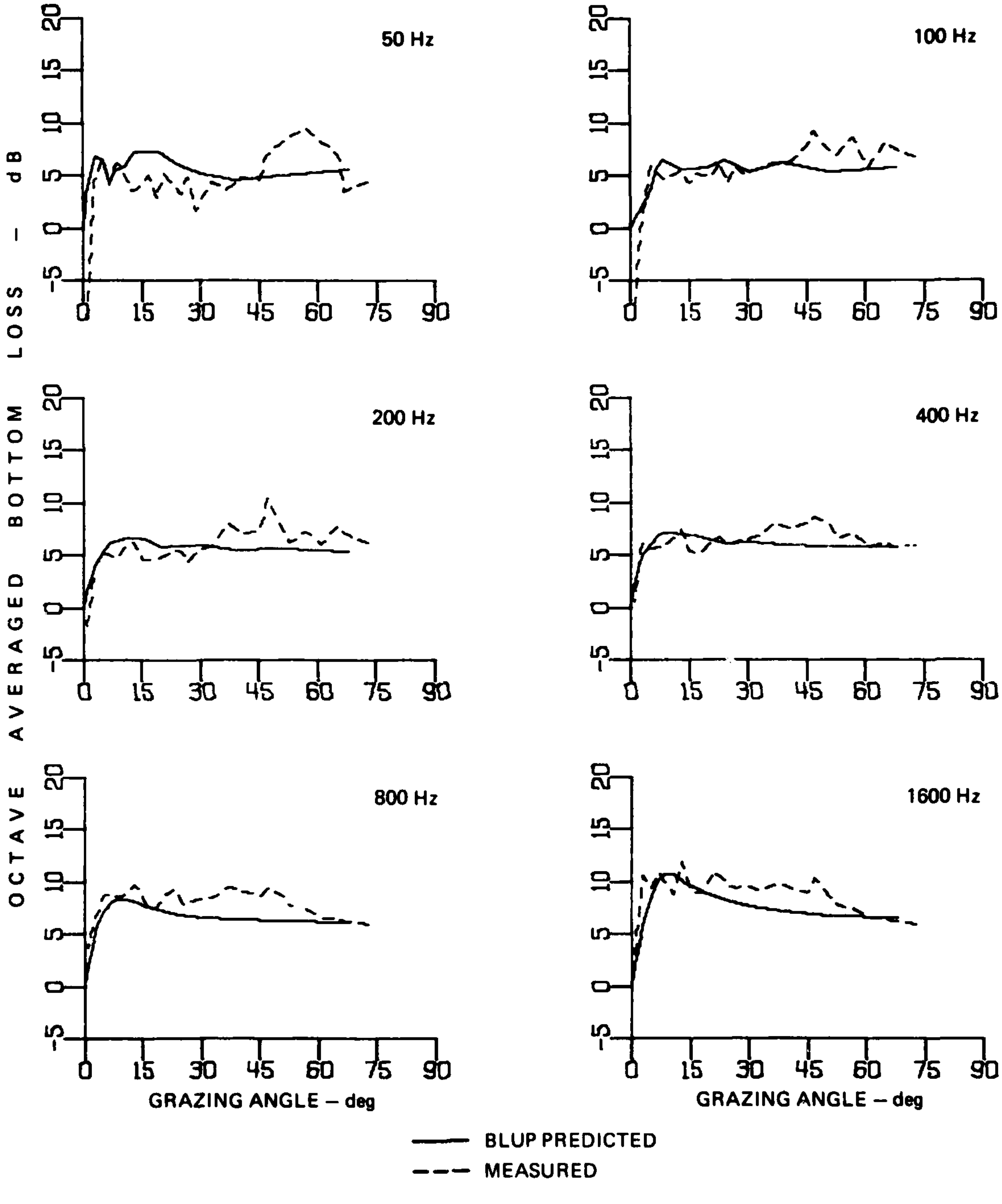

OCTAVE AVERAGED BOTTOM LOSS PREDICTED BY BOTTOM LOSS UPGRADE GEOACOUSTIC PROFILE versus NADC BOTTOM LOSS DATA AT LOCATION 25

ARL:UT
AS-81-1149
DPK - GA
9 - 17 - 81

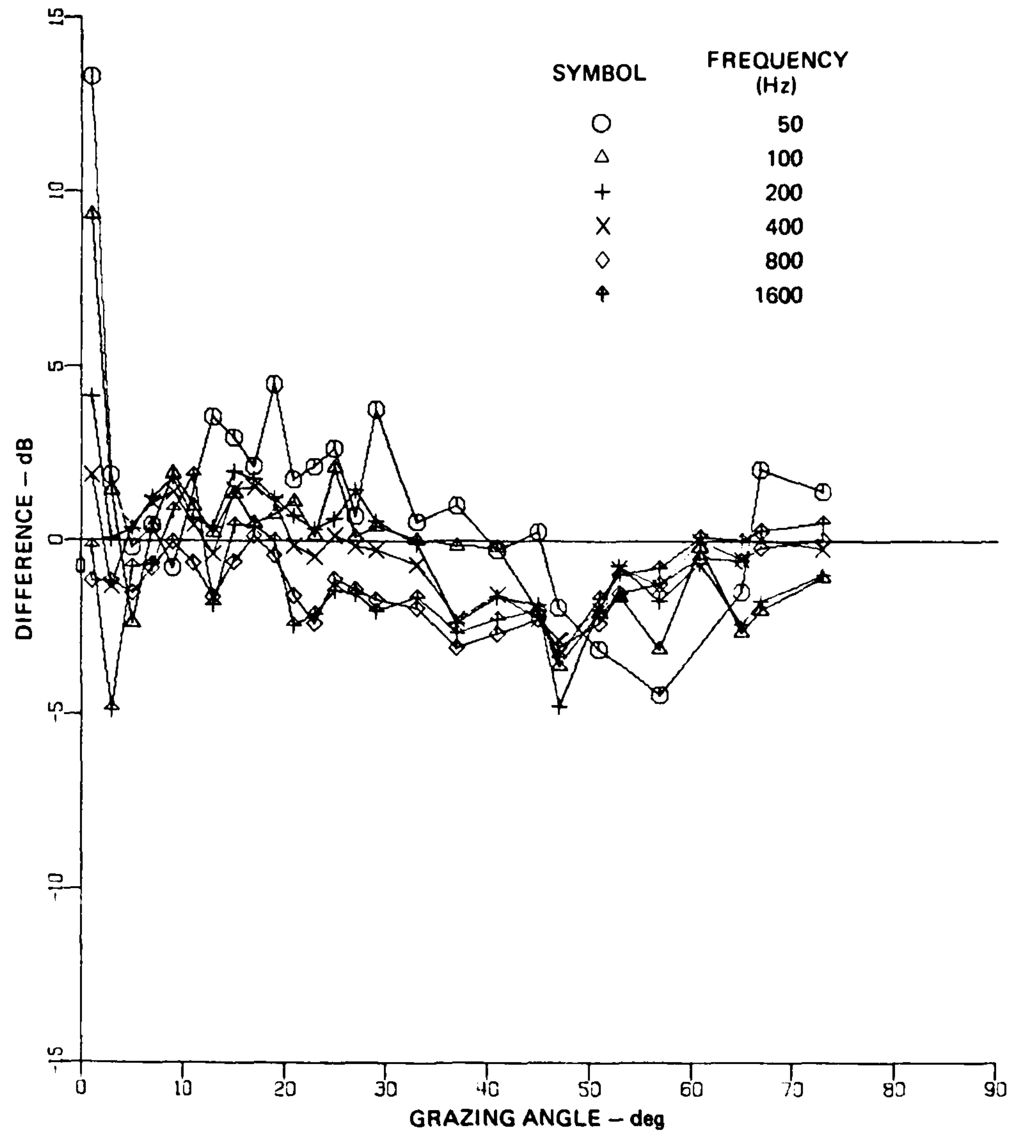

DIFFERENCE BETWEEN BLUP PREDICTED BOTTOM LOSS AND NADC DATA AT LOCATION 25

ARL:UT
AS-81-1180
DPK - GA
9 - 17 - 81

V. Location 30

1. Deficiencies

(1) For 50-800 Hz, BLUP predictions fall below the data (maximum of 5 dB at 200 Hz) in the region $0^{o} < \theta g < 15^{o}$ (problem type 2).

2. Comments

A 20 dB dip in the data appears at 10^{o} at 50 Hz.

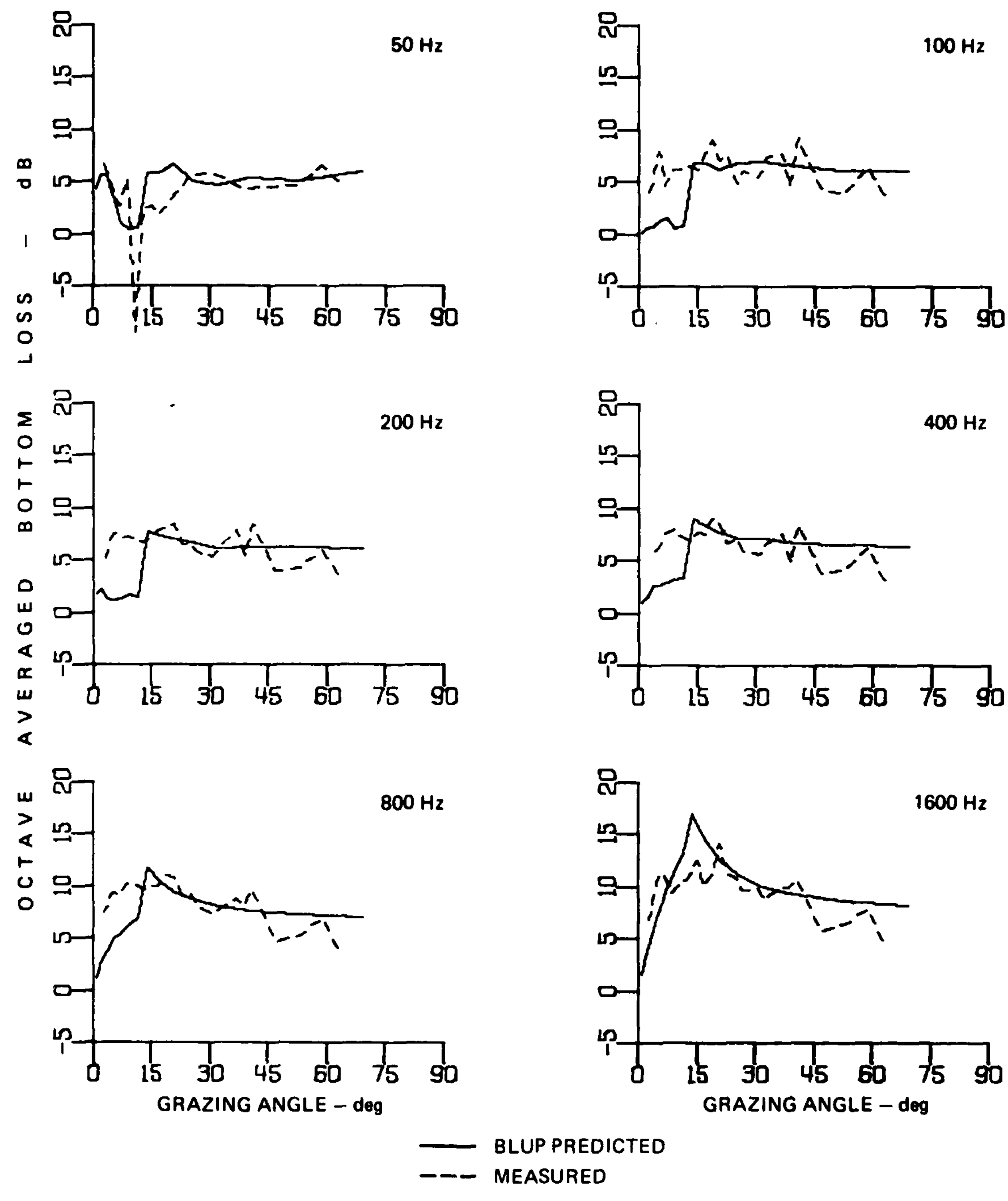

OCTAVE AVERAGED BOTTOM LOSS PREDICTED BY BOTTOM LOSS UPGRADE GEOACOUSTIC PROFILE versus NADC BOTTOM LOSS DATA AT LOCATION 30

ARL:UT
AS-81-1154
DPK - GA
9 - 17 - 81

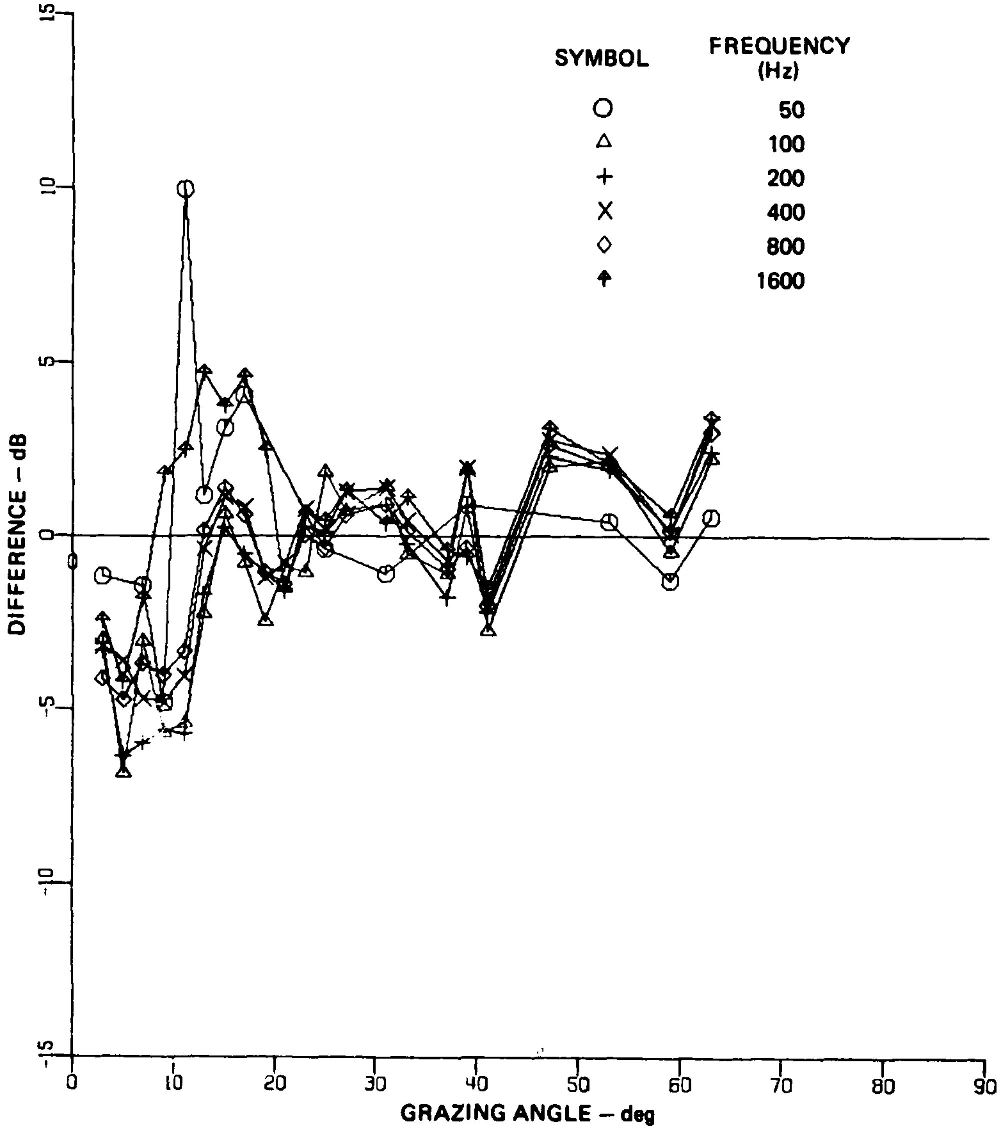

DIFFERENCE BETWEEN BLUP PREDICTED BOTTOM LOSS AND NADC DATA AT LOCATION 30

ARL:UT
AS-81-1185
DPK - GA
9 - 17 - 81

W. Location 31

1. Deficiencies

(1) For all frequencies, BLUP predictions exceed the data (maximum difference of 7.5 dB at 15^{o} at 1600 Hz) (problem type 1).

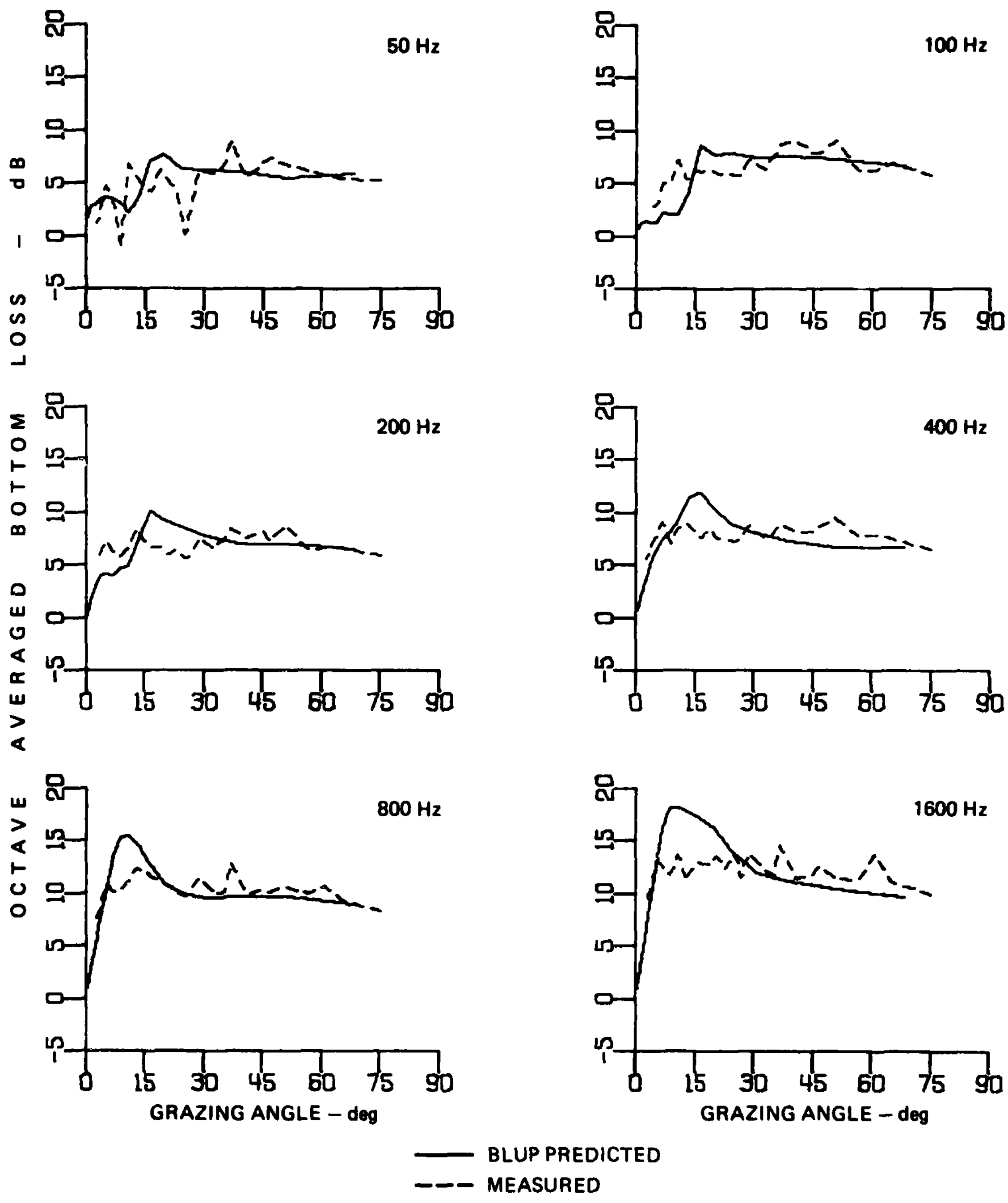

OCTAVE AVERAGED BOTTOM LOSS PREDICTED BY BOTTOM LOSS UPGRADE GEOACOUSTIC PROFILE versus NADC BOTTOM LOSS DATA AT LOCATION 31

ARL:UT
AS-81-1155
DPK - GA
9 - 17 - 81

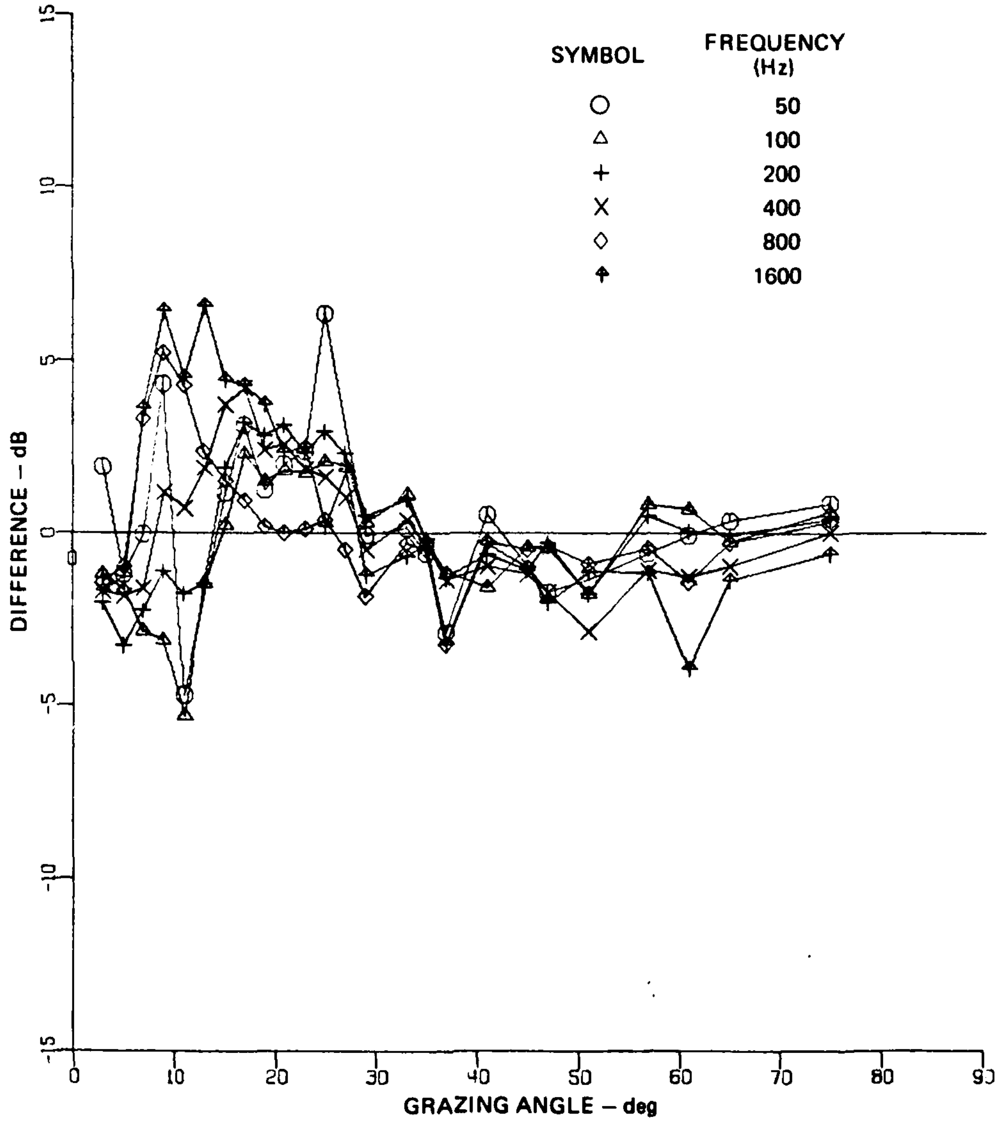

DIFFERENCE BETWEEN BLUP PREDICTED BOTTOM LOSS AND NADC DATA AT LOCATION 31

ARL:UT
AS-81-1186
DPK - GA
9 - 17 - 81

VII. DISCUSSION

This section presents a discussion of the comparisons between the measured bottom loss and BLUP predicted bottom loss. Problems with the data, the frequency, and angle dependence not predicted by BLUP, and the question of sediment thickness are discussed.

An examination of the NADC data for each location shows several anomalies that appear to be due to data collection or analysis problems rather than to the acoustics of bottom interaction. Some examples are: large peaks in bottom loss, e.g., location 1 at 800 and 1600 Hz; deep oscillation in bottom loss with angle, e.g., location 9 at 50 and 1600 Hz; large drops in loss, e.g., location 16 at 50-400 Hz; increases in loss at particular angles, e.g., location 25 at 50 Hz; and very high loss at low angles, e.g., location 17 at 50-1600 Hz. The octave-averaging of the data should have removed much of the detailed structure of acoustical origin, leaving data collection and analysis problems as the most likely source of these anomalies. These anomalies can readily be identified in a particular piece of data and discounted in the "eyeball" average of the comparison curves used to fit the data in obtaining the BLUP parameters. However, the anomalies occur in a less obvious fashion in the difference curves where they influence the estimation of the quality of the overall fit to the data. The presence of these anomalies complicated the analysis of these data by discouraging the use of automation in the procedure for determining the BLUP parameters and requiring human judgment of the quality of the fit to the data.

An examination of the difference curves quickly leads to the conclusion that there are frequency and angle dependencies in the data that the BLUP profile does not predict. At least some of these differences could be eliminated by a frequency and angle dependent basement reflectivity parameter rather than the constant reflectivity BLUP parameter.

Many locations show a general decrease with increasing angle in the difference between BLUP predicted and measured loss. Location 22 is a good example of this angle dependence, termed problem type 2 in earlier discussions. This regular dependence on angle occurs because the BLUP profile causes a clear decrease in loss with angle while much of the data has loss that is nearly independent of angle.

The difference curves also show two distinct dependencies on frequency, one at low angles and the other at high angles. The low angle dependence is most severe at high frequencies where problem type 1 occurs. Location 5 illustrates this dependence. The BLUP predictions are larger than the data. The difference decreases with frequency until it becomes a type 3 problem at low frequencies where BLUP predicts too little loss. The low angle problem occurs at angles generally below that for which a ray first strikes the substrate. Hence, this low angle frequency dependence is due to some combination of sediment parameters, including sediment thickness, or to the necessity for wave theory corrections at low angles for these thin sediments.

The high angle frequency dependence in the difference curves generally starts out as a type 2 problem at high frequencies for which BLUP predicts too little loss. As frequency decreases, the difference increases until at low frequencies BLUP often predicts more loss than seen in the data, i.e., it becomes a type 4 problem. Location 18 illustrates this frequency dependence. Note that the dependence is opposite that of the low angle frequency dependence. Since the rays in the high angle region typically strike the substrate, it is likely that the interaction with the basement is being incorrectly modeled by BLUP. This conclusion is further bolstered by the observation that the switch between the two frequency dependencies occurs at an angle between 15^0 and 30^0 as illustrated by location 4. In this angle range a ray first strikes the substrates for these thin sediments. In particular, the need for a frequency dependent correction to the constant reflectivity is indicated.

The question of the correct value to use for sediment thickness came up repeatedly in the course of determining the BLUP parameters. Typical charts of the Pacific provide sediment thickness contoured in increments of 0.1 sec of two-way travel time. This corresponds to increments of approximately 80 m of actual thickness. This resolution is probably adequate for thick sediment regions where thickness may be 500-1500 m. However, our experience in determining the BLUP parameters shows it to be inadequate for vast areas of the Pacific where thickness is less than 80 m, i.e., less than current resolution. In fact, for several locations nearby, DSDP sites gave thicknesses of about 40 m compared to estimates of 80 m from available charts. The actual values of the sediment parameters obtained will depend to some extent on the choice of sediment thickness, but more importantly, the BLUP predicted bottom loss will depend on the sediment thickness chosen. Figure 8 illustrates this dependence by comparing BLUP predicted bottom loss to measured bottom loss at location 8. The predicted loss was calculated using thicknesses of 20, 40, 60, and 80 m. The average of the curves tends to increase with increasing sediment thickness at about 1 dB/20 m. This is particularly noticeable in the angle range from 10^0 to 45^0. An examination of the frequency dependence in Fig. 8 shows that the uncertainty in sediment thickness can result in a prediction uncertainty of 4 dB on average, smaller at low frequencies, and substantially larger at higher frequencies.

In general, the bottom loss predicted using the BLUP profile for the Pacific locations examined does not compare well with that measured by NADC. While the procedure used to define the BLUP parameters results in a total difference (averaged over frequency and angle) between the two that is small, the spread about this average can be quite large, as much as ± 10 dB. The best fit to the data was obtained at location 2 while the worst occurred at location 14. The pronounced frequency and

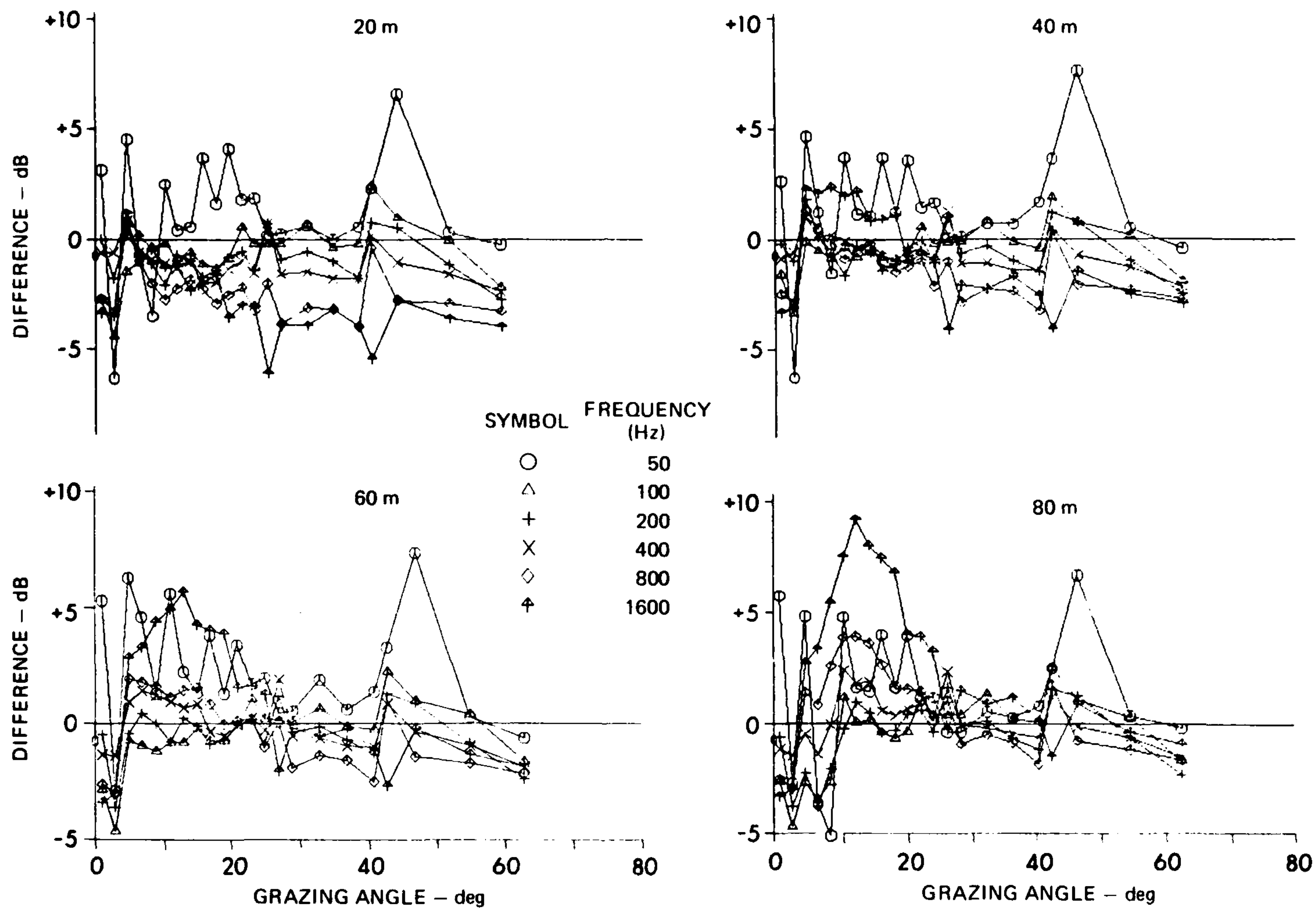

FIGURE 8
COMPARISON OF BLUP PREDICTED TO MEASURED BOTTOM LOSS AT LOCATION 8 FOR SEDIMENT THICKNESSES OF 20, 40, 60 AND 80 m

ARL:UT
AS-82-1138
DPK - GA
7 - 20 - 82

angle dependence seen in the data but not predicted by the BLUP profile suggests the need for use of a frequency and angle dependent basement reflectivity parameter instead of the constant reflectivity now in use. Improved estimates of sediment thickness are needed for the particularly thin regions of the Pacific.

128- Blank

VIII. SUMMARY

This report presents the results of the ARL:UT study of the use of the initial BLUP parameter set in the thin sediment areas of the Northeastern Pacific. The data on which this study is based is NADC measured bottom loss at 31 locations in the Northeastern Pacific. The analysis carried out relied on comparing measured bottom loss with bottom loss predicted by a ray-based simulator of the NADC measurement. The simulation used the BLUP geoacoustic profile to determine the ray paths, intensities, and travel times for rays penetrating the ocean floor. The BLUP geoacoustic parameter values were changed, but kept within accepted geological ranges, to obtain the best fit to the data. The difference between the best-fit prediction and the data was analyzed at each location to identify patterns that could be used to understand the probable source of discrepancies.

This analysis determined that the initial BLUP geoacoustic parameter set does not contain the parameters necessary to accurately predict bottom loss in thin sediment areas. This conclusion is based on the poor fits obtained for at least half of the 31 NADC sites analyzed. These fits are to be contrasted with the generally excellent fits to NADC data that can be obtained in areas of thick sediment cover. The reason for this discrepancy is that the major physical mechanisms governing propagation in thin sediment areas are not well understood while the acoustics of thick, unlayered sediment structures is now well understood and, in fact, forms the basis for the BLUP parameter set. For the thin sediments found in vast areas of the Pacific, a large portion of the incident energy interacts with a rough substrate, an interaction that has little importance in thick sediment areas. This substrate interaction is not well understood at this time. While shear wave generation at the substrate has been studied and can be modeled, scattering from the rough substrate cannot be confidently included at this time in the BLUP parameter set. Uncertainties in sediment thickness in areas of thin sediment cover also play a role in the inadequacy of the BLUP parameter set.

The least-known geoacoustic parameter in the NADC Pacific measurement region is sediment thickness. The typical resolution is only 80 m. This presents a problem for thin sediment modeling since this uncertainty is a significant fraction of sediment thickness. In several instances, sediment thickness values of 20 m were required in our analysis to obtain good fits to the data, while 80 m was used for the majority of the sites. Both values are consistent with present uncertainty in sediment thickness. The actual sediment thickness used in the BLUP implementation has an impact on the accuracy of predicted bottom loss. Studies at one location showed an increase in predicted loss of 1 dB for each 20 m increase in thickness from 20 to 100 m. For better predictive capability, the sediment thickness must be known more accurately than ±80 m in thin sediment areas.

ACKNOWLEDGMENTS

The authors have benefitted from many conversations with K. E. Hawker, S. G. Payne, J. M. Daniels, and T. Foreman of ARL:UT, as well as R. Greene and C. Spofford of Science Applications, Inc. This work was supported by Naval Ocean Research and Development Activity.

132 - Blank

REFERENCES

1. S. K. Mitchell, K. C. Focke, J. J. Lemmon, and M. M. McSwain, "Analysis of Acoustic Bottom Interaction in BEARING STAKE" (U), Applied Research Laboratories Technical Report No. 79-24 (ARL-TR-79-24), Applied Research Laboratories, The University of Texas at Austin, February 1979. (CONFIDENTIAL)

2. S. K. Mitchell, N. R. Bedford, and G. E. Ellis, "Multipath Analysis of Explosive Source Signals in the Ocean," J. Acoust. Soc. Am. 67, 1590-1597 (1980).

3. S. K. Mitchell and K. C. Focke, "New Measurements of Compressional Wave Attenuation in Deep Ocean Sediments," J. Acoust. Soc. Am. 67, 1582-1589 (1980).

4. P. J. Vidmar, "The Effect of Sediment Rigidity on Bottom Reflection Loss in a Typical Deep Sea Sediment," J. Acoust. Soc. Am. 68, 639-648 (1980).

6. S. R. Rutherford, K. E. Hawker, and S. G. Payne, "A Study of the Effects of Ocean Bottom Roughness on Low-Frequency Sound Propagation," J. Acoust. Soc. Am. 65, 381-386 (1979).

7. A. O. Williams, Jr., "Hidden Depths: Acceptable Ignorance about Ocean Bottoms," J. Acoust. Soc. Am. 59, 1175-1179 (1976).

8. S. R. Rutherford and K. E. Hawker, "The Effects of Density Gradients on Bottom Reflection Loss for a Class of Marine Sediments," J. Acoust. Soc. Am. 63, 750-757 (1978).

9. E. L. Hamilton, "Geoacoustic Modeling of the Sea Floor," J. Acoust. Soc. Am. 68, 1313-1340 (1980).

10. C. W. Spofford, R. R. Greene, and J. B. Hersey, "The Estimation of Geo-Acoustic Ocean Sediment Parameters from Measured Bottom-Loss Data," Science Applications, Inc., McLean, Virginia, 1982.

11 H. Holthusen and P. J. Vidmar, "The Effect of Near-Surface Layering on the Reflectivity of the Ocean Bottom," J. Acoust. Soc. Am. 72, 226-234 (1982).

12. J. M. Daniels and P. J. Vidmar, "Occurrence and Acoustical Significance of Natural Gas Hydrates in Marine Sediments," Applied Research Laboratories Technical Paper No. 82-1 (ARL-TP-82-1), Applied Research Laboratories, The University of Texas at Austin, January 1982. Accepted for publication in The Journal of the Acoustical Society of America.

13. J. F. Lynch and K. E. Hawker, "A Statistical Description of Bottom Loss and Propagation Loss for the North Atlantic and Eastern Pacific Ocean" (U), Applied Research Laboratories Technical Report No. 82-26 (ARL-TR-82-26), Applied Research Laboratories, The University of Texas at Austin, May 1982. (CONFIDENTIAL)

14. T. L. Foreman, "Acoustic Ray Models Based on Eigenrays," Applied Research Laboratories Technical Report No. 77-1 (ARL-TR-77-1), Applied Research Laboratories, The University of Texas at Austin, January 1977.

12 August 1982

DISTRIBUTION LIST FOR
ARL-TR-82-17
UNDER CONTRACT N00014-82-C-0049
UNCLASSIFIED

Copy No.	
	Commanding Officer Naval Ocean Research and Development Activity NSTL Station, MS 39529
1	Attn: E. D. Chaika (Code 530)
2	CDR M. McCallister (Code 520)
3	W. Kuperman (Code 320)
	Chief of Naval Research Office of Naval Research Arlington, VA 22217
4	Attn: P. Rogers (Code 425AC)
5	Office of Naval Research Branch Office, Chicago Department of the Navy 536 South Clark Street Chicago, IL 60605
	Commanding Officer Naval Electronic Systems Command Washington, DC 20360
6	Attn: LCDR S. Hollis (Code 612)
7	CDR C. Spikes (PME 124-60)
8	CDR P. Girard (Code 612)
	Director Naval Research Laboratory Department of the Navy Washington, DC 20375
9	Attn: B. B. Adams (Code 8160)
10	W. Mosley
	Commanding Officer Naval Ocean Systems Center Department of the Navy San Diego, CA 92152
11	Attn: E. L. Hamilton
12	H. P. Bucker

Distribution List for ARL-TR-82-17 under Contract N00014-82-C-0049 (Cont'd)

Copy No.

Commander
Naval Sea System Command
Department of the Navy
Washington, DC 20362
13 Attn: R. W. Farwell (Code 63RA)
14 P. R. Tiedeman (Code 630)

Chief of Naval Operations
Department of the Navy
Washington, DC 20350
15 Attn: CAPT E. Young (OP 952D)

Chief of Naval Material
Department of the Navy
Washington, DC 20360
16 Attn: CAPT J. Harlette (Code MAT 08T245)

17 Commander
Naval Surface Weapons Center
White Oak Laboratory
Department of the Navy
Silver Spring, MD 20910

18 Commander
David W. Taylor Naval Ship Research and Development Center
Department of the Navy
Bethesda, MD 20034

Commanding Officer
Naval Oceanographic Office
NSTL Station, MS 39529
19 Attn: W. Jobst (Code 3400)
20 J. Allen

Commander
Naval Air Development Center
Department of the Navy
Warminister, PA 18974
21 Attn: J. Howard

Officer in Charge
New London Laboratory
Naval Underwater Systems Center
Department of the Navy
New London, CT 06320
22 Attn: B. Cole

Distribution List for ARL-TR-82-17 under Contract N00014-82-C-0049 (Cont'd)

Copy No.	
23	Director Naval Warfare Deputy Undersecretary of Defense R&E Room 3D1048, Pentagon Washington, DC 20301
	Superintendent Naval Postgraduate School Monterey, CA 93940
24	Attn: Library
	Commander Naval Coastal Systems Center Department of the Navy Panama City, FL 32407
25	Attn: G. McLeroy
26 - 37	Commanding Officer and Director Defense Technical Information Center Cameron Station, Building 5 5010 Duke Street Alexandria, VA 22314
	Defense Advance Research Projects Agency 1400 Wilson Blvd. Arlington, VA 22209
38	Attn: CDR K. Evans (TTO)
39	Commander Naval Intelligence Support Center 4301 Suitland Road Washington, DC 20390
	Science Applications, Inc. 1710 Goodridge Drive McLean, VA 22101
40 - 41	Attn: C. Spofford
	Ocean Data Systems, Inc. 3255 Wing Street San Diego, CA 92110
42	Attn: K. Osborne
	Bell Telephone Laboratories, Inc. Whippany Road Whippany, NJ 07961
43	Attn: R. Worley

Distribution List for ARL-TR-82-17 under Contract N00014-82-C-0049 (Cont'd)

Copy No.

Planning Systems, Inc.
7900 Westpark Drive, Suite 507
McLean, VA 22101
44 Attn: R. Cavanaugh
45 B. Brunson

TRW, Inc.
TRW Electronics and Defense Sector
Systems Engineering and Applications Division
7600 Colshire Drive
McLean, VA 22102
46 Attn: R. T. Brown

Bolt, Beranek, & Newman, Inc.
50 Moulton Street
Cambridge, MA 02138
47 Attn: H. Cox

Applied Physics Laboratory
The Johns Hopkins University
Johns Hopkins Road
Laurel, MD 20810
48 Attn: J. Lombardo

Western Electric Company, Inc.
P. O. Box 20046 - GC7420
Greensboro, NC 27420
49 Attn: T. Clark

50 Office of Naval Research
Resident Representative
Room 582, Federal Building
Austin, TX 78701

51 Environmental Sciences Division, ARL:UT

52 Robert F. Gragg, ARL:UT

53 Kenneth E. Hawker, ARL:UT

54 Robert A. Koch, ARL:UT

55 Stephen K. Mitchell, ARL:UT

56 Clark S. Penrod, ARL:UT

57 Paul J. Vidmar, ARL:UT

Distribution List for ARL-TR-82-17 under Contract N00014-82-C-0049 (Cont'd)

Copy No.	
58	Library, ARL:UT
59 - 69	Reserve, ARL:UT